Assembly of Omegatetravirus Virus-like Particles in the Yeast *Saccharomyces cerevisiae*

A dissertation submitted in fulfilment of the requirements for the degree of

Doctor of Philosophy

at

Rhodes University

By

Michele Tomasicchio

4th September 2007

DEDICATION

To my loving wife, Andrea, who stood by me and made me realise my dream

ABSTRACT

The *Tetraviridae* are a family of ss (+) RNA viruses that specifically infect lepidopteran insects. Their icosahedral capsids are non-enveloped and approximately 40 nm in diameter with *T*=4 quasi-equivalent symmetry. The omegatetraviruses, which are structurally the best characterised in the family, include *Helicoverpa armigera stunt virus* (HaSV) and *Nudaurelia capensis omega virus* (NωV). The omegatetravirus procapsid is composed of 240 identical copies of the capsid precursor proteins, which undergo autoproteolytic cleavage at its carboxyl-terminus generating the mature capsid protein (β) and γ-peptide. This process occurs *in vitro* following a shift from pH 7.6 to pH 6.0. The viral capsid encapsidates two ss genomic RNAs: The larger RNA1 encodes the viral replicase as well as three small ORFs while RNA2 encodes the capsid precursor protein together with an overlapping ORF designated *P17*. While a wealth of structural data pertaining to the assembly and maturation of omegatetraviruses is available, little is known about how this relates to their lifecycle. The principle aim of the research described in this thesis was to use an experimental system developed in the yeast, *Saccharomyces cerevisiae*, to investigate the assembly of HaSV and NωV virus-like particles (VLPs) in terms of maturation and encapsidation of viral RNAs, *in vivo*.

The yeast expression system used two promoter systems for expression of capsid precursor protein: in the first, a hybrid promoter (P_{GADH}) was used for high-level expression, while the second, $P_{GAL1,}$ produced substantially lower levels of the virus capsid protein precursors. An increase in the level of HaSV capsid protein precursor (p71) via the P_{GADH} promoter resulted in a dramatic increase in VLP assembly as compared with the P_{GAL} system. A protein equivalent to the mature capsid protein (p64) appeared at later time intervals following induction of transcription. Transmission electron microscopic studies showed that p64 correlated with the presence of mature VLPs as opposed to procapsids in cells containing p71. This confirmed that the presence of p64 denoted maturation of VLPs *in vivo*. Further investigation indicated that maturation correlated with cell aging and the onset of apoptosis. It was shown that induction of apoptosis resulted in VLP maturation while

inhibition of apoptosis prevented maturation. These results suggested that the process of apoptosis might be the trigger for maturation of virus procapsids in their host cells.

The increase in the efficiency of VLP assembly observed in the high-level expression system was proposed to be due to an increase in the cellular concentrations of viral RNA. To test this hypothesis, HaSV *P71* was co-expressed with either *P71* mRNA or full length RNA2. An increase in the solubility of p71 was observed in cells expressing increased levels of both RNAs, but there was no increase in the efficiency of VLP assembly. Northern analysis of encapsidated RNAs revealed that there was no selective encapsidation of either *P71* mRNA or viral RNA2. This data indicated that the increase in viral RNA was not the reason for increased efficiency of VLP assembly, but most likely resulted from higher concentrations of p71 itself. It was decided to determine whether a highly efficient nodavirus replication system developed in yeast for heterologous production of proteins, could be used as a method for expressing the capsid protein precursor. The aim of using this system was to determine if VLPs assembled in a replication system specifically encapsidated viral RNA. Transcripts encoding the NωV capsid protein precursor (p70) were generated in yeast cells by replication of a hybrid RNA template by the *Nodamura virus* (NoV) replicase. Western analysis confirmed the presence of p70 as well as a protein of 62 kDa corresponding to the mature NωV capsid protein. Northern analysis of purified VLPs showed that NoV RNA1 and RNA3 were encapsidated, but no RNA2 was detected. Taken together, the data lead to the conclusion that specific encapsidation of tetraviral RNAs required more than close proximity of the viral RNAs and assembling virus-like particles. Encapsidation specificity in the omegatetraviruses may require additional viral proteins such as p17 during encapsidation or specific viral RNA encapsidation was replication-dependent. Replication-dependent assembly has been shown in the nodaviruses.

TABLE OF CONTENTS

LIST OF FIGURES

LIST OF TABLES

LIST OF ABBREVIATIONS

Viruses:

AV	*Aura virus*
BBV	*Black beetle virus*
BMV	*Brome mosaic virus*
DpTV	*Dendrolimus punctatus tetravirus*
FHV	*Flock house virus*
HaSV	*Helicoverpa armigera stunt virus*
HDV	*Hepatitis delta virus*
NβV	*Nudaurelia beta virus*
NωV	*Nudaurelia omega virus*
NoV	*Nodamura virus*
PrV	*Providence virus*
PaV	*Pariacoto virus*
STMV	*Satellite tobacco mosaic virus*
TaV	*Thosea asigna virus*
ToRSV	*Tobacco ringspot virus*

General:

ARS	autonomous replication sequence
bp	base pair
CEN	yeast centromeric sequence
cpm	counts per minute
cryoEM	cryo-electron microscopy
$dddH_2O$	triple-distilled water
DAB	3,3'-diaminobenzidine
DAPI	4,6-diamidino-2-phenylindole
DEPC	diethyl pyrocarbonate
DIG	digoxigenin
DNA	deoxyribonucleic acid
DTT	dithiothreitol

EB	extraction buffer
EDTA	ethylenediaminetetra acetic acid
GAPDH	*Saccharomyces cerevisiae glyceraldeyde-3-phosphate dehydrogenase* gene
H_2O_2	hydrogen peroxide
HC ribozyme	hairpin cassette ribozyme
HDV ribozyme	*Hepatitis delta virus* ribozyme
HOAc	acetic acid
Ig-like	immunoglobulin-like
kb	kilobase
kDA	kilo dalton
LA	Luria-Bertani agar
LB	Luria-Bertani broth
LHB	larval homogenisation buffer
MOPS	3-(*N*-morpholino)propanesulfonic acid
M_R	relative molecular weight
mRNA	messenger RNA
NaAc	sodium acetate
NaCl	sodium chloride
nt	nucleotide
OD_{600nm}	optical density at 600nm
ORF	open reading frame
P_{ADH2}	*Saccharomyces cerevisiae ADH2* promoter
PCD	programmed cell death
PCR	polymerase chain reaction
PEG	polyethylene glycol
$P_{ADH2\text{-}GAPDH}$ / P_{GADH}	*Saccharomyces cerevisiae alcohol dehydogenase*-2 / *glyceraldeyde-3-phosphate dehydrogenase* hybrid promoter
P_{GAL1}	*Saccharomyces cerevisiae GAL1* promoter
PMSF	phenylmethyl-sulfonyl fluoride
RNA	ribonucleic acid
RNase	ribonuclease
POD	horseradish peroxidase
RdRp	RNA-dependent-RNA-polymerase

ROS	reactive oxygen species
SDS	sodium dodecyl sulphate
SDS-PAGE	sodium dodecyl sulphate polyacrylamide gel electrophoresis
Sf 21	*Spodpoptera frugiperda* 21
SMM	synthetic minimal medium
ss (+) RNA	single stranded, positive sense RNA
Tcyc_1	*Saccharomyces cerevisiae CYC1* terminator
TEM	transmission electron microscopy
Tris	tris(hydroxymethyl)aminomethane
TUNEL	terminal deoxynucleotidyl transferase-mediated dUTP nick end labelling
tRNA	transfer RNA
VLPs	virus-like particles
YEPD	yeast extract, peptone, dextrose medium
YNB	yeast nitrogen base

ACKNOWLEDGEMENTS

My sincere thanks to the following people:

- My supervisor Professor Rosemary Dorrington for guiding me through this project and making it a success. Her passion for this project and science in general is inspiring.
- My parents and brother for their love and support.
- My wife Andrea for supporting me.
- My friends especially to Mez Jiwaji for proofreading my thesis and members of lab 417 who constantly made me smile.
- To Dr Arno Venter who started the yeast project and provided the tools for my project.
- To Petra Gentz, Jeremy Baxter, Mez Jiwaji, Andrew Grant, Jo and Clinton de la Mare and James Short for all their hospitality during the final preparation of this thesis.
- To Professor Andrew Ball, Dr Lance Eckerle and Dr Kyle Johnson at University of Alabama at Birmingham who offered me the opportunity to work in their lab and generate the data presented in chapter 4.
- To Professor Jack Johnson and Professor Annette Schneemann for interesting discussions.
- To Frank Madeo at the University of Tübingen, Germany for protocols on the TUNEL test and DAPI staining techniques.

This project was funded by the National Research Foundation of South Africa.

PUBLICATION

Chapter 2, in part or in full, is a reprint of the material as it appears in Tomasicchio, M., Venter, P.A., Gordon, K.H., Hanzlik, T.N and Dorrington, R.A. 2007. Induction of apoptosis in *Saccharomyces cerevisiae* results in the spontaneous maturation of tetravirus procapsids *in vivo*. Journal of General Virology. **88 (5):** 1576-1582. The dissertation author was the primary investigator and author of this paper.

CHAPTER 1. LITERATURE REVIEW

CHAPTER 1. LITERATURE REVIEW

1.1 THE *TETRAVIRIDAE*

The *Tetraviridae* are a group of small insect RNA viruses which encapsidate one or two single strands of positive sense genomic RNA into a non-enveloped icosahedral capsid of approximately 40 nm in size with a *T*=4 quasi-equivalent symmetry (reviewed in Hanzlik *et al.,* 1997). The family is classified into the monopartite *Betatetraviridae* and the bipartite *Omegatetraviridae* genera. The *Tetraviridae* are highly tropic for lepidopteran insects (Fauquet *et al*., 2005).

1.1.1 History

In the early 1970s the first tetravirus, *Nudaurelia β virus* (NβV) was isolated from infected larvae of the pine emperor moth (*Nudaurelia cytherea capensis*), in South Africa (Table 1.1; Juckes, 1970). In addition to NβV the larvae were also infected with *Nudaurelia* γ, δ, α, and ε viruses (Juckes, 1970). NβV, the dominant virus characterised by Struthers and Hendry in 1974, had a major capsid protein of approximately 60 to 62 kDa. Later, Finch and Crowther (1974) determined that the capsid was composed of 240 subunits which had a *T*=4 quasi-equivalent symmetry. *Thosea asigna virus* (TaV) was later isolated from *Setothosea asigna* larvae, which were serologically related to NβV and had an identical buoyant density of 1.275 g/cm^3 in CsCl (Table 1.1; Reinganum *et al*., 1978). Biophysical analysis of *Nudaurelia* β and ε viruses named the new virus group *Nudaurelia* β-like virus (NβV), which was the first genus of the family *Tetraviridae* (Matthews, 1982; Juckes, 1979). The two viruses had different sedimentation coefficients and buoyant densities but more importantly the particles had a diameter of between 39 to 40 nm (Juckes, 1979). Later a third member of the family, *Nudaurelia ω virus* (NωV) was isolated from *Nudaurelia* larvae (Table 1.1; Hendry *et al*., 1985). This virus was serologically distinct from NβV and differed further by having a bipartite RNA genome as opposed to the monopartite genome of NβV. The family was named *Tetraviridae* referring to the Greek word *tettares* (four) because their capsid was characterised as having a *T*=4 quasi-equivalent symmetry (Francki *et al*., 1991).

Table 1.1. Members of the family *Tetraviridae* (Fauquet *et al.*, 2005).

Virus name	**Abbreviation**	**Host Family**	**Location Discovered**	**References**
Genus: Betatetraviruses				
Nudaurelia capensis β *virus*	NβV	*Saturniidae*	South Africa	Juckes, 1970
Antheraea eucalypti virus	AeV	*Saturniidae*	Australia	Grace and Mercer, 1965
Darna trima virus	DtV	*Limacodidae*	Malaysia	Reinganum *et al*., 1978
*Dasychira pudibunda virus**	DpV	*Lymantriidae*	United Kingdom	Greenwood and Moore, 1984
Philosamia Cynthia x ricini virus	PxV	*Saturniidae*	United Kingdom	Reinganum *et al*., 1978
Pseudoplusia includens virus	PiV	*Noctuidae*	United States	Chao *et al*., 1983
*Thosea asigna virus***	TaV	*Limacodidae*	Malaysia	Reinganum *et al*., 1978
Euprosterna elaeasa virus	EeV	*Noctuidae*	-	Zeddam *et al*., unpublished
Trichoplusia ni virus	TnV	*Noctuidae*	United States	Morris *et al*., 1979
Providence virus	PrV	*Noctuidae*	United States	Pringle *et al*., 2003
Genus: Omegatetraviruses				
Nudaurelia capensis ω *virus*	NωV	*Saturniidae*	South Africa	Hendry *et al*., 1985
Helicoverpa armigera stunt virus	HaSV	*Noctuidae*	Australia	Hanzlik *et al*., 1993
Dendrolimus punctatus tetravirus	DpTV	*Lasicampidae*	China	Yi *et al*., 2005

* Known previously as *Calliteara pudibunda virus*.
** Known previously as *Sethosea asigna virus*.

The second genus named, *Nudaurelia* ω-like, was joined by *Helicoverpa armigera stunt virus* (HaSV), which was isolated by Hanzlik *et al*. (1993) from infected *Helicoverpa armigera* larvae (Table 1.1). In 2003 a betatetravirus, named *Providence virus* (PrV), was described from a persistently infected *Helicoverpa zea* cell line

(Table 1.1; Pringle *et al*., 2003). To this day PrV remains the only tetravirus, which is able to infect a cell line and thus offer the potential to study the infectious cycle of the *Tetraviridae*. Recently a new member of the *Omegatetraviridae* named *Dendrolimus punctatus tetravirus* (DpTV) was isolated from *Dendrolimus punctatus* larvae in China (Yi *et al*., 2005). To date the *Betatetraviridae* have 10 confirmed members, while the *Omegatetraviridae* have 3 confirmed members (Fauquet *et al*., 2005; Table 1.1).

1.1.2 Pathology

The *Tetraviridae* are highly pathogenic to the hosts they infect (reviewed in Hendry and Agrawal, 1994). The symptoms of infection by the *Nudaurelia* viruses involve the larvae becoming increasingly lethargic, discoloured and flaccid followed by vomiting and death (reviewed in Hendry and Agrawal, 1994). Infected larvae have been shown to hang from their prolegs following infection (Hendry and Agrawal, 1994; personal observation). The primary site of infection has been elucidated as the midgut for a number of tetraviruses (Grace and Mercer, 1965; Greenwood and Moore, 1984; Brookes *et al*., 2002), but the pathobiology of infection has only been well document for HaSV (Brookes *et al*., 2002). The response of *H. armigera* larvae to HaSV infection of its goblet and regenerative cells is cell sloughing or cell removal, which is linked to the cells undergoing programmed cell death (PCD) or apoptosis (Brookes *et al*., 2002). Older *H. armigera* larvae in the fourth or fifth instar are less sensitive to infection than younger larvae. This decreased susceptibility to infection is thought to be as a consequence of the larvae having an increased ability to remove their midgut cells during infection (Brookes *et al*., 2002).

1.1.3 Tetravirus genome organisation

Currently among the tetraviruses the entire genomes of two omegatetraviruses (HaSV and DpTV) and three betatetraviruses are known (NβV, TaV and EeV) (Zeddam *et al*., unpublished; Hanzlik *et al*., 1995; Gordon *et al*, 1995; Gordon *et al*., 1999; Pringle *et al*., 1999; Yi *et al*., 2005). In addition, the partial genome sequence is available for PrV (capsid precursor protein coding sequence) and NωV (RNA2) (Agrawal and Johnson, 1992; Pringle *et al*., 2003; du Plessis *et al*., 2005).

1.1.3.1 The betatetraviruses.

NβV, the type member of the genus, contains a single (+) RNA molecule which is approximately 6.5 kb in size and represents 10% of the particle mass (Fauquet *et al*., 2005). This RNA encodes both the RNA dependent RNA polymerase (replicase) and capsid protein precursor (Figure 1.1). The major open reading frame (ORF) from nucleotides 93 to 5870 encodes the replicase with a predicted molecular mass of 216 kDa (Figure 1.1). This ORF accounts for 87% of the genome and is at the 5' end (Gordon *et al*., 1999). The replicase contains a methyltransferase, helicase and RNA-dependent RNA polymerase (RdRP) domain, which are conserved among the (+) RNA Alphaviruses (Gordon *et al*., 1999). The capsid precursor gene overlaps the replicase gene at the 3' end between nucleotides 4039 to 5874. The capsid precursor protein (66.4 kDa) is encoded by a subgenomic RNA (Figure 1.1). During assembly 240 copies of the capsid precursor protein associate to form the procapsid. The capsid precursor is cleaved between Asn 536 and Gly 537 to generate the mature capsid (β protein) of 58.4 kDa and a smaller γ-peptide of 8 kDa (Gordon *et al*., 1999).

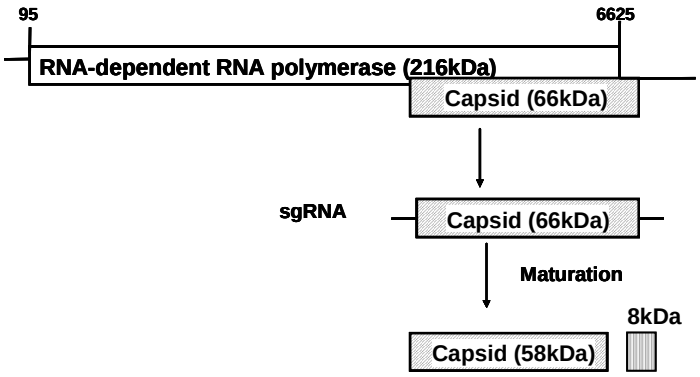

Figure 1.1 The genome organization for NβV (Gordon *et al*., 1999).

The 3' end of the NβV genome can be folded into a tRNA-like structure, with a valine anticodon (Gordon *et al*., 1999). This structure has been identified in some plant viruses, but is different because it forms without a pseudoknot (Gordon *et al*., 1999). The function of the authentic $tRNA^{Val}$ has been hypothesised to aid in replication of the genome and is a common feature in both tetravirus genera (Hanzlik *et al*., 1995; Gordon *et a*l., 1999).

The genome of TaV is 6.5 kb in size and contains two overlapping ORFs (Pringle *et al*., 1999). The first encodes a putative replicase and the second, a capsid precursor polyprotein (Pringle *et al*., 1999). The capsid precursor protein in TaV is cleaved twice to generate an *N*-terminal cleavage product of 17 kDa (P17), the large capsid protein of 58.3 kDa (L) and a small capsid protein of 6.8 kDa (S) (Pringle *et al*., 1999). The 17 kDa protein has been hypothesised to stabilise the capsid during assembly (Pringle *et al*., 2001). In TaV a NPGP tripeptide was identified between the P17/L cleavage site in the polyprotein, which are conserved domains among the picornaviruses where cleavage occurs, and are called 2A-like domains (Donnelley *et al*., 2001). These 2A-like domains have also been identified in PrV, indicating that the processing of their polyprotein occurs in a similar way (Pringle *et al*., 2003). Cleavage of the procapsid in PrV results in the generation of a 60 kDa mature capsid and two smaller proteins of 7.4 kDa and 13 kDa (Pringle *et al*., 2003).

1.1.3.2 The omegatetraviruses.

The larger genome segment (RNA1) of HaSV is 5312 nucleotides in length and is capped at the 5' end. The RNA molecule contains a major ORF encoding the 1704 amino acid replicase (Figure 1.2). The replicase has a predicted molecular mass of 187 kDa (Gordon *et al*., 1995). Three additional ORFs are located at the 3' end of the replicase ORF called p11, p15 and p8 with no known functions. In DpTV RNA1 is 5492 nucleotides in length and encodes a replicase with predicted molecular weight of 180 kDa (Yi *et al*., 2005). Additionally there are also three ORFs at the 3' end designated ORFp15, ORFp13 and ORFp11 (Yi *et al*., 2005). Sequence analysis of the replicase protein revealed that like HaSV, DpTV contains the three domains (methyltransferase domain, the helicase domain and the polymerase domain), which are conserved among other Alphaviruses (Yi *et al*., 2005). The replicase was shown to have polymerase activity, which was lost when the GDD motif within the polymerase domain was mutated (Zhou *et al*., 2006). The different domains of the DpTV replicase display different sequence identities with other viruses in the family. The methyltransferase domain shares 67% homology with HaSV and 38% with NβV (Yi *et al*., 2005). The helicase domain is more distantly related to HaSV with 63% identity and the polymerase domain is 76% and 36% similar to HaSV and NβV respectively (Yi *et al*., 2005).

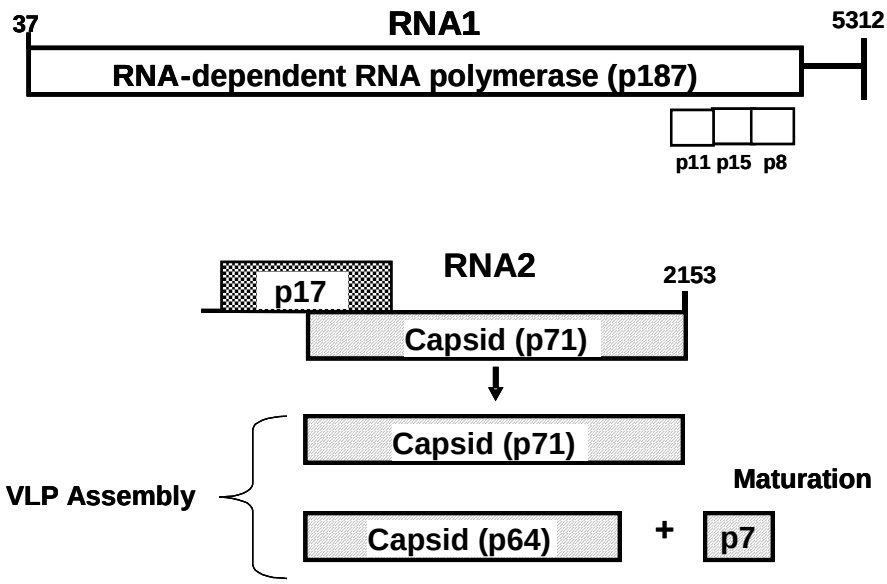

Figure 1.2 The genome organization for HaSV (Gordon *et al*., 1995; Hanzlik *et al*., 1995).

The sequence of HaSV RNA2 is 2478 nucleotides in length and is capped at the 5' end. RNA2 encodes two overlapping ORFs (Figure 1.2). The first ORF (p17) encodes a protein with predicted mass of 17 kDa, which has been hypothesised to function as a movement protein (Hanzlik *et al*., 1995). The p17 ORF protein is conserved among the omegatetraviruses (Hanzlik *et al*., 1995; Hanzlik and Gordon, 1997; du Plessis *et al*., 2005; Yi *et al*., 2005). The second ORF of HaSV RNA2 encodes a 647 amino acid capsid precursor protein with a molecular mass of 71 kDa (p71) (Figure 1.2). During maturation p71 is cleaved at an Asn-Phe site after amino acid 575 to generate the mature capsid protein of 64 kDa and a small gamma peptide of 7 kDa. Cleavage of p71 has been shown to occur upon assembly of the capsid in baculoviruses (Hanzlik *et al.,* 1995) and release of the minor protein by the assembly dependent cleavage reaction is proposed to be essential for viral infectivity (Hanzlik and Gordon, 1997).

The RNA2 molecules of NωV and DpTV contain a major ORF which encodes a capsid precursor protein with predicted molecular weight of 70 kDa, that is cleaved at a similar Asn-Phe site to HaSV resulting in a mature protein of approximately 62 kDa and a smaller protein of 8 kDa (Agrawal and Johnson, 1992; Yi *et al*., 2005).

Table 1.2. Sequence similarity and identity between the capsid encoding sequences of the omegatetraviruses (HaSV, NωV and DpTV) and three betatetrarviruses (NβV, TaV and PrV) (adapted from Pringle *et al*., 2003)

		SIMILARITY				
Virus	PrV	TaV	HaSV	NβV	NωV	DpTV
PrV		35	47	35	46	42
TaV	28		33	43	35	31
HaSV	38	27		36	72	76
NβV	27	35	29		35	35
NωV	37	27	66	29		92
DpTV	30	21	66	23	86	

IDENTITY

As in NβV the 3' termini of NωV, HaSV and DpTV RNA2 have been shown to have the potential to fold into secondary structures resembling tRNAs with a valine codon (Hanzlik *et al*., 1995; Yi *et al*., 2005). These structures can also from in HaSV and DpTV RNA1 (Gordon *et al*., 1995; Yi *et al*., 2005). This ability of the RNA to fold is not localised to the 3' end in HaSV. The 5' end and an internal region of the RNAs can also fold into loop structures (Hanzlik *et al*., 1995). These structures are thought to play a role in virus replication, RNA encapsidation and gene regulation. It has been suggested that they may even protect the RNA from degradation by the host cell (Hanzlik and Gordon, 1997).

1.1.4 Virus structure- the theory of quasi-equivalence

The theory of quasi-equivalence, first described by Casper and Klug (1962), proposed that an icosahedral virus particle is formed from hexameric and pentameric structures of the same protein. In order for the icosahedral structure to form, it must be composed of 12 pentamers. The greater the *T* number, the greater the number of hexamers there are between the pentamers. For a given quasi-equivalent symmetry the subunits associate through either a two-fold, three-fold or five-fold axis.

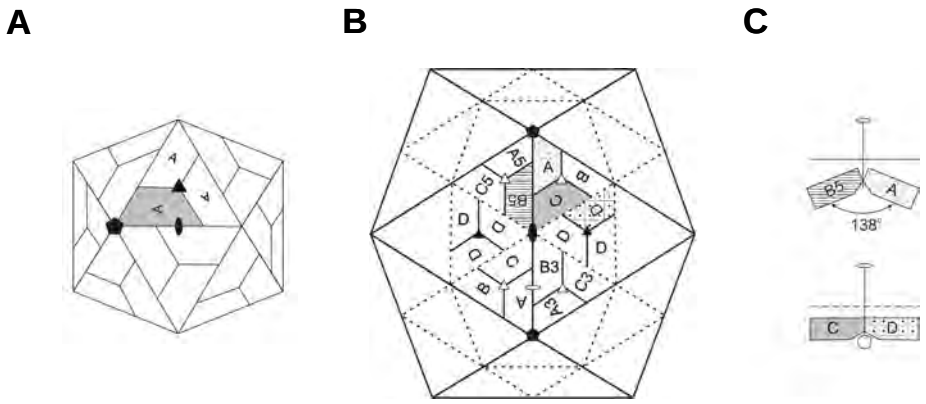

Figure 1.3 Diagrammatic representation of a virus particle with *T*=1 (**A**) and *T*=4 (**B**) quasi-equivalent symmetry. (**A**) The arrangement of the identical subunits A in the *T*=1 particle are in the same environment and only form a bent contact. (**B**) The subunits A, B, C and D in the *T*=4 particle, indicate subunits from identical gene products in a different environments in the icosahedral shell. The symmetrical two-fold, three-fold and five-fold axes are depicted by solid eclipses, triangles and pentagons respectively. (**C**) The bent contact and flat contact formed between the A/B and C/D subunits respectively at the two-fold axis of the *T*=4 particle are shown (Johnson and Reddy, 1998).

Viruses with the simplest structure have identical subunits which adopt a *T*=1 quasi-equivalent symmetry and are composed of 60 subunits (Figure 1.3, A). According to the theory of quasi-equivalence this dictates that each subunit lies in an identical environment, and associates through a 2-fold axis with a bent contact (138°). The small size of the particle indicates that they are unable to encapsidate their genome (Johnson, 1996). The formation of particles with more than 60 subunits requires that while all the subunits are identical, they must adopt slightly different conformation in the capsid shell. The theory of quasi-equivalence states that all capsids adopt their structure through a given vertex and the way in which different environments are occupied dictates the *T* number (Baker *et al.*, 1999). The number of possible subunits for a given viral conformation indicate that the number is equal to 60*T*, where *T* refers to the number of subunits in different environments.

1.1.4.1 The *T*=4 quasi-equivalent structure of the tetraviruses

In the tetraviruses, the *T*=4 quasi-equivalent capsid shell is composed of subunits A, B, C, D, which are derived from the same gene product in slightly different environments. A total of 240 subunits make up the viral shell (Figure 1.3, B). The

shell forms two different trimers ABC and DDD (Munshi *et al.*, 1996; Canady *et al.*, 2000; Helgstrand *et al.*, 2004). The ABC trimers surround the 5–fold axis and the DDD trimers associate at the 3–fold axis. Three ABC trimers and one DDD trimer form each face of the capsid. Additionally, at the 2–fold axis there are two copies of subunits BCD making a quasi 6–fold axis. There are also two distinct 2–fold axes. One related to 6–fold axes and the other to a 5 and 6–fold axes (Helgstrand *et al.*, 2004). The interactions between these axes have two types of contacts; a flat contact where the angle between the subunits is 180°, and a bent contact, where the angle between the subunits is 144°. The flat contacts occur at the 2–fold axis between C/D subunits and the 6–fold axis between B/D subunits. The bent contacts have been shown at the 5–fold axis between B/C subunits and the 6–fold axis between A/B subunits (Helgstrand *et al.*, 2004).

1.1.5 Tetravirus subunit structure

The structure of wild-type NωV was solved to 2.8 Å resolution by Munshi *et al.*, (1996) and subsequently refined by Helgstrand *et al.*, (2004). Each capsid subunit is composed of three domains: the internal helical domain, a β-sandwich domain and an external immunoglobulin (Ig)-like domain (Figure 1.4). The β-sandwich domain located in the centre of the capsid subunit is composed of eight anti-parallel β-sheets designated βB, βC etc. to βI and the loops connecting the strand are designated BC, CD etc. (Munshi *et al.*, 1996). The β-sandwich domain relates to residues 121 through 543. The boundary between the β-sandwich domain and internal helical domain interact with each other at Asp 44, Phe 121 and Gln 543 (Munshi *et al.*, 1996).

The internal helical domain resides at both the *N* and *C*-terminus of the protein (Figure 1.4) comprising helices, designated αN1-αN4 and αC1-αC4 respectively (Helgstrand *et al.*, 2004). The two regions represent residues 1 to 43 at the *N*-terminus and 591 to 607 at the *C*-terminus (Munshi *et al.*, 1996, Helgstrand *et al.*, 2004). Helix αC4 and αC2 are the γ-peptides, which are cleaved during maturation.

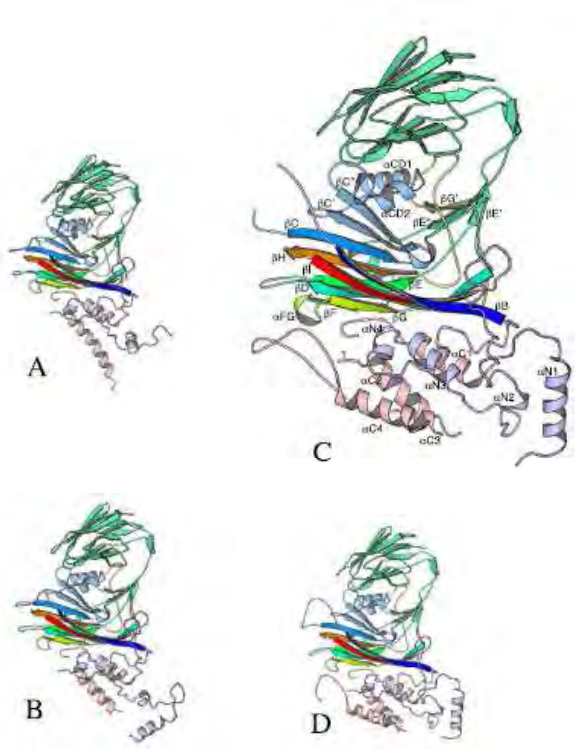

Figure 1.4 The structure of the NωV subunits A, B, C and D. The three domains of each subunit are shown: internal helical domain, β-sandwich domain and the external or immunoglobulin (Ig)-like domain (Helgstrand *et al.*, 2004).

The γ-peptides formed from cleavage of the helical domain in NωV were originally thought to be arranged in a similar way to the nodaviruses. This led to assumptions that the helical bundle, formed at the 5-fold axis between the A subunit γ-peptides, of NωV and the nodaviruses had conserved functions in membrane translocation of RNA (Cheng *et al.*, 1994; Munshi *et al.*, 1996). Since then the refined structure of NωV revealed a number of differences between the helical domains in the two virus families (Helgstrand *et al.*, 2004). Firstly, the γ-peptide of NωV is longer [(74 amino acids in NωV versus 44 amino acid in *Flock house virus* (FHV) or *black beetle virus* (BBV)] than FHV or BBV. Secondly, the helical bundle is formed from five *C*-terminal γ-peptides of the A subunit and five *N*-terminal γ-peptides of the B subunit in NωV, whereas in the nodaviruses the bundle only consists of five C-terminal γ-peptides of the A subunit (Cheng *et al.*, 1994; Helgstrand *et al.*, 2004). This would indicate that externalisation of the helical bundle for RNA translocation would almost certainly be impossible in NωV because the bundle would have to move 75 Å in order to be exposed (Helgstrand *et al.*, 2004).

The internal domain includes a number of positively charged residues. At the *C*-terminus, the last twenty residues have a net charge of +8 while the first 40 residues of the *N*-terminus have a net charge of +11 (Agrawal and Johnson, 1995). For this reason it is possible that the genomic RNA interacts with this region, which has the potential to neutralise up to 50% of the genomic RNA charge (Agrawal and Johnson, 1995; Helgstrand *et al*., 2004). The difference in the individual subunits A, B, C and D primarily exists at the α-helix N1 and N2 (Figure 1.4). The C and D subunits are very similar, with the A and B subunits differing in the loop that connect αN1 and αN2 (Helgstrand *et al*., 2004). The external domain exists between the βF and βE strands of the internal domain, and folds into a structure representing an Ig-like domain (Figure 1.4). The structure is formed by 10 folded β-sheets and consists of 133 amino acids (Munshi *et al*., 1996).

1.1.6 Tetravirus capsid structure.

The first structural study on the tetraviruses was the cryo-electron microscopic (cryoEM) examination of frozen hydrated NβV particles by Olson *et al*. (1990). The surface structure of this virus revealed that each of the twenty triangular faces was composed of twelve protein subunits grouped into four Y–shaped trimeric aggregates (Figure 1.5, B).

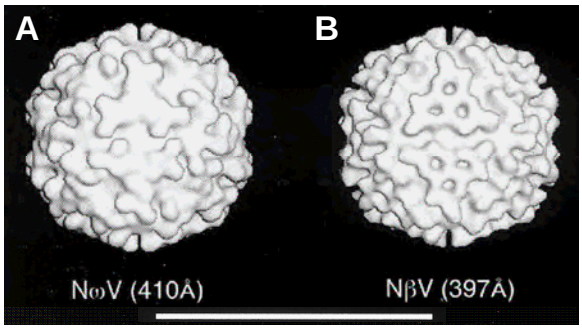

Figure 1.5 Cryo-EM reconstructions of NωV (**A**) and NβV (**B**) virions. The bar represents 500 Å (Baker *et al*., 1999).

Comparisons of the NωV and NβV surface structures by cryoEM show that NβV is pitted and more porous (Figure 1.5, B). Three pits were visible on each triangular face, while NωV has a solid trimeric face (Figure 1.5, A). Since 1990, a wealth of structural information has been generated by cryoEM and X-ray crystallographic

analysis of NωV (Munshi *et al.*, 1996; Canady *et al.*, 2000; 2001; Taylor *et al.*, 2002; Helgstrand *et al.*, 2004; Bothner *et al.*, 2005). This data will be discussed in detail below.

1.1.6.1 Procapsids and mature capsids are structurally distinct

The procapsid and capsid are structurally distinct (Figure 1.6). Cryo-EM reconstruction of baculoviral-derived NωV VLPs purified at a pH of 7.6 revealed that the particles exist as procapsids (Canady *et al.*, 2000). At an acidic pH of 5.0 a transition occurs from the procapsid state to the mature capsid (Canady *et al.*, 2000, 2001).

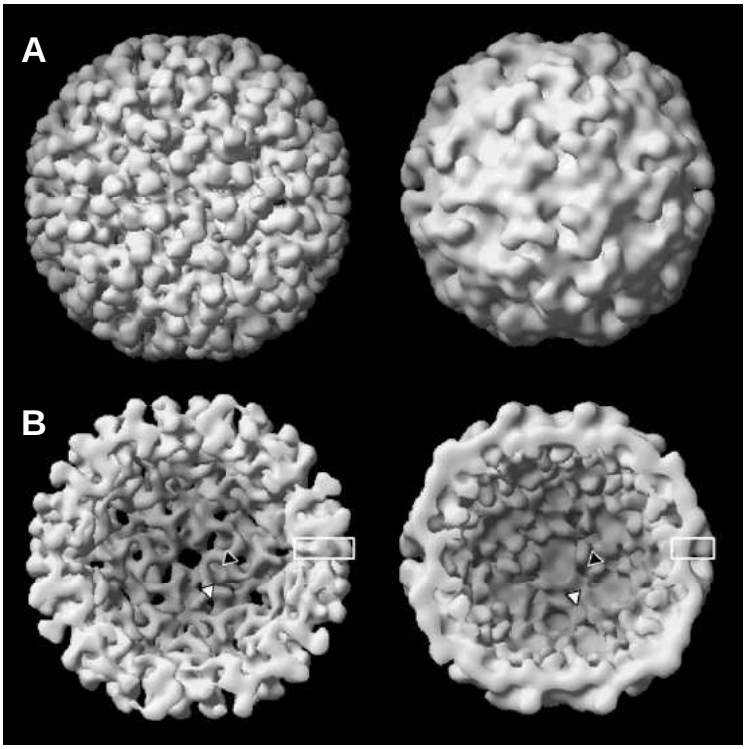

Figure 1.6 Cryo-EM reconstruction of the NωV procapsid and capsid structures. (**A**) Three-dimensional view of the NωV particle and (**B**) a section through the procapsid (left) and capsid (right) down the 2-fold axis, showing 3-fold (black triangle) and quasi 3-fold (white triangle) axis (Canady *et al.*, 2000).

As a result large structural changes occur causing the shrinking of the rounded, porous, procapsid (spanning 450 Å), into the compact, polyhedral capsid (spanning 410 Å) (Figure 1.6, compare A to B). The inner surface of the procapsid is larger than the capsid and spans 240 Å compared to 220 Å (Canady *et al.*, 2000).

Furthermore, the external or Ig-like domains at the surface of the particle are dumbbell shaped in the procapsid as opposed to trimeric in the mature capsid (Figure 1.6, A). The structural rearrangements from the procapsid to the capsid state at an acidic pH of 5.0 occurs rapidly (100 ms), while autocatalytic cleavage has a half-life of hours (Canady *et al.*, 2001). This extended time period is believed to be as a result of the initial expansion of the procapsid during the transition as protein-protein and protein-RNA interactions need to be broken (Taylor *et al.*, 2002).

1.1.7 Capsid assembly

The first model for procapsid assembly was proposed by Canady *et al.* (2000). In the procapsid AB and CD dimers are predominant, while in the mature capsid the trimeric ABC and DDD interactions are predominant (Candy *et al.*, 2000). The porous nature of the procapsid exists because of the disordered configuration of the subunits at the 6–fold axis.

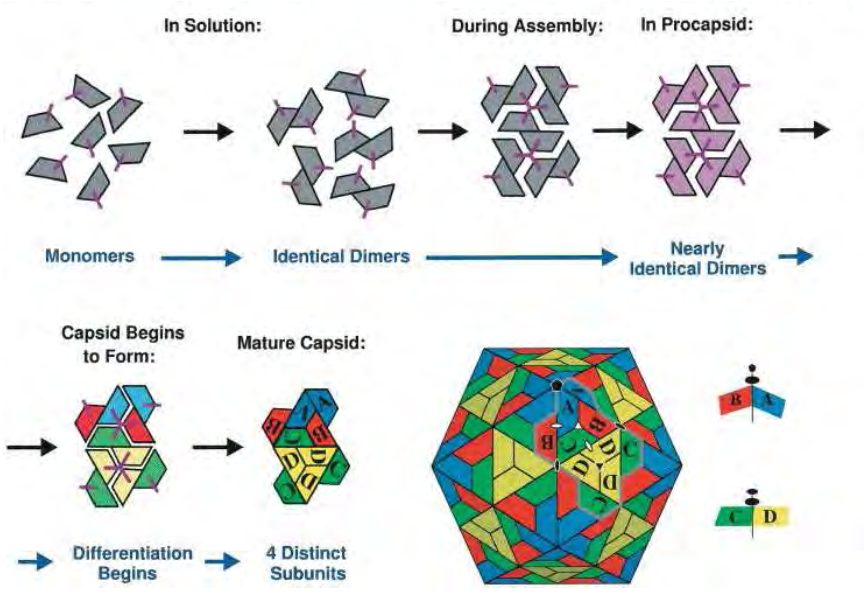

Figure 1.7 Proposed mechanism of NωV assembly through subunit dimer association. The colour change (from grey to purple) represents slight structural changes upon assembly into procapsids (Canady *et al.*, 2000).

Assembly of the procapsid initially involves the formation of AB and CD subunit dimers (Figure 1.7). These dimers further associate through their internal domains resulting in the procapsid shell. It is possible that the genomic RNA plays a role in

the assembly process by gathering the individual subunits and forming the dimers, which are believed to be essential during assembly. This mechanism is based on the refined structural data of NωV where genomic RNA is believed to interact with the internal domain offering the particle structural stability (Helgstrand *et al*., 2004).

1.1.8 The mechanism of capsid maturation

The proposed mechanism of capsid maturation by Canady *et al*. (2000) was based on X-ray solution scattering. The model proposed that arginine residues within the molecular switch have low pK_a values that become positively charged at an acidic pH. This causes the repulsion of arginine residues resulting in the bent A/B contacts between the two subunits (Canady *et al*., 2000). The transition causes a shift from the 3-fold axes to the quasi 2-fold axes resulting in the "shrinking" of the particle causing the trimeric associations.

Two mechanisms of cleavage have been proposed from the refined structure of NωV (Taylor *et al*., 2002; Helgstrand *et al*., 2004). The first proposes that when cleavage occurs, residues Thr 246 and Glu 103 position Asn 570 to enable the cleavage event (Figure 1.8, A and B). A succinimide intermediate is formed by the nucleophilic attack of the asparagine side chain on the carbonyl group (Figure 1.8, B). The ring structure is then opened by hydrolysis, forming either an iso-asparagine or asparagine intermediate at the *C*-terminus of the 62 kDa β-peptide. Cleavage of the γ-peptide does not occur if Asn 570 is replaced by threonine, glutamine or aspartic acid, indicating that asparagine is vital for the maturation process. Cleavage of the γ-peptide was shown to be essential for stabilising the mature capsid (Taylor *et al*., 2002).

The second mechanism of cleavage proposed that the aspartate and glutamate residues at the 2–fold bent contact may be important during the maturation of procapsids at low pH (Helgstrand *et al*., 2004). A number of acidic residues (Asp 83, Asp 85, Asp 87, Glu 110 and Asp 124) exist at the surface of the A subunit in the flat contact between C and D subunits. These interact with the *N*-terminus in the subunit. At an acidic pH of 6.5, an expansion above the pI of the residues results in a charge repulsion causing the bent contact to form (Helgstrand *et al*., 2004; Bothner *et al*.,

2005). The maturation models indicate that an acidic pH is required for cleavage to occur by allowing the normally hydrophobic *N*-terminal regions of the subunits to interact (Helgstrand *et al*., 2004).

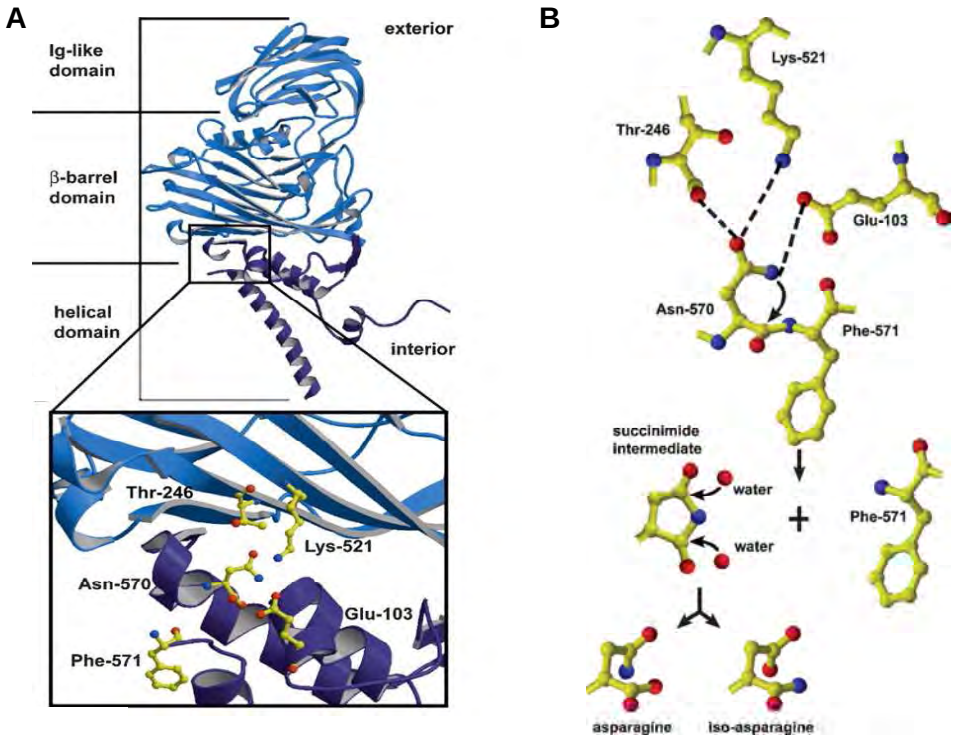

Figure 1.8 Side view of a NωV A subunit (**A**) and mechanism of Asn 570/Phe 571 cleavage in the helical domain (**B**). The inset in (**A**) depicts residues in the helical domain where cleavage occurs (Taylor and Johnson, 2005).

Taylor *et al*., (2002) proposed that during cleavage, the irreversible transition of a helix to coil was induced by an acidic pH within the helical domain. The change from a helix state to a coil state occured upon lowering the pH from 7.6 to 5.0 at residues 1 to 44 and 571 to 644 (Figure 1.9). The model proposed that at a pH of 5.0 the helix transformed into a coil resulting in cleavage of the γ-peptide causing the coils to migrate to the centre of the particle (Figure 1.9, compare A to C). In this state the process is irreversible and if the pH is raised to 7.4 the coil reverts back to helices, but the particle resembles a capsid (Figure 1.9, D). If cleavage does not occur at pH 5 the process is reversible (Figure 1.9, B).

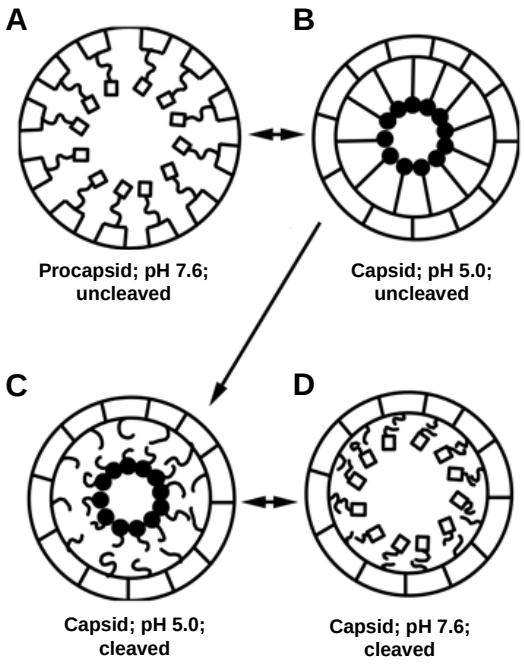

Figure 1.9 Schematic representation of the helix ( ) to coil (•) transition of the NωV particle from a procapsid state at pH 7.6 to a capsid state at pH 5.0 See text for details (Taylor *et al*., 2002).

1.1.9 RNA and assembly

Baculoviral-derived expression of the NωV capsid encoding sequence (*P70*) in a *Spodoptera frugiperda* 21 (Sf 21) cell line resulted in the assembly of NωV VLPs, which represented native virions (Agrawal and Johnson, 1995). The VLPs specifically encapsidated their own message, indicating that the NωV particles do not require full length genomic RNA1 or RNA2 for assembly. These authors concluded that the specific manner in which *P70* mRNA was encapsidated indicated that the capsid-encoding sequence may contain an encapsidation signal. Similarly expression of HaSV RNA1, RNA2 and *P71* in plant protoplasts resulted in the assembly of VLPs that had the ability to encapsidate their capsid-encoding message and RNA1 (Gordon *et al*., 2001). The encapsidation of the viral RNA in the VLPs implied that viral RNA was importantant during the assembly process. This is interesting to note because viral RNA has been observed to interact with the highly positively charged γ-peptide (Helgstrand *et al*., 2004). Viral RNA has been hypothesised to stabilise the

virus particle during maturation through the neutralisation of the particle interior (Agrawal and Johnson, 1995; Taylor *et al*., 2002).

The replication and RNA encapsidation strategy of the *Nodaviridae* (a virus family which also infects insects) is well understood and offer important clues for studying the *Tetraviridae* (Venter *et al*., 2005; Schneemann, 2006; Venter and Schneemann, 2007).

1.2 THE *NODAVIRIDAE*

The *Nodaviridae* are a family of non-enveloped icosahedral bipartite (+) ss RNA viruses which are 29 to 39 nm in diameter with a *T*=3 quasi-equivalent symmetry (Fauquet *et al*., 2005). The family consists of two genera; the *Alphanodaviridae*, which predominately infect insects and the *Betanodaviridae*, which infect fish (reviewed in Ball and Johnson, 1998). The two genera are classified by the hosts they infect, their serological relatedness and their structural and genomic characteristics (van Rogenmortel *et al*., 2000). The alphanodaviruses include the type member *Nodamura virus* (NoV) and FHV for which the replication systems have been well characterised (Ball and Johnson, 1998). The alphanodaviruses have been shown to replicate in a number of organisms, which include yeast, insects, mammals and plants (Garzon *et al*., 1990; Selling *et al*., 1990; Ball *et al*., 1992; Price *et al*., 1996; Dasgupta *et al*., 2001; Dasgupta *et al*., 2003; Price *et al*., 2005; Dasgupta *et al*., 2007). More importantly, the yeast *Saccharomyces cerevisiae* has been shown to support robust FHV and NoV replication, with the replicated genomic RNA approaching ribosomal RNA levels (Price *et al*., 1996; 2005). For the scope of this thesis the review of the literature will focus on NoV, FHV and BBV.

1.2.1 Genomic organisation.

Like the omegatetraviruses, the nodaviruses have a bipartite genome consisting of two ss (+) RNA molecules; RNA1 and RNA2 (Dearing *et al*., 1980; Scotti *et al*., 1983). Both RNAs are capped at their 5’ ends, co-packaged in the viral shell and are non-polyadenylated (Dasgupta *et al*., 1984; Krishna and Schneemann, 1999).

The large genomic segment of FHV (RNA1) is 3107 nucleotides in length and encodes 3 ORFs designated proteins A, B1 and B2 (Figure 1.10). Protein A, the replicase, is 998 amino acids in length with a predicted molecular weight of 112 kDa (Dasgupta *et al*., 1994). The replicase was shown to form its own group (group 2) in the classification scheme according to Koonin *et al*., (1992). The RNA1 sequence of BBV is 3106 nucleotides in length and also encodes a 998 amino acid replicase with a predicted molecular weight of 101 kDa (Dasmahapatara *et al*., 1985). The two smaller ORFs are translated from a subgenomic RNA, RNA3, (which is approximately 390 nucleotides in length) with predicted M_Rs of 10.8 kDa and 11.6 kDa for B1 and B2 respectively (Figure 1.10). RNA3 corresponds to nucleotides 2719-3107 of RNA1 with the ORF for protein B1 overlapping the ORF for protein A. Protein B1 has an unknown function. Protein B2 has been shown to be involved in inhibiting RNA interference in NoV (Sullivan and Ganem, 2005) and FHV (Li *et al*., 2002; Chao *et al*., 2005) and facilitating viral RNA accumulation in NoV (Johnson *et al*., 2004).

FHV RNA2 is 1400 nucleotides long and encodes the capsid precursor protein, α (44 kDa) (Friesen and Rueckert, 1981; Gallagher and Rueckert, 1988). During assembly 180 copies of protein α associate to form the procapsid. The procapsid is autoproteolytically cleaved to yield the mature protein, β (39 kDa) and the γ-peptide (4.4 kDa) (Gallagher and Rueckert, 1988; Schneemann *et al*, 1992). The NoV and BBV RNA2 is 1335 and 1399 nucleotides in length respectively (Dasgupta *et al*., 1984; Dasgupta and Sgro, 1989). Protein α, the capsid precursor protein, is 407 and 399 amino acids in size for BBV and NoV respectively.

The 3' end of BBV RNA1, RNA2 and FHV RNA2 fold into a stem-loop structure. This differs from the tRNA-like structure of the omegatetraviruses (Dasgupta *et al*., 1984; Kaesberg *et al*., 1990; Hanzlik *et al*., 1995). While the tRNA-like structure has no known function, it has been hypothesised that it may have a function in virus replication (Kaesberg *et al*., 1990; Hanzlik *et al*., 1995).

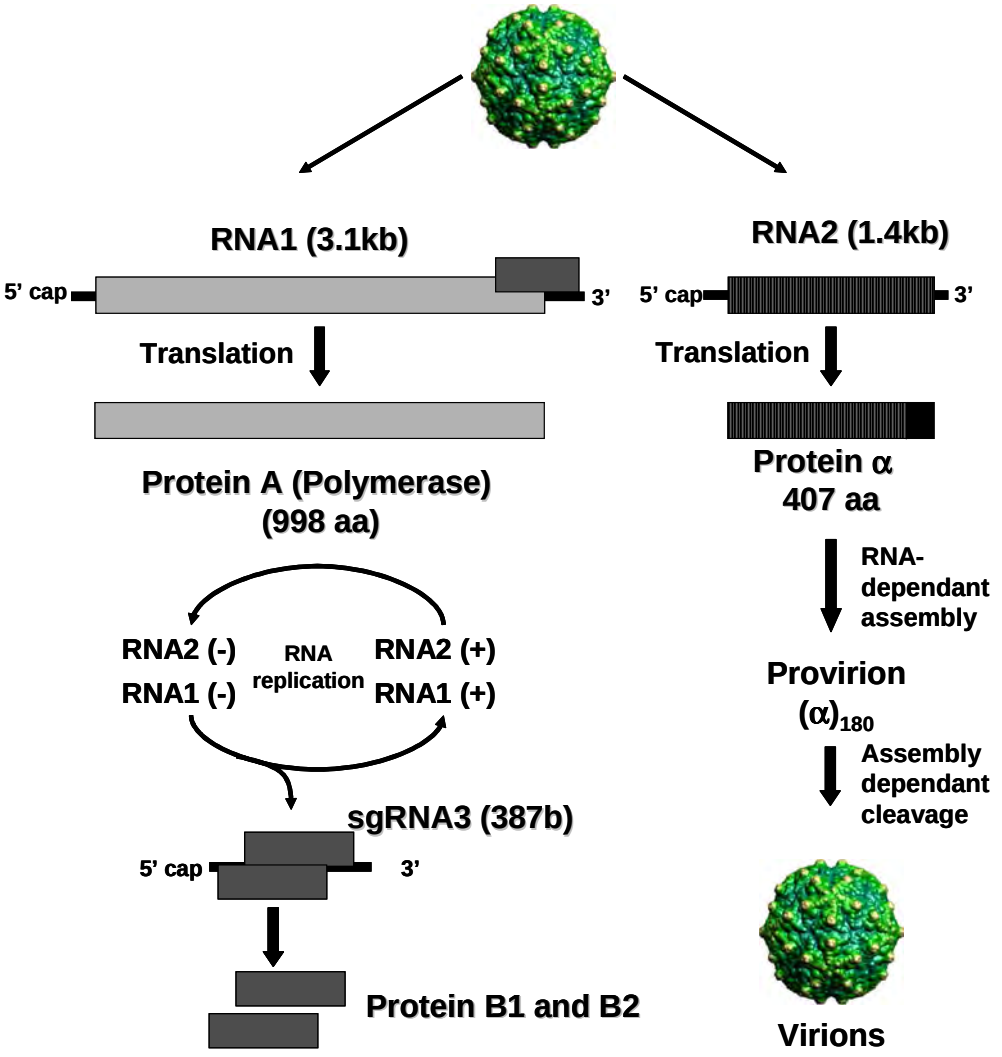

Figure 1.10 Schematic representation of the genome organisation and replication strategy for FHV (adapted from van Rogenmortel, 2000 and Ball and Johnson, 1998). The FHV particle depicted was taken from the Viper database (http://viperdb.scripps.edu/info_page.php?VDB=fhv).

1.2.2 RNA replication

FHV replication occurs on the outer mitochondrial membranes in *Drosophila* cells, with replication resulting in major structural changes (Miller *et al*., 2001). Later during infection spherules are formed, which encompass the replicating virions, and the matrix swells. The major protein encoded from RNA1, protein A, contains a mambrane localisation signal (Miller and Ahlquist, 2002). The protein is the RNA polymerase, which has the ability to replicate RNA1 *in trans* (Gallagher *et al*., 1983;

Ball, 1995). During the replication cycle the RdRp binds to the 3' end of the (+) RNA1 and uses it as a template for (-) RNA1 synthesis (Figure 1.10). The RdRP then binds to the 3' end of the negative sense RNA1 strand, synthesizing (+) RNA1. RNA3 is in turn believed to be synthesized from RNA1 through either an internal transcription mechanism or a termination mechanism (Zhong and Ruekert, 1993). The internal transcription mechanism involves the initiation of (+) RNA3 synthesis from an internal site in the (-) RNA1. The termination mechanism describes that as (-) RNA1 is synthesised, premature termination occurs producing a (-) RNA3. This negative strand is then used as a template for (+) RNA3 synthesis. The replication of RNA2 occurs in the same way as RNA1. RNA1 can regulate the synthesis of RNA3 and the replication of RNA2 through interaction (Lindenbach *et al*., 2002). Replication of RNA1 is dependent on an intact RNA3 3' end and RNA3 has the ability to regulate RNA2 replication (Albarino *et al*., 2003; Eckerle *et al*., 2003). The replication of RNA2 down-regulates the production of RNA3 (Zhong and Rueckert, 1993). Extensions at the 5' and 3' ends of the genomic RNAs were shown to abolish replication (Ball and Li, 1993; Ball, 1995). The regions on RNA1 and RNA2 which are important during replication will be discussed in chapter 4.

1.2.3 Nodavirus capsid structure

The nodaviruses form their capsid shell from three subunits corresponding to the same gene product, which are in slightly different conformations A, B, and C (Figure 1.11, A). Each of the 60 capsid faces are composed of three trimers A, B and C. The *T*=3 particle is related at the 5-fold axis by A subunits and B/C subunits at the three fold axis (Johnson, 1996). At the two icosahedral two-fold axes, one relates two C subunits and the other A/B subunits. The two C subunits form a flat contact while the A/B subunits form a bent contact of 144° (Figure 1.11, B). The genomic RNA interacts with or lies between the two C subunits at the flat contact offering the subunits stability (Fisher and Johnson, 1993). Cleavage of the γ–peptide occurs at the C/C contacts, forming the flat and bent contacts (Johnson, 1996).

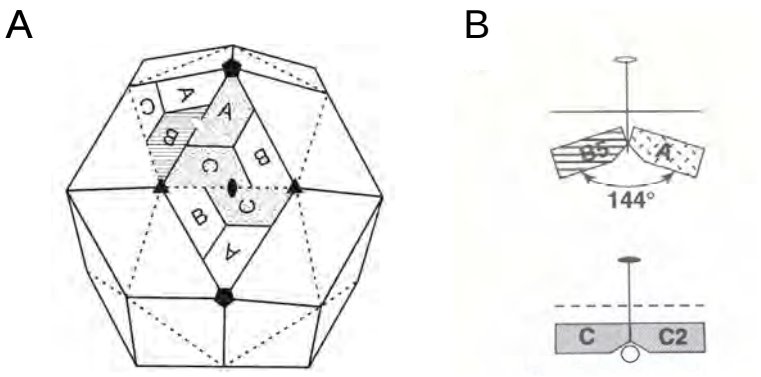

Figure 1.11 Diagrammatic representation of the *T*=3 quasi-equivalent particle. (**A**) The quasi 2-fold, 3-fold and 5-fold axis are depicted as solid eclipses, triangles and pentagons respectively. (**B**) The flat and bent contacts occurring at the 2-fold axis between two C and the A/B subunits respectively (Taken from Johnson, 1996; Johnson and Reddy, 1998).

The structures of both BBV and FHV have been determined by X-ray crystallography at a resolution of 3.0 Å (Hosur *et al*., 1987; Fisher and Johnson, 1993). Like NωV, each capsid subunit consists of an internal helical domain and a β-sandwich domain (Figure 1.12, A and B). However, the two structures differ from each other in that the NωV subunit has an external Ig-like domain (Munshi *et al*., 1996) while in the nodaviruses, this domain is a continuation of the β-sandwich domain, formed by three β sheets. In the nodaviruses this domain is proposed to be the receptor binding domain (Hosur *et al*., 1987; Dasgupta *et al*., 1994; Wery *et al*., 1994). Like NωV, the nodavirus β-sandwich domain consist of eight anti-parallel β sheets designated βB, βC…etc to βI (Rossmann and Johnson, 1989).

The internal domain of the nodaviruses consists of 3 helices named helix I (residues 61 to 73), helix II (residues 341 to 353) and helix III (residues 365 to 379) (Figure 1.12, A; Hosur *et al*., 1987). Helix II and helix III are cleaved during autoproteolytic cleavage between Asn 363 and Ala 364 releasing helix III that is referred to as the γ-peptide. The contacts between the genomic RNA occur at helix I and the γ-peptide (Fisher and Johnson, 1993).

1.2.4 Nodavirus assembly

Schneemann *et al*. (1994) demonstrated that FHV capsid assembly begins with genomic RNA interacting with individual capsid subunits. These interactions enable the rapid formation of the viral capsid. The function of RNA in the assembly process was proposed to be both structural and physical. RNA could recruit individual subunits into the assembly process and either chaperone these subunits into a stable conformation or act like a scaffold bringing the individual subunits together (Schneemann *et al.*, 1994; Schneemann, 2006). In so doing the RNA could associate different subunits together, ensuring the highly compact nature of the RNA in the interior of the particle.

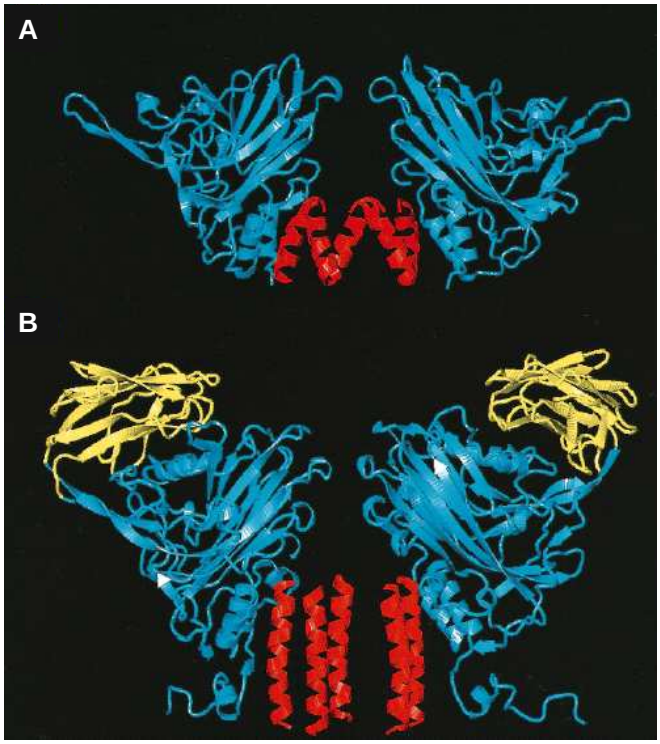

Figure 1.12 Structural similarity between the capsid subunits of BBV and NωV. Side view of the 5-fold axis between the BBV (**A**) and NωV (**B**) subunits, showing the similarity between the β-sandwich domains (blue). The γ-peptides are shown in red and the Ig-like domain (yellow) in NωV was not present in BBV (Taken from Munshi *et al*., 1996).

A more model proposed by Larson and McPherson (2001) and reviewed by Schneemann (2006) for *Satellite tobacco mosaic virus* (STMV), suggests that the viral RNA is packaged while it is being synthesised. In this way the packaging of the

genome is controlled and energetically efficient producing a stable icosahedral structure (Schneemann, 2006). Because of the stability offered by this mechanism, the uncoating and re-folding of the viral genome during translation and transcription is thought to be feasible (Schneemann, 2006).

1.2.5 Nodavirus maturation

In FHV cleavage of the γ-peptide is assembly-dependent (Schneemann *et al.*, 1992). The proposed cleavage mechanism of the nodaviruses during maturation is believed to involve the protonation of Asp 75, which in turn causes the polarization of Asn 363 (Figure 1.13; Zlotnick *et al.*, 1994; Johnson and Reddy, 1998). This protonation makes Asn 363 more susceptible to nucleophilic attack by a water molecule. This leads to the formation of a tetrahedral intermediate causing the loss of an amide group and leading to the generation the γ-peptide and the *N*-terminal peptide (Zlotnick *et al.*, 1994).

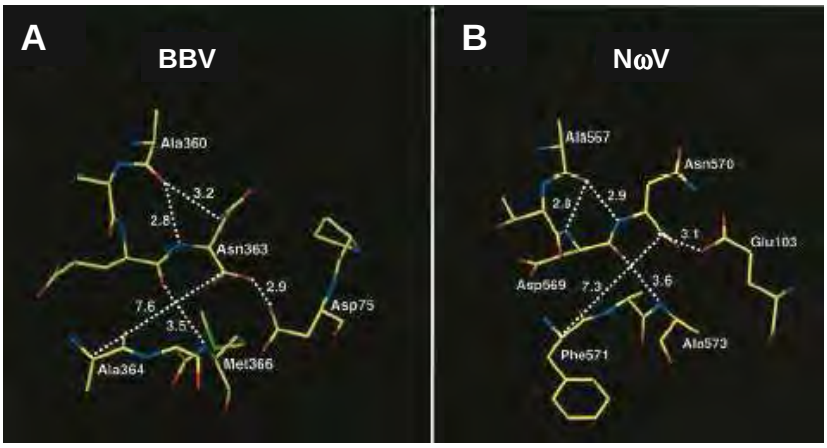

Figure 1.13 Similarity between the cleavage sites of BBV (**A**) and NωV (**B**). Cleavage of the γ-peptide in BBV and NωV occur between Asn 363-Ala 364 and Asn 570-Phe 571 respectively. The mechanism of cleavage between the two viruses is strikingly similar. The hydrophobic nature of the cleavage region leads to the protonation of Asp 75 (BBV) or Glu 103 (NωV). This results in positioning Asn 363 (BBV) or Asn 570 (NωV) in such a way that they are more susceptible to nucleophlic attack by a water molecule leading to cleavage of the γ-peptide. The dotted lines represent hydrogen bonding distances (Munshi *et al.*, 1996).

Viral RNA has been shown to be important in capsid assembly and maturation in the *Nodaviridae* (Schneemann *et al.*, 1992; Fisher and Johnson 1993; Schneemann *et al.*,

1994; Zontnick *et al*., 1994; Schneemann and Marshall, 1998). The mechanisms used by these viruses has provided insight into the complex nature by which RNA and the capsid protein interact during the assembly of (+) ss RNA insect viruses. X-ray crystallographic analysis of the FHV and BBV capsids shows the genomic RNA as an integral component of the viral shell. The RNA controls the interactions between subunits at the two-fold symmetrical axes (Figure 1.14). The amino acids that interact with the sugar phosphate backbone of the RNA in FHV are conserved glutamine (Glu 61) and lysine residues (Lys 68, 371 and 375) (Fisher and Johnson, 1993; Wery *et al*., 1994; Schneemann and Marshall, 1998). This interaction is thought to position the RNA correctly between subunits, such that optimal protein-protein contacts can form (Schneemann and Marshall, 1998).

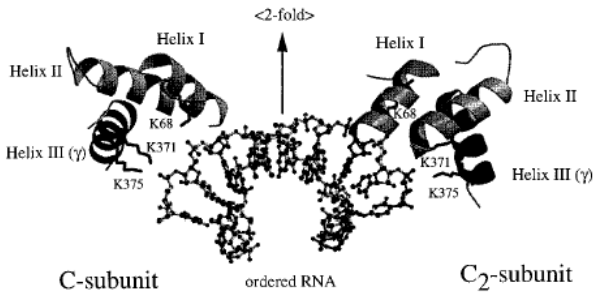

Figure 1.14 Interaction between the viral RNA and internal helical regions in FHV. Organization of the γ-peptides at the 2-fold axis in the FHV particle and their interactions with genomic RNA (Schneemann and Marshall, 1998).

The RNA also lies in close association with the Asn–Phe cleavage site indicating that RNA–protein interaction may not only be important for assembly, but also in the maturation of the virus particle (Schneemann and Marshall, 1998). The viral RNA has been proposed to polarize water molecules that allow nucleophilic attack of the carbonyl group at the cleavage site (Cheng *et al*., 1994). Furthermore, deletions of residues 2-31 from the *N*-terminus of FHV coat protein interfered with its ability to recognize RNA2 (Marshall and Schneemann, 2001).

Using crystallography and cryoEM analysis, Tang *et al* (2001) later resolved the structure of another nodavirus, *Pariacoto virus* (PaV) (Figure 1.15). They showed that RNA was in close association with the inner surface of the protein shell. The RNA is a structural component of the viral shell, which forming a highly ordered

dodecahedral cage of duplex RNA (representing 35% of the total genomic RNA) through interactions with the capsid at the two-fold and three-fold axes. The amino acids involved are twelve arginine and lysine positioned between residues 7 and 43 of the coat protein subunits. The other 65% of the RNA is packaged within the interior of the particle. Similarly, cellular RNA has been shown to form a highly ordered structure in FHV and PaV VLPs, indicating that nodavirus capsids can encapsidate heterologous RNAs which are compatible (Johnson *et al.*, 2004; Tihova *et al.*, 2004). The degree of plasticity displayed by these capsids is difficult to determine. It is assumed that the genomic RNA would be preferentially packaged if it is available, which means the viral RNA must have a function in maintaining stability within the particles.

Figure 1.15 Cryo-EM reconstruction of a section through a PaV virus particle revealing the dodecahedral cage of duplex RNA (Tang *et al.*, 2001).

1.2.6 RNA encapsidation in the nodaviruses

The two genomic RNA molecules in the nodaviruses are co-packaged in equimolar concentrations (Krishna and Schneemann, 1999). The exact mechanism of RNA encapsidation has until recently been poorly understood. The ability of baculoviral-derived PaV and FHV VLPs to encapsidate a mixture of highly ordered cellular and genomic RNA indicates that the packaging mechanism of viral RNA may be random (Johnson *et al.*, 2004; Tihova *et al.*, 2004). Venter *et al.* (2005) demonstrated that the packaging of viral RNA in FHV was coupled to replication and that encapsidation of RNA1 was dependent on the replication of RNA2. However, encapsidation of RNA2 was not dependent on the replication of RNA1. Further evidence for replication-dependent encapsidation was provided by the assembly of two distinct

populations of FHV VLPs from replicating and non-replicating coat protein (Venter and Schneemann, 2007). Virus particles which were purified from replicating coat protein templates had the ability to specifically encapsidate RNA1 and RNA2. In contrast VLPs purified from non-replicating templates encapsidated mostly cellular RNA. In the absence of replication, FHV VLPs package random cellular RNAs, presumably due to insufficient amounts of RNA produced by transcription as opposed to replication (Venter and Schneemann, 2007). The advantage of replication-dependent RNA encapsidation ensures that there is a high initial concentration of viral RNA, which can interact with the capsid subunits in the vicinity of one another (Venter *et al.*, 2005). In this way the replicating viral RNA and synthesis of capsid protein occur within a "microenvironment" in the cell.

1.3 PROJECT PROPOSAL

The tetraviruses are some of the genetically simplest ss (+) RNA viruses, but studying these viruses has proved to be a challenge. PrV was the only tetravirus shown to replicate in a *Helicoverpa zea* cell line (Pringle *et al*., 2003) and HaSV failed to replicate in 13 different insect and 1 mammalian cell line (Bawden *et al*., 1999). Expression of HaSV *P71* and the capsid encoding sequence of PrV, in a bacterial expression system, resulted in formation of insoluble aggregates (Hanzlik *et al*., 1995; Taylor *et al*., 2005). A similar result was obtained when HaSV RNA1 and RNA2 were transfected into plant protoplasts. No replicating virus was detected, but the authors did speculate that p71 had the ability to assemble *in vivo* (Gordon *et al*., 2001). Venter (2001) exploited the possibility of using the yeast *S. cerevisiae* to produce authentic HaSV VLPs by expressing the capsid encoding sequence (*P71*) with the genomic RNAs using P_{GAL1}. There was some evidence that infectious virus was produced and VLPs had the ability to assemble, but the system was largely inefficient.

In contrast when the capsid encoding sequence of NωV (*P70*) or the full length genomic RNA of TaV were expressed using a baculoviral expression system in a Sf 21 cell line, VLPs were detected (Agrawal and Johnson, 1995; Pringle *et al*., 2001) and in the case of NωV shown to encapsidate their own *P70* mRNA (Agrawal and Johnson, 1995). This system was extensively and successfully used to study the

assembly and maturation of NωV *in vitro* by cryoEM and crystallographic reconstruction (Munshi et al., 1996; Canady *et al*., 2000; 2001; Taylor *et al*., 2002; Helgstrand *et al*., 2004; Bothner *et al*., 2005). From all the data generated from the *in vitro* studies, little is known about how the omegatetraviruses assemble and mature *in vivo*.

The aim of the research presented in this thesis was to develop an alternative expression system in the yeast *S. cerevisiae* to produce substantially higher levels of capsid protein. This system was then used to study VLP assembly and RNA encapsidation.

CHAPTER 2. ASSEMBLY OF HaSV VLPs IN YEAST

CHAPTER 2. ASSEMBLY OF HaSV VLPs IN YEAST

2.1 INTRODUCTION

Yeast cells have been successfully used as a non–host system for the production of several different types of VLPs including *Hepatitis B virus* surface antigen particles (Valenzuela *et al*., 1982; Fu *et al*., 1996), *Hepatitis delta virus* (Wu *et al*., 1997), polio subviral particles (Rombaut and Jore, 1997), *Human papillomavirus* (Hofmann *et al*., 1995; 1996; Neeper *et al*., 1996) and *Influenza A virus* non–structural protein NS_1 (Ward *et al*., 1994). From here forward yeast will refer to *S. cerevisiae* because there is no mention of another strain.

The coding sequence of the HaSV capsid precursor (*P71*) was expressed via the *GAL1* promoter on a multicopy plasmid or from a single copy of the *P71* gene under control of the same promoter inserted on the chromosome (Venter, 2001). The presence of p71 was detected and a small amount of immature VLPs were purified. These VLPs appeared to mature *in vitro* at pH 6.5. However, Venter (2001) was unable to confirm the presence of VLPs by TEM due to the low levels of VLPs he was able to purify. He concluded that the system was permissive to VLP production, but inefficient. Thus an alternative system was required to study assembly and maturation of HaSV VLPs in yeast. Venter (2001) suggested that an increase in the levels of transcription of *P71* mRNA might result in more efficient VLP assembly. Venter (2001) concluded this from the observation that higher concentrations of NωV capsid precursor mRNA (*P70*) were expressed from insect cells infected with baculovirus vectors and this mRNA could be encapsidated (Agrawal and Johnson, 1995). The polyhedrin promoter used for the baculoviral–derived expression is a strong promoter, which drives the expression of the desired protein such that it constitutes 25–50% of the total cellular protein (Miller, 1988). This is in direct contrast to P_{GAL1}–dependent expression that drives expression of the protein of interest such that it constitutes 0.3 to 1.5% of total yeast protein (Johnson, 1987).

The alcohol dehydrogenase-2 (*ADH2*) promoter has been the promoter of choice for the expression of many heterologous proteins (Price *et al*., 1990, Romanos *et al*., 1992; La Grange *et al*., 1996; Ramjee *et al*., 1996). The amount of P_{ADH2}-derived

protein can represent up to 1% of soluble cellular protein (Price *et al.*, 1990). The promoter is repressed several hundred fold in the presence of glucose and is referred to as de-repression (Price *et al.*, 1990; Verdone *et al*, 1996; 1997). The method of P_{ADH2} expression is uncomplicated and involves the depletion of glucose in the growth medium (Price *et al.*, 1990; Donoviel *et al.*, 1995; Verdone *et al*, 1996, 1997; Görgens *et al.*, 2001) or the induction of the promoter by incubation in a non-fermentable carbon source (i.e. ethanol) (Denis *et al.*, 1982).

A hybrid promoter with dramatically increased levels of transcriptional activation has been created. This was achieved by fusing the 5' end of the *ADH2* promoter, containing the 22 bp dyad sequence (important for *ADH2* de-repression) and placing it approximately 320 nucleotides from the glyceraldehyde-3-phosphate dehydrogenase (*GAPDH*) TATA element (see Appendix 3 for the entire sequence). In this way Cousens *et al*. (1987) believed that the hybrid promoter, $P_{ADH2\text{-}GAPDH}$ (P_{GADH}) increased expression levels above that of the *ADH2* promoter alone. However, transcription was still repressed in the presence of glucose and was still induced by glucose depletion or growth in ethanol.

The hybrid promoter was able to support the production of 100 mg/L of superoxide dismutase (SOD)–proinsulin in yeast (Cousens *et al.*, 1987). Expression of the protein using this promoter represented more than 15% of total cellular yeast protein, which is substantially higher than the maximum reported for P_{GAL1} (1.5%) or P_{ADH2} (5%) (Johnson, 1987; Shuster, 1989). The number of mRNA copies transcribed from this hybrid promoter can be greater than 50 per cell, which is in contrast to mRNAs in yeast that are present at 1 or 2 copies per cell (Cousens *et al.*, 1987; Johnson, 1987; Shuster, 1989; Wodicka *et al.*, 1997).

This chapter describes the construction and optimisation of a HaSV *P71* expression system based upon the *ADH2-GAPDH* promoter (P_{GADH}). The effect of increased expression levels on VLP assembly was investigated and a possible *in vivo* maturation mechanism elucidated.

2.2 MATERIALS AND METHODS

2.2.1 Microbial strains and plasmids.

Recombinant plasmids were maintained in *Escherichia coli* DH5α (Appendix 1; Table A1.1) or *E. coli* JM110 (Appendix 1; Table A1.1), which was used to prepare plasmids carrying methylated restriction sites. Plasmids were purified from *E. coli* cells using the Qiagen plasmid purification kit and the inserts sequenced using an Applied Biosystems 373A DNA sequencer.

Yeast strain INVScI (Appendix 1; Table A1.1; Invitrogen) was used for *P71* expression and VLP assembly studies described chapters 2 and 3. The HaSV capsid coding sequence, *P71* (pAV3; Figure 2.1) was obtained from P.A. Venter (Venter, 2001). The vectors pUC18 (Figure 2.1) and pGEMT-Easy (Promega) were used for sub-cloning of restriction fragments and PCR products. Plasmid pYES2 (Invitrogen) was used as the backbone for *P71* expression in yeast while plasmid pY2TG (Figure 2.1), which carried P_{GADH}, was obtained from Professor Laszlo Szilagyi (Department of Biochemistry at Eotvos Lorand University, Budapest, Hungary).

2.2.2 Microbial culture conditions

E. coli cells were grown in Luria-Bertani broth (LB) or on LB agar (Sambrook *et al.*, 1989) plates at 37°C with the relevant antibiotic for plasmid selection (Appendix 6). Competent *E. coli* cells were prepared using a $CaCl_2$ method. *E. coli* DH5α cells cultured on LA overnight at 37°C were inoculated into 5 mL LB broth and allowed to incubate for a further 16 hours at 37°C. Four 250 mL Erlenmeyer flasks containing 100 mL of LB were inoculated with 1.5, 1.0, 0.7 and 0.3 mL of the pre-inoculum, and incubated on an orbital shaker at 37°C for approximately 2 hours. When the optical density (OD_{600nm}) of the culture inoculated with the 1.5 mL pre-inoculum reached the mid–log phase of growth (OD_{600nm} = 0.6-0.8), all the flasks were cooled for 5-10 min on ice and the cells harvested by centrifugation at 5000 rpm for 10 minutes at 4°C in a Beckman JA–14 rotor (Beckman centrifuge T2-21). The pellets were re-suspended in 25 mL of buffer RF1 (100 mM KCl; 50 mM $MnCl_2$; 30 mM CH_3COOK; 10 mM $CaCl_2$; 15% glycerol (volume/volume) pH 5.8), followed by a further 20 minutes incubation on ice. The cultures, which were

inoculated with the 1.5 mL and 0.3 mL pre-inoculum and 1.0 mL and 0.7 mL pre-inoculum, were pooled. The cells were pelleted as described above and both pellets re-suspended in 4 mL buffer RF2 (10 mM MOPS; 10 mM KCl; 75 mM CaCl; 15% (weight/volume) glycerol pH 6.8). All the cultures were pooled, aliquoted and stored at -80°C.

YEPD [2% yeast extract (weight/volume), 1% peptone (weight/volume) and 2% glucose (volume/volume)] was used as the medium for preparation of the competent yeast cells. Competent yeast cells were prepared and transformed using the Frozen-EZ Yeast Transformation II Kit (Zymo Research). Transformations were plated onto SMM [0.17% (weight/volume) yeast nitrogen base (YNB) without amino acids or ammonium sulphate (DIFCO); 0.5% (weight/volume) ammonium sulphate] agar (1.5%) with 0.002% histidine, 0.002% tryptophan, 0.01% leucine and 2% glucose (volume/volume) (Kaiser *et al*., 1994). The plated cells were incubated at 28°C for 3 days. Colonies were patched onto fresh selective SMM agar plates and incubated at 28°C for an additional 2 days. Freshly transformed yeast cells were used for each experiment to ensure that the 2µ-based expression vector/s were not lost during subsequent cell divisions. All liquid cultures were incubated on an orbital shaker at 200 rpm.

2.2.3 Preparation of wild-type HaSV

Wild-type HaSV was purified from infected *H. armigera* larvae according to Hanzlik *et al*. (1993). Approximately 25 g of infected larvae, which were stored at -80°C, were homogenized in 50 mL of 50 mM Tris-HCl (pH 7.4) and filtered through cheesecloth. The homogenate was centrifuged at 9000 rpm in a Beckman JA-20 rotor for 30 minutes at 4°C. The supernatant was layered upon 4 mL of 30% sucrose [prepared in 50 mM Tris-HCl (pH 7.4)] and centrifuged at 23500 rpm for 3 hours in a Beckmann SW-28 rotor at 11°C. The supernatant was discarded and the pellet was allowed to re-suspend in 250 µL of 50 mM Tris-HCl (pH 7.4) at 4°C overnight. The virus suspension was then layered upon a 10-40% sucrose gradient [prepared in 50 mM Tris-HCl (pH 7.4)] and centrifuged at 40000 rpm in a Beckman SW-41 rotor for one hour and fifteen minute. The virus band was removed with a syringe and the

virus re-pelleted in a Beckman SW-41 rotor at 24150 rpm for 3 hours at 11°C. The pellet was allowed to re-suspend overnight in 100 μL of 50 mM Tris-HCl (pH 7.4).

2.2.4 Construction of *P71* expression vector, pMT9

The *GADH* promoter sequence used in the cource of this study varies from that published by Cousens *et al*., (1987). The 22 bp dyad sequence of the *ADH2* promoter is placed 101 bps from the TATA box of the *GAPDH* gene.

A 1443 bp *Hind* III fragment carrying the *GADH* hybrid promoter was excised from pY2Tg and inserted into pUC18 generating pAV16MT (Figure 2.1, Step I). Next, a 1026 bp *Bam* HI / *Pvu* II fragment from pAV3, which carries the 5' end of HaSV *P71*, was inserted into the *Bam* HI / *Sma* I site of pAV16MT, downstream of the *GADH* promoter sequence, generating pMT7 (Figure 2.1, Step II). The 236 bp sequence between the *GAPDH* translational start and the translational start of p71, was deleted by reverse PCR. At the same time an optimal Kozak sequence (Table 2.1) for efficient translational initiation was inserted using primers MT1 (Appendix 4; Table A4.1) and MT2 (Appendix 4; Table A4.1; Figure 2.1 Step III). In this was the *GAPDH* TATA box is placed 127 bps from the AUG of HaSV *P71*, placing the coding sequence in frame with the AUG of the *GAPDH* gene. The thermal cycling conditions are shown in Appendix 5, program 1. A 935 bp *Bcl* I / *Bgl* II fragment from the resulting plasmid (pMT8) was removed and inserted into pAV17 generating pMT9 (Figure 2.1 Step IV). Plasmid pMT9 is a multi-copy yeast expression vector for P_{GADH} –derived *P71* expression flanked by a *CYC1* (T_{CYC1}) terminator at the 3' end, a uracil 3 auxotophic marker (*URA3*) and a β-lactamase for ampicillin resistance.

2.2.5 *P71* expression in yeast

2.2.5.1 Comparison of P_{GAL1} versus P_{GADH}-derived *P71* Expression

Yeast cells transformed with pAV3 or pMT9 were grown on SMM agar plates supplemented with 0.002% histidine, 0.002% tryptophan, 0.01% leucine and 2% glucose (volume/volume) for three days at 28°C. The colonies were patched onto

fresh selective plates and incubated at 28ºC for an additional two days. Cells were scraped from the patches, re-suspended in a small volume of sterile triple distilled water and then inoculated into SMM with 0.002% histidine, 0.002% tryptophan, 0.01% leucine, 0.1% glucose and 5% glycerol (volume/volume) at an OD_{600nm} of 0.1. After 12 hours incubation at 28°C, 0.01% galactose was added to cells containing pAV3 for P_{GAL1} induction (galactose induction medium) and either no additional carbon source added (carbon-limiting medium) or ethanol added to a final concentration of 3% (volume/volume) to cells containing pMT9 for P_{GADH} induction.

Table 2.1 Comparison of the sequences surrounding the start codon of HaSV *P71* mRNA to the yeast translational initiation consequence sequence. The nucleotide which varies from the consensus is underlined.

Origin	**Sequence surrounding start codon**	**Reference**
S.cerevisiae consensus	Y A X A A U G U C U	Cigan and Donahue, 1987
P71 (pMT9)	A A C A A UG G G A	This study
P71 (pAV3)	C A C A A U G G G A	Venter, 2001

X = A/U
Y = A/C/T

2.2.5.2 Optimisation of growth conditions for P_{GADH} expression

To investigate the effect of glycerol on P_{GADH}–derived *P71* expression, cells containing pMT9 were patched as indicated above. The patched cells were scrapped off the plates re-suspended in a small volume of sterile triple distilled water and inoculated into SMM with 0.002% histidine, 0.002% tryptophan, 0.01% leucine and either 0.1% glucose (glucose-starvation medium) or 0.1% glucose and 5% glycerol (carbon-limiting medium). The culture was incubated at 28°C for up to 50 hours.

2.2.5.3 Growth conditions for apoptosis experiments

Cells containing pMT9 were patched as indicated before. The patched cells were scrapped off the plates and inoculated into a small volume of sterile triple distilled water. The cell suspension was inoculated into carbon-limiting medium as indicated and incubated at 28°C for 28 hours.

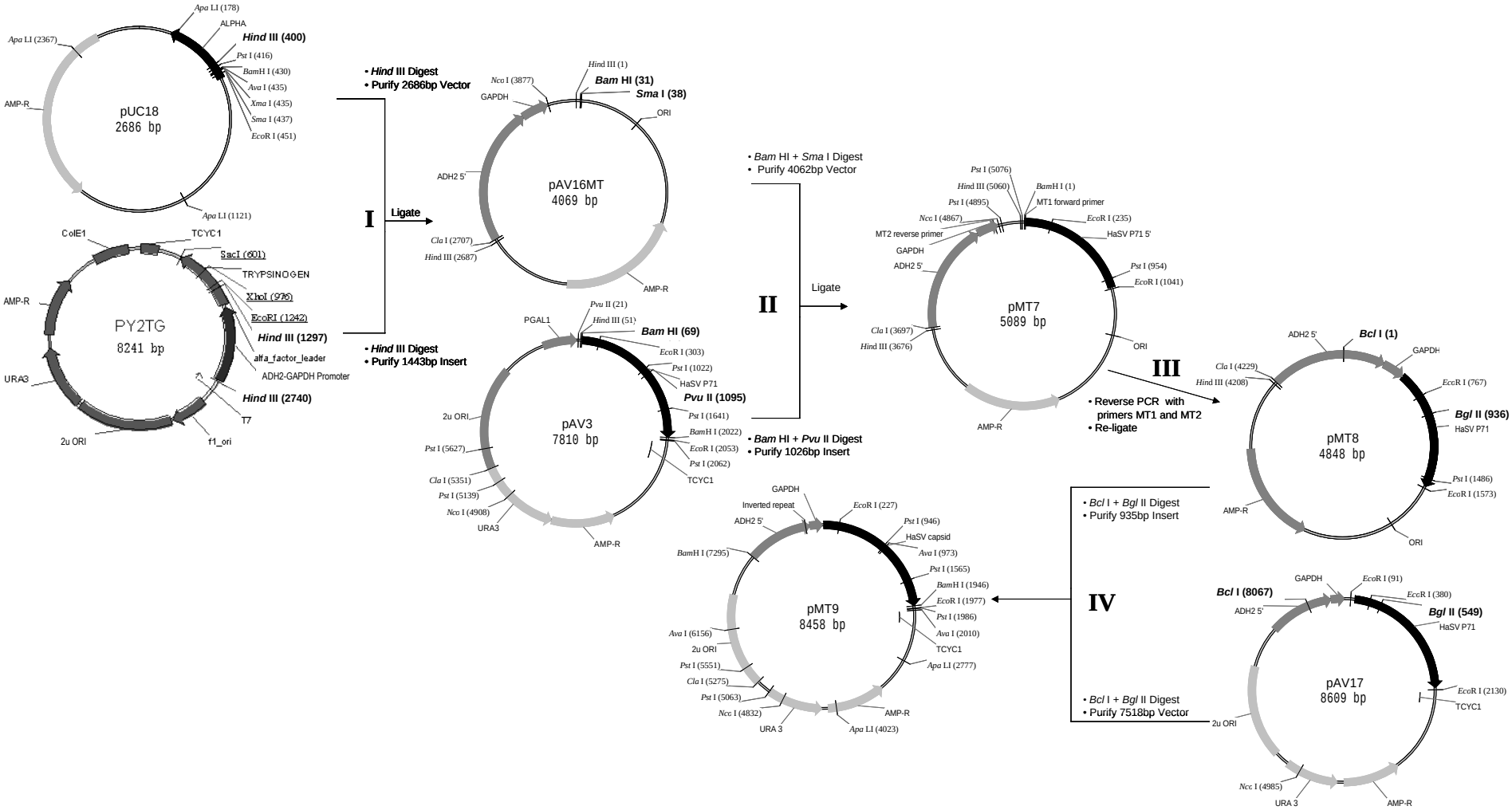

Figure 2.1 Diagrammatic representation of the process followed for construction of the yeast HaSV *P71* expression vector, pMT9. The restriction enzymes utilized for each cloning step are highlighted in larger font and the steps followed represented by Roman numerals The 5' end of the *ADH2* promoter and 5'end of the *GAPDH* untranslated region are represented by *ADH2* 5' and *GAPDH* respectively. HaSV *P71*, the capsid encoding sequence of HaSV (*P71*); TCYC1, *CYC1* terminator (T_{CYC1}); *AMP*-R, β-lactamase gene for ampicillin resistance; ORI, *E. coli* origin of replication; 2μ *ORI*, yeast origin of replication; *URA*3, uracil 3 auxotrophic marker.

2.2.6 Protein analysis

To monitor *P71* expression, two OD_{600nm} units of culture were removed, the cells harvested by microfuging at 2500 ×g for 5 minutes at 4°C, and the pellet re-suspended in 30 µL of extraction buffer (EB: 50 mM Tris-HCl (pH 7.4), 250 mM NaCl, 1 mM DTT, 1 mM PMSF, 1 µM Pepstatin A). The cells were lysed by homogenisation with 0.1 g of 0.2 mm acid-washed glass beads (Sigma) in 30 second intervals on ice, with a total time of 10 minutes. The yeast lysate was then diluted by addition of 60 µL EB and vortexed briefly. After vortexing the supernatant that represented the total yeast extract was collected with an autopipette and placed into a fresh eppendorf tube. For soluble yeast extracts, the total yeast lysates were microfuged at 15500×g for 5 minutes at 4ºC and the supernatant used directly for Western analysis.

The Bradford method was used to determine the protein concentration of samples (Bradford, 1976). Approximately 1 µg of total yeast protein was subjected to SDS-PAGE on a 7.5% polyacrylamide gel according to Laemmli (1970). Coomassie staining was used to confirm that equal concentrations of total yeast protein were loaded onto the polyacrylamide gel (Sambrook *et al*., 1989). Electrophoretic transfer to Hybond-C+ membranes (Amersham) and immunoblot processing was performed according to the manufacturers instructions (Amersham). A premixed unstained protein molecular marker (116-14 kDa; Fermentas) was used to determine the relative molecular mass of visualised protein bands. For Western analysis, the polyclonal antibody RB2 (Andrew Dinsmore, Syngenta, UK) specific for the HaSV virus was used as a primary antibody at a dilution of 3.5×10^5 to detect p71. The Roche Chemiluminescence Western Blotting Kit was used for immunodetection.

2.2.7 Induction and detection of apoptosis

The growth conditions for these experiments are described in section 2.2.5.3. Apoptosis was induced by the addition of either 80 mM acetic acid or H_2O_2 was added at varying concentrations between 0 and 180 mM. The cells were incubated for three hours and twenty minutes at 28ºC. To inhibit the onset of apoptosis,

cycloheximide was added to a final concentration of 15 μg/mL in conjunction with 80 mM acetic acid or 40 mM H_2O_2.

Terminal deoxynucleotidyl transferase (TdT)-mediated dUTP nick end-labelling (TUNEL) and 4,6-diamidino-2-phenylindole (DAPI) were used to test for apoptosis according to the method described by Madeo *et al* (1999) (Appendix 7, A7.1 and A7.2). In the TUNEL test, DNA fragments were end-labelled using the *in situ* Cell Death Detection kit, POD (Boehringer Mannheim). Yeast cells were fixed with formaldehyde, digested with lyticase (Sigma) and applied to a polylysine coated slide (MP biomedicals) (Adams *et al*., 1984; Appendix 7, A7.1). Cellular permeabilization, treatment of the cells with the TUNEL mixture and detection of peroxidase were carried out according to Madeo *et al* (1999). Three hundred cells were counted using an Olympus BX-60 reflected light microscope to determine the number of TUNEL positive cells. DAPI stained nuclei were viewed with an Olympus BX-61 fluorescence microscope. Cell viability was determined by staining with methylene blue (counting 1000 cells under the light microscope), or plate counts.

2.2.8 VLP purification

VLP purification was performed essentially according to the method described by Taylor *et al* (2002). Three litres of induced yeast cells were harvested at the appropriate time by centrifugation at 2500 ×g for 5 minutes at 4°C and the pellet re-suspended in 2 ml EB per gram wet cell mass. Cells were lysed with 0.2 mm acid-washed glass beads (Sigma) in a bead beater (Biospec Products), followed by centrifugation in a Beckman JA-20 rotor at 12500 rpm for 15 minutes at 4°C. The supernatant was layered on 4 mL of 30% sucrose, and centrifuged at 25000 rpm in a Beckman SW-28 rotor for 5.5 hours at 11ºC. The supernatant was discarded and the pellet re-suspended overnight in 100 μL EB at 4ºC. The VLP suspension was then layered on a 10-40% sucrose gradient followed by centrifugation at 40000 rpm in a Beckman SW-41 rotor for 75 minutes at 11ºC. Selected fractions were either collected by fractionation or the viral band was removed from the gradient with a syringe. Fractions, which had an absorbance at 260 nm, were pooled and centrifuged at 25000 rpm in a SW-28 rotor for 5.5 hours at 11ºC to pellet the VLPs. The

supernatant was discarded and the pellet re-suspended overnight in 100 µL EB at 4ºC. The purified VLPs were then used directly for Western or TEM analysis.

2.2.9 Electron microscopy

Virus particles were stained with 2% uranyl acetate according to the method of Dong *et al*., (1998) and viewed using a JOEL JEM-1210 electron transmission microscope**.** Approximately, 5×10^{11} virus particles representing 5 µL of the VLP suspension were placed on each copper coated grid.

2.3 RESULTS

Previously, Venter (2001) had shown that P_{GAL1}-derived expression of *P71* in yeast cells resulted in low concentrations of assembled VLPs, and the majority of p71 appeared to be insoluble. In contrast baculoviral expression of the same *P71* coding sequence resulted in more efficient VLP assembly (Mosisili, 2003). Since the levels of expression in the P_{GAL1} system are several orders of magnitude lower than those achieved from baculovirus promoters, it was decided to investigate the effect of a higher expression level on VLP assembly in yeast cells.

2.3.1 Construction of the *P71* expression vector, pMT9

An expression system based upon P_{GADH}, which activates transcription under glucose limiting conditions and is induced by the presence of ethanol in the growth medium, was selected. This promoter supports at least a 10-fold increase in RNA when compared to levels produced from P_{GAL1} (Denis *et al*., 1982). The expression vector, pMT9, which was derived from Venter's (2001) expression construct pAV3, is based on the multicopy expression vector pYES2 with a *URA3* auxotrophic marker and *CYC1* terminator (T_{CYC1}). However the P_{GAL1} promoter was replaced with the *GADH* promoter derived from the vector pY2Tg as described in the materials and methods (Section 2.2.4).

2.3.2 P_{GADH}-derived expression of *P71* in yeast

It has been reported that transcription from P_{GADH} is repressed several hundred-fold in the presence of glucose and induced when glucose is depleted from the growth media or when the cells are grown in glycerol or ethanol as carbon sources (Denis *et al*., 1982). Upon induction, the promoter can produce greater than 50 copies of the mRNA per cell (Shuster, 1989). To determine whether the P_{GADH} promoter would produce significantly higher levels of p71, cells containing pAV3 (P_{GAL}) or pMT9 (P_{GADH}) were initially grown in SMM supplemented with 0.1% glucose and 5% glycerol for 12 hours at 28°C. Galactose was then added at a concentration of 0.01% to cells containing pAV3. Cells containing pMT9 were either grown further without additional carbon (carbon-limiting) or in the presence of 3% ethanol. Cell free lysates were subjected to Western analysis to determine the level of *P71* expression

As observed previously by Venter (2001), p71 was detected in cells containing pAV3 4 hours after induction but after 12 hours no p71 was detected (Figure 2.2, lane 7 versus 16). In cells containing pMT9, p71 was detected immediately and was still present in cells after 26 hours, irrespective of whether cells were grown under carbon-limiting conditions or in medium containing ethanol (Figure 2.2 lanes 2 and 3 versus 17 and 18). There was a significant increase in the levels of p71 in cells carrying pMT9 as opposed to pAV3, in which *P71* expression was directed by P_{GAL1}. More importantly after 4 hours of incubation in carbon-limiting medium a band was detected which co-migrated with wild-type HaSV, indicating that the HaSV VLPs may be maturing in the yeast cells (Figure 2.2, lanes, 9, 12, 15 and 18). Induction of the hybrid promoter in carbon-limiting medium produced higher levels of p71 as opposed to when cells were incubated in the presence of 3% ethanol after 4 hours incubation (Figure 2.2). In the presence of ethanol, p71 levels appeared to decrease substantially after 12 hours (Figure 2.2, lanes 14 and 17), suggesting that the presence of ethanol in the growth medium might inhibit P_{GADH} –derived expression or result in increased levels of protein degradation. It was therefore decided to select the carbon-limiting growth medium for further optimisation, to increase the yield of p71.

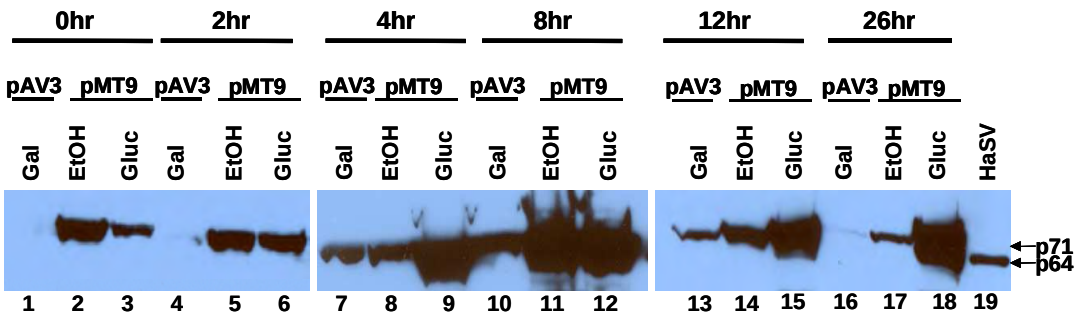

Figure 2.2 Comparison of P_{GAL1} versus P_{GADH}-directed *P71* expression levels. Western analysis of total yeast lysates, which were prepared from cells that were expressing *P71* under control of P_{GAL1} or P_{GADH}. Cells containing pAV3 (P_{GAL1}-derived expression of *P71*) or pMT9 (P_{GADH}–derived expression of *P71*) were initially incubated in SMM with 0.1% glucose and 5% glycerol for 12 hours at 28°C. For expression of *P71* cells were incubated in the presence of 0.01% galactose (Gal) for P_{GAL1} and either 3% ethanol (EtOH) or depletion of glucose in the growth media (Gluc) for P_{GADH}. The arrows indicate the position of bands migrating at an approximate molecular weight of 64 kDa (p64) and 71 kDa (p71), 1 ng of wild-type virus was loaded as a positive control (HaSV).

2.3.3 Optimisation of growth conditions for P_{GADH}-derived expression of *P71*

While glucose limitation induces P_{GADH} activity, low levels of carbon in the medium can also limit the amount of biomass produced and therefore, the yield of p71. It was important to characterise the growth of INVScI cells containing pMT9 to determine the general growth profile. Accordingly, yeast cells containing pMT9 were inoculated into medium containing various concentrations of glucose and the level of p71 production relative to cell growth determined.

When cells containing pMT9 were grown in the presence of 0.5, 1 or 1.5% glucose a significant higher concentration of biomass was produced, than when the cells were incubated in 0.1% glucose (OD_{600} = 2.3 in 0.5, 1 and 1.5% glucose versus OD_{600} =1.5 in 0.1% glucose; Figure 2.3, A). Cells grown in the different glucose concentrations had the same growth profile irrespective of the glucose concentration in the growth medium (Figure 2.3, A). Western analysis of yeast lysates after 24 and 39 hours showed that p71 was only expressed in cells grown in 0.1% and 0.5% glucose (Figure 2.3, B). Higher levels of p71 were produced when cells were incubated in a

glucose concentration of 0.1% compared to 0.5% and no p71 could be detected when cells were incubated in glucose concentrations of 1 or 1.5%. This most likely indicated that the glucose was significantly depleted in the medium, which contained 0.1% and 0.5% glucose to induce expression of the promoter.

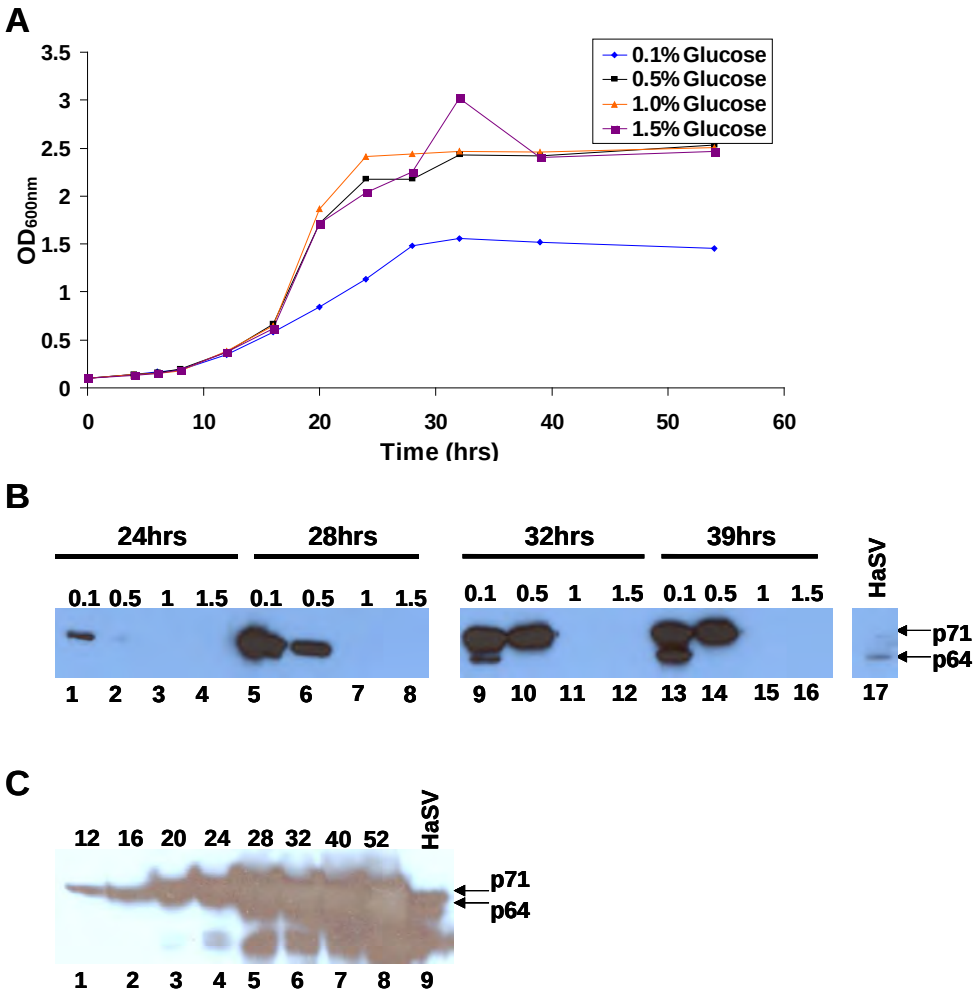

Figure 2.3 Growth and expression of *P71* in yeast cells. (**A**) Growth curve of yeast cells containing pMT9 incubated in SMM with various concentrations of glucose at 28°C. (**B**) Western analysis of selected total yeast lysates from cells expressing P_{GADH} –derived *P71* incubated in SMM with various concentrations of glucose. (**C**) Western analysis of total yeast lysates from cells expressing *P71* incubated in 0.1% glucose. The contrast in (**C**) was adjusted to make the protein bands clearer. Arrows indicate the position of bands migrating at an approximate molecular weight of 64 kDa (p64) and 71 kDa (p71). HaSV represents wild-type HaSV.

As the incubation time progressed a protein band, which co-migrated with wild-type HaSV could be detected when cells were grown in 0.1% glucose (Figure 2.3, B,

lanes 9 and 13). This was in direct contrast to when cells were grown in the presence of 0.5% glucose where only p71 was detected. Cells grown in 0.1% glucose produced the highest levels of p71 and it was important to determine if p71 had the ability to be expressed after 39 hours of incubation.

The increase in p71 levels as incubation time progressed and its presence after 52 hours of incubation (Figure 2.3, C) was in contrast to P_{GAL1}-derived expression, where p71 could not be detected after 12 hours post-induction (Compare Figure 2.2 with Figure 2.3, C). As observed previously, a protein which co-migrated with p64 after 32 hours of incubation was detected, which was possibly linked to glucose depletion or starvation in the cells (Figure 2.3, C, lane 6).

To determine if the appearance of p64 was dependent on glucose starvation, cells were grown in 0.1% glucose with (carbon-limiting) or without (glucose-starvation) 5% glycerol. If there was a link between starvation and p64 glycerol would prolong the growth phase of the cells and possibly delay the appearance of p64.

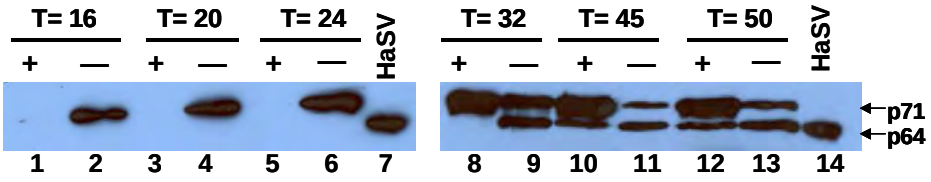

Figure 2.4 P_{GADH} –derived expression of HaSV *P71*in yeast cells. Western analysis of total protein extracts from P_{GADH}-derived expression of *P71*. Cells were incubated at 28°C in glucose–starvation (-) or carbon–limiting medium (+). Arrows indicate the position of bands migrating at an approximate molecular weight of 64 kDa (p64) and 71 kDa (p71). HaSV refers to wild-type HaSV used as a positive control.

High-level expression of p71 was detected after 16 hours of growth in glucose-starvation medium while p71 was detected only after 32 hours in cells grown in carbon-limiting medium (Figure 2.4). In both sets of cells p71 was still present after 50 hours (Figure 2.4, lanes 12 and 13) and as observed previously, a band co-migrating with the wild-type virus (p64) was detected after 32 hours growth in glucose-starvation medium (Figure 2.4, lane 9 compared with lane 14). In cells grown in carbon-limiting medium, a band co-migrating with p64 was observed after 45 hours (Figure 2.4, lane 10 vs lane 14). The appearance of p64 suggested the possibility that the VLPs were undergoing maturation cleavage.

2.3.4 Assembly and maturation of HaSV VLPs in yeast cells

To determine whether VLPs were assembling in the yeast cells, cells grown under glucose-starvation or carbon-limiting conditions were subjected to a VLP purification protocol. Selected fractions from sucrose gradients were examined for the presence of p71 and p64 by Western analysis. Both p71 and p64 were detected in the glucose-starved sample, but p64 was the major protein band (Figure 2.5, A, lane 1). Similarly both p71 and p64 were present in VLP samples prepared from carbon-limited cells, but here p71 was the major protein band (Figure 2.5, A, lane 2).

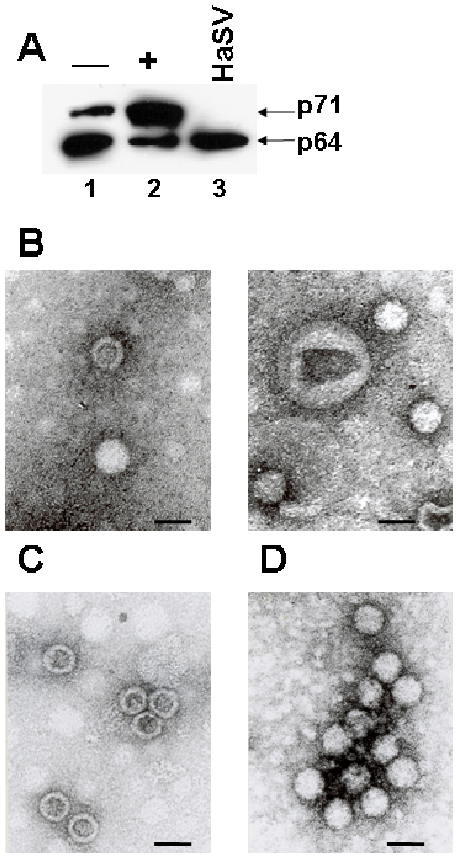

Figure 2.5 Purification of HaSV VLPs from yeast cells expressing *P71*. (**A**) Western analysis of VLPs purified from cells containing pMT9 incubated in SMM under glucose–starvation (-) or carbon–limiting conditions (+). Arrows indicate the position of bands migrating at an approximate molecular weight of 64 kDa (p64) and 71 kDa (p71). HaSV indicates wild-type HaSV. (**B**) Transmission electron micrograph of VLPs purified from cells expressing *P71*, incubated in SMM under glucose–starvation or (**C**) carbon–limiting conditions. (**D**) Wild-type HaSV. The bar represents 50 nm.

Transmission electron microscope (TEM) analysis revealed that both preparations contained two types of VLPs: a proportion of approximately 42 nm in diameter that were penetrable to the stain or 38 nm in diameter that were indistinguishable from wild-type HaSV (Figure 2.5). These virus particles are consistent with the presence of procapsids and mature capsids respectively. The proportion of procapsids to mature capsids correlated to the relative levels of p71 versus p64 observed by Western analysis. Mature capsids were predominant in the glucose-starved sample (Figure 2.5, B) while procapsids were in the majority in the carbon-limiting sample (Figure 2.5, C). These results confirmed that the presence of p64 indicated that the HaSV VLPs had the ability to assemble and mature in the yeast cells.

2.3.5 Induction of apoptosis results in spontaneous maturation of tetravirus procapsids *in vivo*.

The data presented thus far shows a correlation between the carbon (and therefore energy) status of yeast cells and the appearance of p64 as opposed to p71. It has been shown that nutritional starvation leads to programmed cell death (PCD) or apoptosis (Herker *et al*., 2004). This raises the possibility that the appearance of p64 could be linked to the onset of PCD in the yeast cells.

To determine whether the appearance of p64 and hence VLP maturation correlated with the onset of apoptosis, yeast cells expressing *P71* (pMT9) were grown in carbon–limiting medium for 28 hours to ensure the production of procapsids only, after which apoptosis was induced by adding either H_2O_2 or acetic acid. Cells were grown for a further 3 hours and 20 minutes. Both p64 and p71 were present in cells treated with acetic acid (Figure 2.6, A, lane 2) or H_2O_2 at concentrations of 40 mM and higher (Figure 2.6, A, lanes 10-13). In contrast only p71 was present in untreated cells (Figure 2.6, A, lanes 1 and 3) or when H_2O_2 was added at concentrations lower than 40 mM (Figure 2.6, A, lanes 4-6). The viability of the treated cells, determined by counting methylene blue-stained cells in a haemocytometer, was significantly lower than the untreated control (Figure 2.6, B). This data suggested that apoptosis might be correlating with VLP maturation of the procapsids *in vivo*.

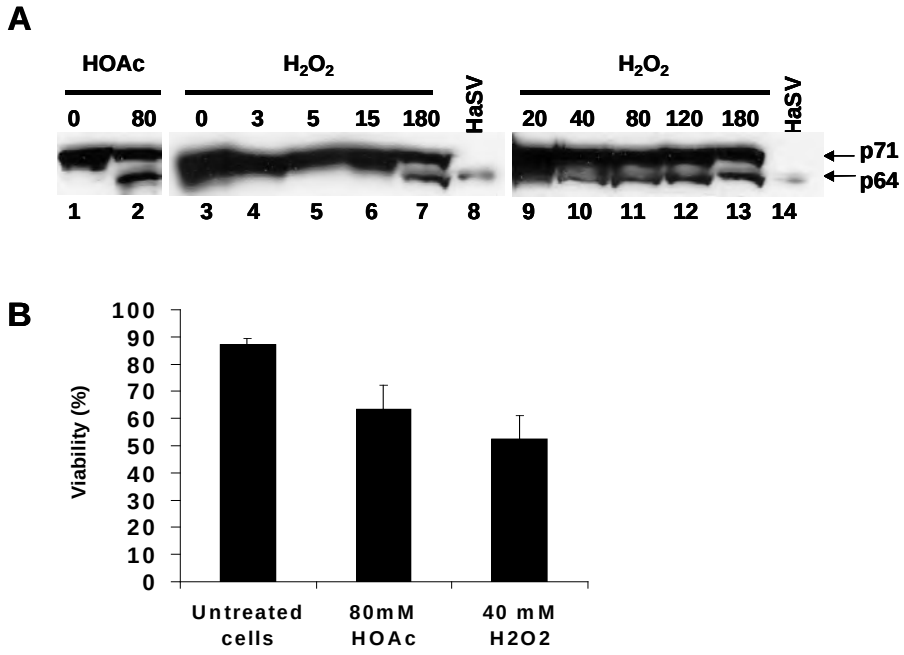

Figure 2.6 Induction of apoptosis and spontaneous maturation of HaSV VLPs *in vivo*. (**A**) Western analysis of crude protein extracts from cells expressing *P71* under control of P_{GADH} (pMT9) treated with either acetic acid (HOAc) or varying concentrations of H_2O_2. Arrows indicate the position of bands migrating at an approximate molecular weight of 64 kDa (p64) and 71 kDa (p71), while HaSV indicates wild-type HaSV. (**B**) Viability of untreated cells or cells treated with 80 mM acetic acid (HOAc) or 40 mM H_2O_2.

Apoptosis can be differentiated from necrosis on the basis that apoptosis requires *de novo* protein synthesis while necrosis does not (Madeo *et al.*, 1999; Ludovico *et al.*, 2001). To confirm that the onset of apoptosis and not cell necrosis was promoting VLP maturation, yeast cells transformed with pMT9, were treated with either acetic acid or H_2O_2 in the presence or absence of cycloheximide, a compound which inhibits *de novo* protein synthesis.

Western analysis of cell-free extracts showed only p71 present in untreated cells or cells treated with cycloheximide alone (Figure 2.7, lanes 1 and 2). When cells were treated with acetic acid or H_2O_2, both p64 and p71 were detected (Figure 2.7, lanes 3 and 5). VLP maturation occurred in cells treated with acetic acid in the presence of cycloheximide (Figure 2.7, lane 4), but p64 was not observed when cells were exposed to H_2O_2 in conjunction with cycloheximide (Figure 2.7, lane 6). Thus,

cycloheximide appeared to inhibit maturation of VLPs in cells treated with H_2O_2 but not in those treated with acetic acid. This data confirmed that at least in the case of H_2O_2, maturation of the VLPs was dependent upon *de novo* protein synthesis in the yeast cells.

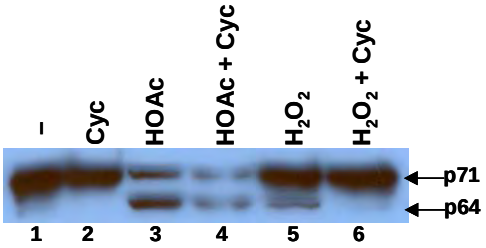

Figure 2.7 Inhibition of apoptosis and VLPs maturation. The methods for this experiment are described in section 2.2.7. (-) Indicates cells incubated without cycloheximide (Cyc), acetic acid (HOAc) or H_2O_2 and arrows show the position of p71 and p64.

The TUNEL test and DAPI staining were used to confirm that the yeast cells treated with acetic acid or H_2O_2 were undergoing apoptosis. TUNEL was selected because it is a useful and specific test to label free 3'-OH termini from fragmented DNA as a result of apoptosis. Essentially, terminal deoxynucleotidyl transferase (TdT), transfer fluorescien labelled nucleotides to the free 3'-OH DNA ends of fragmented DNA. The fluorescent signal can then be converted by the detection of the fluorescien with anti-fluorescien conjugated with horseradish peroxidase (POD). Finally the substrate 3,3'-diaminobenzidine (DAB) is added, which utilizes cobalt and nickel chloride in the presence of POD resulting in the formation of a brown precipitate, which can be visualised by light microscopy.

DAPI staining was used to confirm the results from the TUNEL test, because the fluorescent molecule complexes with double-stranded DNA. In this way the morphology of the nuclei can be viewed with a fluorescence microscope and apoptotic nuclei characterised by chromatin condensation, which are observed as semi-circles (Madeo *et al*., 1999).

As expected, p64 was detected in the lysates of cells treated with acetic acid and H_2O_2, while no p64 was detected in untreated cells (Figure 2.8, A, lanes 2 and 3 versus 1). Samples of cells were fixed and subjected to a TUNEL test to detect

fragmented DNA represented by a brown precipitate, which could be visualised using light microscopy. The test showed that approximately 80% of cells treated with either acetic acid or H_2O_2 were TUNEL positive (Figure 2.8, B), while only 5% of untreated cells exhibited a positive reaction (Figure 2.8, B).

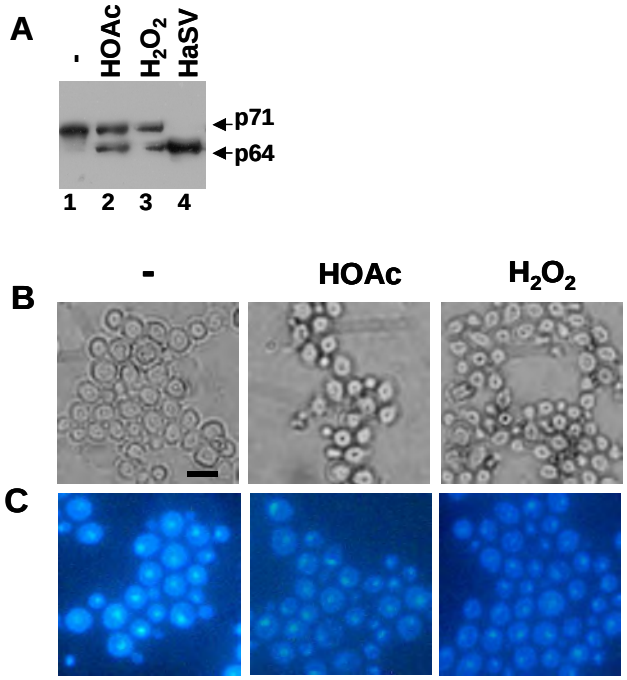

Figure 2.8 TUNEL test and DAPI staining to confirm the onset of PCD in yeast cells treated with acetic acid or H_2O_2. (**A**) Western analysis of total yeast lysates from cells expressing *P71*, untreated (-), treated with 80 mM acetic acid (HOAc) or 40 mM H_2O_2 for 200 minutes at 28ºC. Arrows indicate the position of bands migrating at an approximate molecular weight of 64 kDa (p64) and 71 kDa (p71). HaSV indicates wild-type HaSV. TUNEL reaction (**B**) or DAPI stained (**C**) untreated cells (-), cells treated with 80 mM acetic acid (HOAc) or cells treated with 40 mM H_2O_2 as indicated. The bar represents 5 μm.

The DAPI stains confirmed that the majority of nuclei of treated cells were fragmented, with the chromatin forming a semi circle, which is indicative of chromatin condensation (Figure 2.8, C). This observation was consistent with reports of chromatin condensation induced by apoptosis (Madeo *et al.*, 1998; 1999; 2002; Herker *et al.*, 2004). In contrast, the nuclei of untreated cells were solid, round and no chromatin condensation was evident (Figure 2.8, C). These tests confirmed that apoptosis was induced by the addition of acetic acid and H_2O_2 which correlated in VLP maturation.

2.3.6 H_2O_2 treatment does not result in maturation *in vitro*

To rule out the possibility that maturation of procapsids was as a result of direct interaction with H_2O_2, yeast cells expressing *P71* were grown in carbon-limiting medium for 24 hours to ensure the presence of procapsids only. The cells were lysed and the cell-free extract treated with acetic acid or H_2O_2, followed by Western analysis. Acetic acid caused maturation of the procapsids *in vitro* after 3.5 hours (Figure 2.9, lane 2), but no maturation was observed when the lysates were untreated or treated with H_2O_2 even after 19 hours of incubation (Figure 2.9, lane 9). VLPs have previously been shown to mature in the presence of a 70 mM sodium acetate (pH 5.0) buffer *in vivo* (Canady *et al*., 2000; Venter, 2001), which could explain why the VLPs had the ability to mature in the presence of acetic acid. These results showed that induction of VLP maturation by H_2O_2 could only occur *in vivo*, supporting the hypothesis that VLP maturation correlated with the onset of apoptosis.

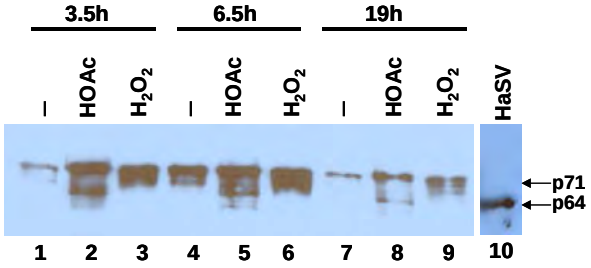

Figure 2.9 Maturation of VLPs *in vitro* in the presence of acetic acid and H_2O_2. Western analysis of crude yeast lysates from cells expressing *P71* under control of P_{GADH} (pMT9) lysed in EB containing either 80 mM acetic acid (HOAc) or 40 mM H_2O_2 over time (3 to 19 hours). Cells were initially incubated in carbon-limiting medium for 28 hours at 28ºC. (-) Indicates cells lysed in EB alone while HaSV indicates wild-type HaSV. Arrows indicate the position of bands migrating at an approximate molecular weight of 64 kDa (p64) and 71 kDa (p71).

2.4 DISCUSSION

The aim of this chapter was to develop a high-level HaSV *P71* yeast expression system based upon the *GADH* promoter to study the assembly of VLPs *in vivo*. The increase in expression levels from P_{GADH} compared to P_{GAL1} resulted in the assembly of VLPs, which had the ability to mature *in vivo*. Evidence was provided by the ability of the VLPs to mature and the detection of VLPs by TEM analysis that represented wild-type HaSV.

2.4.1 HaSV VLP assembly in yeast

Venter (2001) observed that more than 95% of p71 produced in cells under control of P_{GAL1} were insoluble. He postulated that the disappearance of p71 after 12 hours induction could be attributed to proteolytic degradation of insoluble aggregates. Increasing the expression levels of a poorly soluble protein traditionally results in even higher levels of an insoluble protein. However, this was not the case with P_{GADH}-directed expression of *P71*, which resulted in increased protein expression, solubility, and assembly of the VLPs, which were still detected after 50 hours incubation

Evidence that p71 had the ability to assemble *in vivo* was provided by detection of mature VLPs by TEM analysis, which had identical average diameters (38 nm) to wild-type HaSV. However, even though it appeared that assembly had improved, a large proportion of p71 remained indicating that the protein which remained, may have been insoluble. The insolubility of p71 may be attributed to the protein forming aggregates within the yeast cells (Venter, 2001).

The differences in efficiency between the P_{GAL} and P_{GADH} promoter systems with respect to p71 assembly cannot be attributed to the increase in p71 concentrations only, but may also be as a consequence of elevated *P71* mRNA levels transcribed from the hybrid promoter, which are encapsidated by the VLPs. This seems likely because; firstly, NωV VLPs produced using a baculoviral expression system in a Sf 21 cell line encapsidated *P70* mRNA; secondly, the stability of NωV particles appear to be governed by the necessity of viral RNA to neutralize the highly charged inner surfaces; thirdly, viral RNA forms a structural component of the inner surface of the nodaviruses which offer the capsid support and stability; and finally, in the nodaviruses, viral RNA was preferentially encapsidated ahead of cellular mRNA in competition experiments (Fisher *et al*., 1992; Schneemann *et al*., 1992; Agrawal and Johnson, 1995; Tang *et al*., 2001). From the above argument it seems highly unlikely that HaSV VLPs would form empty particles devoid of RNA. Both the tetraviruses and nodaviruses have the ability to package random cellular RNAs, but packaging non-viral RNA has been shown to result in particles which are less stable and more susceptible to proteolytic degradation (Bothner *et al*., 1999; Krishna *et al*., 2003).

The low number of VLPs detected by TEM analysis representing wild-type HaSV, most likely represent particles which solely or partly encapsidate *P71* mRNA. However one cannot rule out the possibility that high concentration of p71 produced off the hybrid promoter resulted in the elevated assembly rates experienced. In this way a certain percentage of particles would encapsidate viral RNA or cellular RNA during assembly, depending on which was available and in close proximity.

2.4.2 Apoptosis and HaSV VLP maturation *in vivo*.

Apoptosis is a translation-dependent pathway, which is energy-dependent and is a form of cellular suicide. It differs from necrosis in that apoptosis is a defined orchestrated pathway dependent on *de novo* protein synthesis by the cell in response to negative stimuli or mechanical cellular damage. In addition to cellular ageing compounds such as H_2O_2 or acetic acid can induce apoptosis in yeast cells (Madeo *et al*., 1999; Ludovico *et al*., 2001; Herker *et al*., 2004). The well orchestrated process initially involves the production of reactive oxygen species (ROS) in the cytosol, leading to expression of the caspase pathway, DNA fragmentation, chromatin condensation, the release of cytochrome C from the mitochondria and exposition of phosphatidyl serine on the cell surface (reviewed in Madeo *et al*., 2004). Release of cytochrome C from the mitochondria has been implicated in the acidification of the cytosol (Ludovico *et al*., 2002).

Mitochondria play a central role in the regulation of apoptosis, since changes in the permeability of the mitochondrial membranes result in the release of apoptosis inducing factors into the cytoplasm which trigger the pathway (van Gurp *et al*., 2003). It has been reported that the onset of apoptosis results in a drop of cytosolic pH due to release of cytochrome C from the mitochondria (Matsuyama and Reed, 2000). This acidification was shown using pH-sensitive green fluorescent protein mutants and is critical for caspase activity (Matsuyama *et al*., 2000). Acidification of the cytosol has also been reported to occur from the release of protons from lysosomes (Nilsson *et al*., 2006). So it would be reasonable to propose that maturation could occur due to acidification of the cytosol from the onset of apoptosis.

NωV VLPs, have been shown to mature spontaneously in baculovirus-infected Sf 21 cells as they age (Agrawal and Johnson, 1995) and *in vitro* at an acidic pH (Canady *et al*., 2000). So while the molecular mechanisms of autoproteolytic cleavage of the capsid precursor protein are well understood (Canady *et al*., 2001; Taylor *et al*., 2002), the relevance of maturation in the context of the virus and its interaction with the host cell remains unclear. The ability of acetic acid and H_2O_2 to induce apoptosis provides a possible way to link this process to maturation. When acetic acid or H_2O_2 were added to cells expressing *P71,* the VLPs had the ability to mature. The TUNEL tests confirmed that approximately 80% of the treated cells were undergoing apoptosis. DAPI staining of the nuclei indicated chromatin condensation, which is a characteristic of PCD. In the case of acetic acid it is impossible to distinguish between acetic acid-triggered maturation directly (by acidification of the cytosol) or indirectly (by induction of apoptosis) (Ludovico *et al*., 2001; this study). Either way the ability of H_2O_2 to cause maturation *in vivo* and not *in vitro* indicated a possible link between apoptosis and HaSV VLP maturation in yeast cells.

To investigate the effect viral RNA has on the assembly of HaSV VLPs, assembly efficiency will be determined by co–expressing *P71* with either *P71* mRNA or RNA2. The VLPs purified from cells co–expressing protein and viral RNA will be assessed for encapsidated viral RNA with the aim of relating assembly to viral RNA encapsidation.

CHAPTER 3. RNA ENCAPSIDATION BY HaSV VLPS ASSEMBLED IN YEAST

CHAPTER 3. RNA ENCAPSIDATION BY HaSV VLPS ASSEMBLED IN YEAST.

3.1 INTRODUCTION

In the previous chapter the high-level expression system resulted in assembly of HaSV VLPs in yeast. The increase in the efficiency of assembly by expressing P_{GADH}–*P71* when compared to P_{GAL1}–*P71* could result from increased protein production. Alternatively the increase in assembly efficiency of the VLPs could be the result of increased *P71* mRNA transcribed by the hybrid promoter, which may function (as in the nodaviruses) to nucleate capsid precursor association during assembly (Schneemann and Marshall, 1998). If the mRNA was being encapsidated it may contain an encapsidation signal.

This chapter describes experiments to determine whether the co-expression of *P71* with viral RNA results in the VLPs specifically encapsidating viral RNA.

3.2 MATERIALS AND METHODS

3.2.1 Construction of HaSV RNA expression vectors

***P71* mRNA expression vector (pMT9–AUG).** The methionine start of HaSV p71 was mutated by site–directed mutagenesis using the QuickChange II Site-Directed Mutagenesis Kit (Stratagene). To enable co-selection of the mRNA expression vector with pMT9 or pAV3, the *URA3* selectable marker on pMT9 (section 2.2.4) was replaced with the *LEU2* auxotrophic marker by ligating the 7017 bp *Bcl* I / *Mlu* I backbone from pPG45 (obtained from Petra Gentz, Department of Microbiology, Biochemistry and Biotechnology, Rhodes University), containing the *LEU2* auxotrophic marker into pMT9, generating pMT9Leu (Figure 3.1, Step I). Plasmid pMT9Leu was then used as a template for reverse PCR amplification with primers MT6F (Appendix 4; Table A4.1) and MT7R (Appendix 4; Table A4.1; Appendix 6, program 2). These overlapping primers altered the nucleotides encoding the p71

translational start, (ATG was mutated to ACG) introducing an *Aat* II restriction site. The plasmid pMT9-AUG was generated for the high-level expression of HaSV *P71* mRNA (Figure 3.1, Step II).

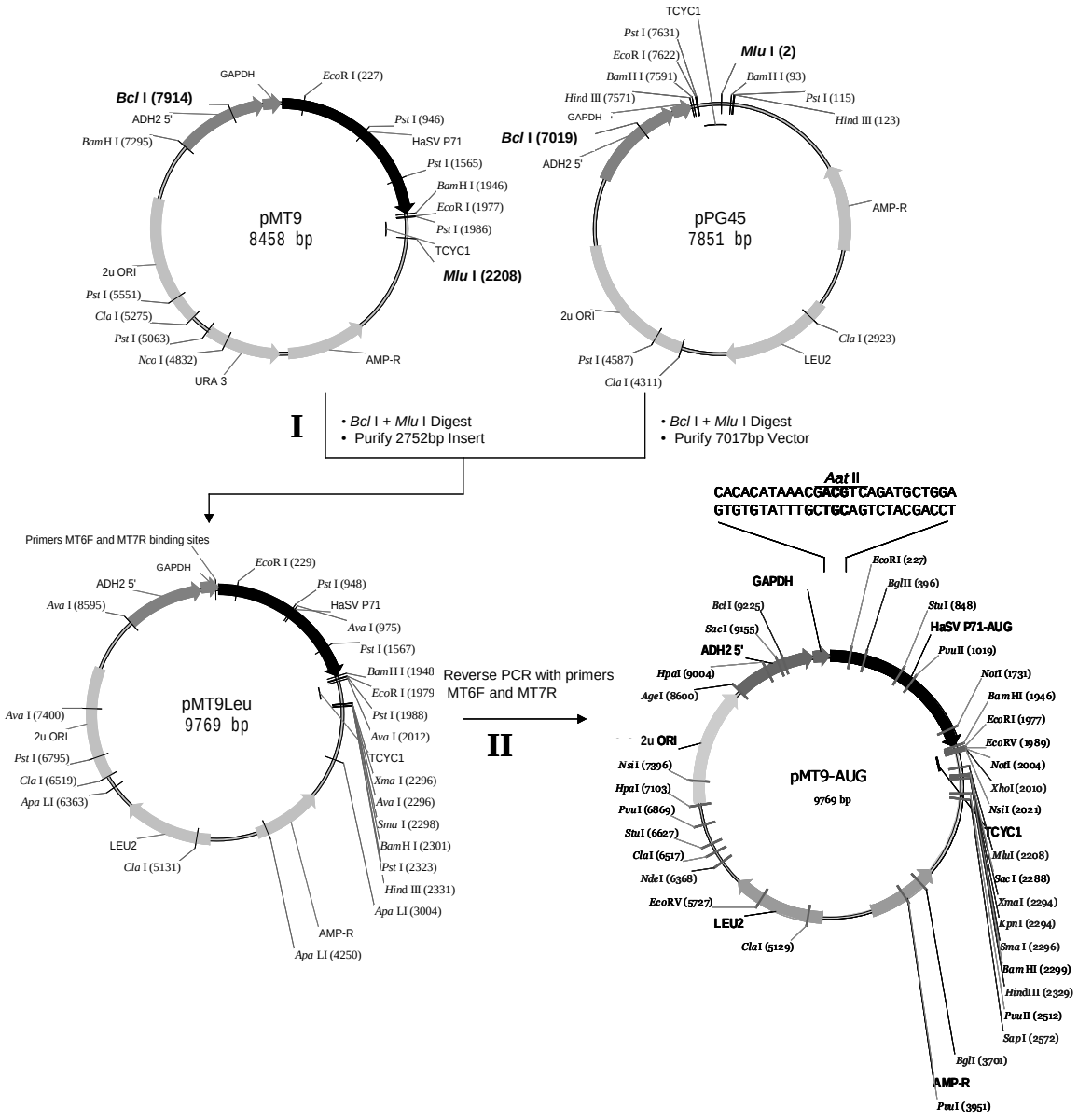

Figure 3.1 Construction of *P71* mRNA expression vector, pMT9-AUG. The restriction enzymes utilized for each cloning step are highlighted in a larger font and the steps followed are represented by Roman numerals. The resulting mutation of the HaSV *P71* methionine (AUG mutated to ACG) is shown above the plasmid map of pMT9-AUG. ADH2, 5' end of the *ADH2* promoter; GAPDH, 5' end of the *GAPDH* untranslated region; HaSV *P71*, the capsid encoding sequence of HaSV (*P71*); TCYC1, *CYC1* terminator (T_{CYC1}); AMP-R, gene encoding the β-lactamase enzyme for ampicillin resistance; 2μ *ORI*, yeast origin of replication; *URA*3, uracil 3 auxotrophic marker; *LEU2*, leucine 2 auxotrophic marker.

Vectors for the expression of RNA2 (pMT22L and pMT29). The RNA2 expression vectors were constructed with expression directed either by P_{GAL1} or P_{GADH}. Venter (2001) constructed an RNA2 expression vector (pAV14HPTrp) in which the 5' end of HaSV RNA2 was fused to the -1 nucleotide of the *GAL1* promoter. The vector pAV14HPTrp carries a low copy number CEN/ARS replication origin (Figure 3.2), which replicates at approximately 1 to 2 copies per cell (Lundblad, 1997). To increase the plasmid copy number, the *CEN/ARS* origin of replication was replaced with the 2µ origin, which replicates at approximately 20-50 copies per cell (Rose and Broach, 1990). To accomplish this, the entire P_{GAL1} promoter and RNA2 sequence were removed from pAV14HPTrp by digesting with *Age* I and *Kpn* I. The resulting 3212 bp insert was ligated into identical restriction sites in the 2µ-based vector, pYES2 (Figure 3.2, Step I) with the resulting plasmid (pMT22) replicating at high copy number, and encoding a *URA*3 marker for selection in yeast. To ensure that pMT22 could be co-selected with pAV3 (which also carries a *URA*3 marker) the backbone of the plasmid was replaced with the backbone from pMT9Leu. The 6654 bp *Age* I / *Bam* HI fragment from pMT9Leu, encoding the *LEU2* gene, was ligated into the 3320 bp *Age* I / *Bam* HI fragment from pMT22, replacing the *URA*3 marker with *LEU*2 (Figure 3.2, Step II). The resulting plasmid (pMT22L) supports higher levels of expression of RNA2 under control of P_{GAL1} than that of pAV14HPTrp and carries an exact fusion between P_{GAL1} and RNA2 (Table 3.1). The plasmid contains a *cis*–cleaving tobacco ringspot virus (ToRSV) hairpin cassette (HC) ribozyme at the 3' end of RNA2 (Figure 3.2).

P_{GADH}, was used for high-level expression of RNA2. A 2100 bp *Bam* HI / *Not* I fragment from pMLY2 (constructed by Michelle Williams, CSIRO Entomology, Canberra, ACT Australia), which represented the 5' end of HaSV RNA2 was cloned upstream from P_{GADH} into the vector pPG37 (obtained from Petra Gentz, Department of Microbiology, Biochemistry and Biotechnology, Rhodes University), resulting in pMT28 (Figure 3.3, Step I). Next a 5354 *Age* I / *Not* I fragment from pMT28, which represents the entire P_{GADH} and RNA2 sequence were cloned into identical restriction sites in pMT22L, generating pMT29 (Figure 3.3, Step II; Table 3.1). Plasmid pMT29 is a 2µ-based plasmid, contains a HC ribozyme at the 3'end of RNA2 and a *LEU2*

auxotrophic marker. This would place the start of the HaSV RNA2 159 bps from the TATA element of *GAPDH*.

3.2.2 Chromosomal versus episomal expression of *P71*

The yeast strain INVScI 3#20.1 (Matα, *his*3, *P71*:*LEU2*, *trp*1, *ura*3) (Venter, 2001) transformed with pYES2 was used for the expression of *P71* under control of P_{GAL1} from a single copy of the gene inserted into the *LEU2* chromosomal locus. The yeast strain, INVScI L+ (Matα, *his*3, *LEU*2, *trp*1, *ura*3) (Venter, 2001) was used for the P_{GAL1} (pAV3) and P_{GADH} (pMT9)-dependent expression of *P71* from plasmid vectors. The cells were grown in SMM supplemented with 0.002% histidine, 0.002% tryptophan, 0.1% glucose and 5% glycerol (volume/volume) for 20 hours at 28°C. The cells were harvested and washed twice in sterile triple distilled water and re-suspended in SMM supplemented with 0.002% histidine, 0.002% tryptophan, 0.01% galactose and 5% glycerol (volume/volume).

Table 3.1. Nucleotide sequences around junctions between P_{GADH} or P_{GAL1} and the 5' ends of HaSV *P71* or RNA2

Plasmid Name	Selectable Marker	Promoter	Promoter-RNA junction	Translational start
pMT9Leu	URA3	P_{GADH}	AACACACAUAAACA**AUGGGAGAU**	CA**AUGGGA**
pMT9 (-AUG)	LEU2	P_{GADH}	AACACACAUAAACG**ACGUCAGAU**	CG**ACGUCA**
pMT22L	*LEU2*	P_{GAL1}	UGUAAUAAA**GUUUUUCUUUCUUU**	CA**AUGUAC**
pMT29	*LEU2*	P_{GADH}	AACACACAUAAACA…36bp…**GUUUUUCUUUCUUU**	CA**AUGUAC**

The plasmid name, selectable auxotrophic marker and promoter are depicted. The RNA sequence of *P71* and RNA2 are shown in bold font. The promoters are double underlined and the region of the translational start in pMT9Leu which was mutated underlined, generating an *Aat* II site.

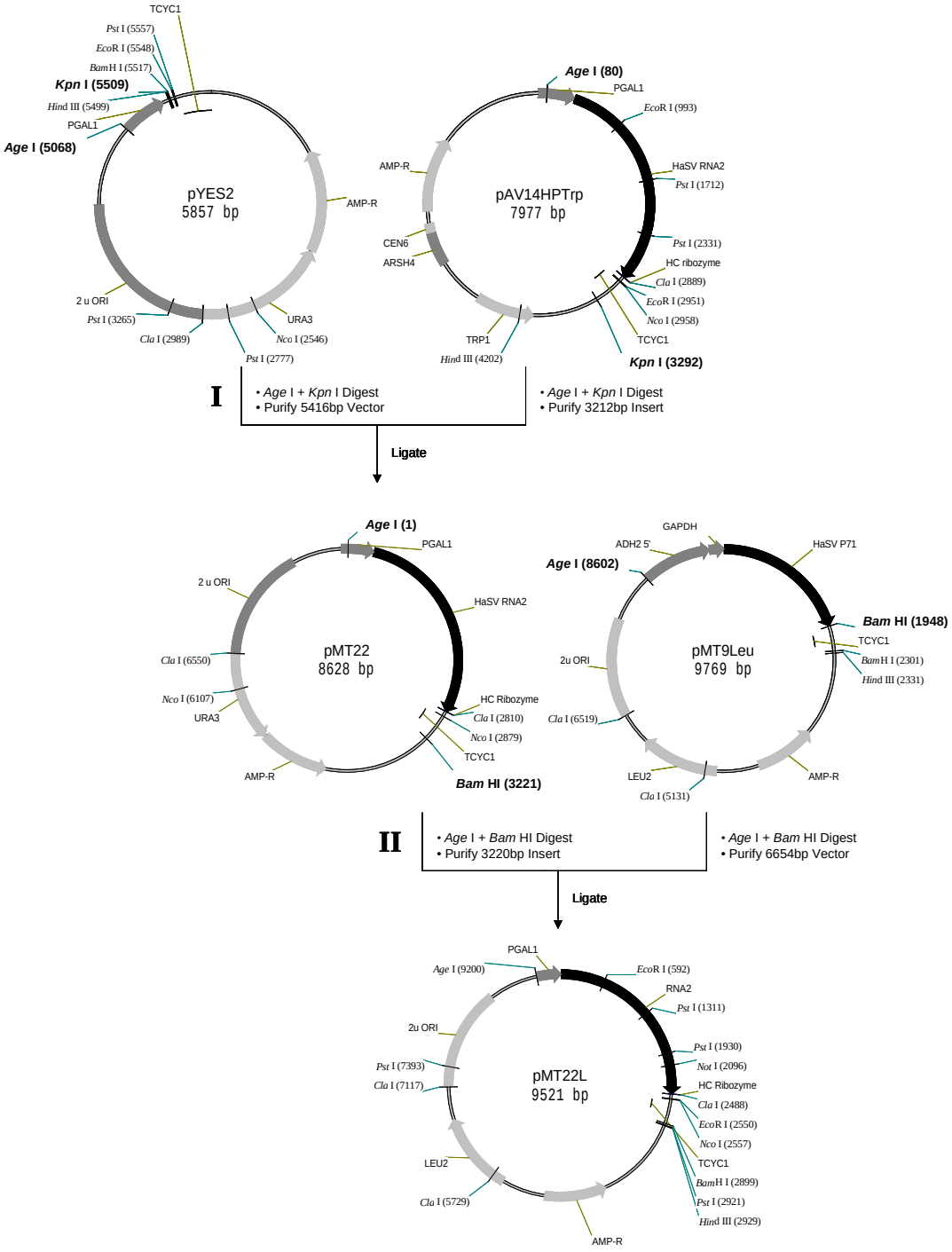

Figure 3.2 Construction of the P_{GAL1}-derived HaSV RNA2 expression vector, pMT22L. The restriction enzymes utilized for each cloning step are highlighted in a larger font and the steps followed are represented by Roman numerals. ADH2, 5' end of the *ADH2* promoter; GAPDH, 5' end of the *GAPDH* untranslated region; P_{GAL1}, *GAL1* promoter; HaSV *P71*, the capsid encoding sequence of HaSV (*P71*); TCYC1, *CYC1* terminator (T_{CYC1}); *AMP*-R, gene encoding the β-lactamase enzyme for ampicillin resistance; 2μ *ORI*, yeast origin of replication; *URA*3, uracil 3 auxotrophic marker; *LEU2*, leucine 2 auxotrophic marker; *Tobacco ringspot virus* (ToRSV) hairpin cassette ribozyme, HC ribozyme; *ARS*, autonomous replication signals; *CEN*, yeast centromeric sequence.

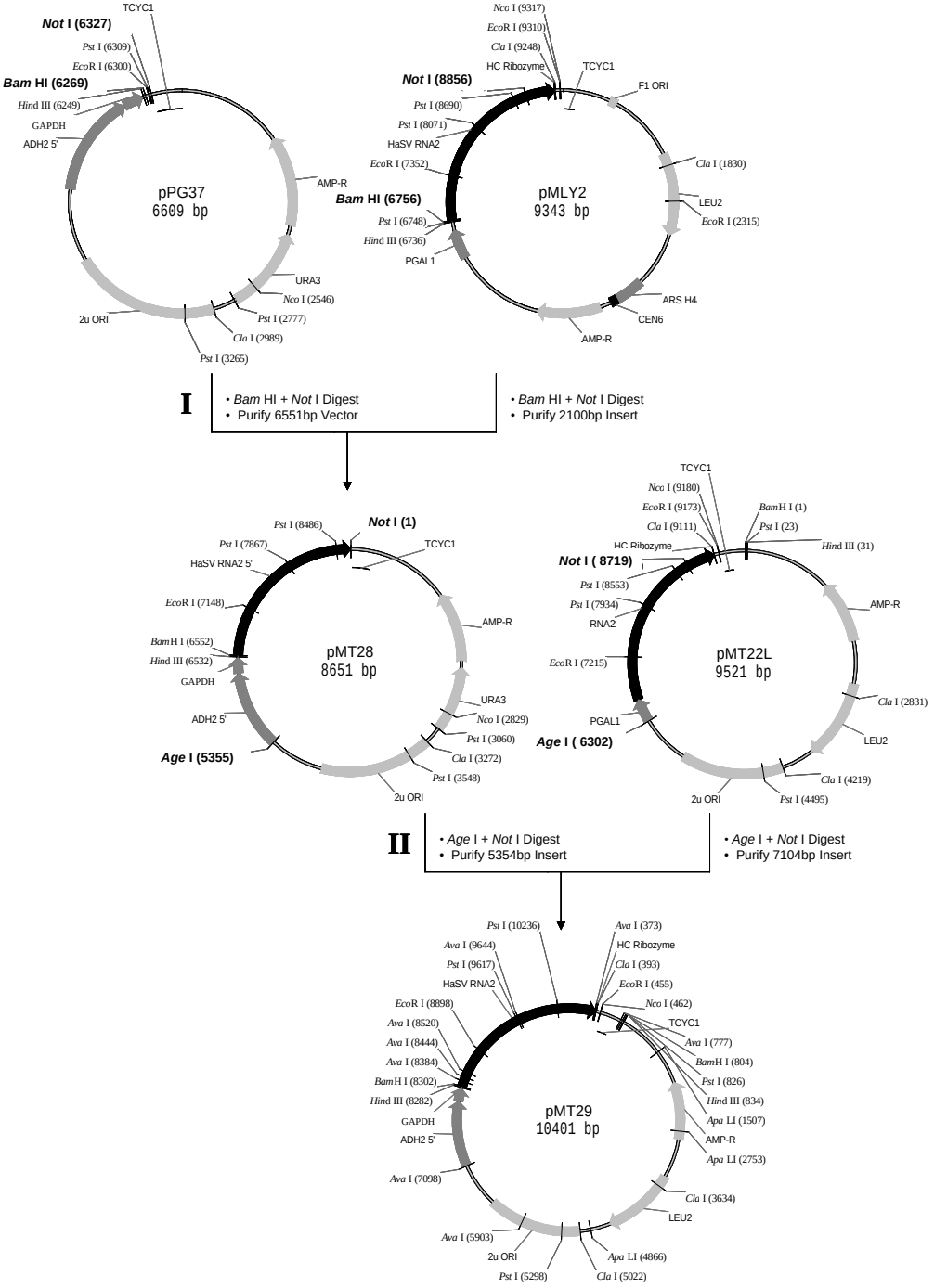

Figure 3.3 Diagrammatic representation of the process followed for construction of the P_{GADH}–derived HaSV RNA2 expression vector, pMT29. The restriction enzymes utilized for each cloning step are highlighted in a larger font and the steps followed are represented by Roman numerals. ADH2, 5' end of the *ADH2* promoter; GAPDH, 5' end of the *GAPDH* untranslated region; P_{GAL1}, *GAL1* promoter; TCYC1, *CYC1* terminator (T_{CYC1}); *AMP*-R, gene encoding the β-lactamase enzyme for ampicillin resistance; 2μ *ORI*, yeast origin of replication; *URA*3, uracil 3 auxotrophic marker; *LEU2*, leucine 2 auxotrophic marker; (ToRSV) hairpin cassette ribozyme, HC ribozyme; autonomous replication signals *ARS*; yeast centromeric sequences, *CEN*.

3.2.3 Co-expression of *P71* with viral RNA

Yeast strain INVScI was either transformed with pAV3 (medium-level expression of *P71*) or pMT9 (high-level expression of *P71*) in conjunction with the high-level *P71* mRNA (pMT9-AUG) expression vector. Cells containing the relevant plasmids were incubated in SMM supplemented with 0.002% histidine, 0.002% tryptophan, 0.1% glucose and 5% glycerol (volume/volume) for 20 hours at 28°C. The cells were harvested washed twice in triple distilled water and then re-suspended in SMM supplemented with 0.002% histidine, 0.002% tryptophan, 0.01% galactose and 5% glycerol (volume/volume).

For the *in vivo* maturation of HaSV VLPs, cells were co-transformed with pAV3 (medium-level expression of *P71*) and either the low–level RNA2 (pMT22L) or high-level *P71* mRNA (pMT9-AUG) expression vectors. The cells were grown in SMM supplemented with 0.002% histidine, 0.002% tryptophan, 0.1% glucose and 5% glycerol (volume/volume) for 12 hours at 28°C. Acetic acid was added to a final concentration of 80 mM and the cells were grown for a further 200 minutes at 28°C.

To ensure that an equal amount of total yeast protein was analysed from each preparation the total yeast lysates were probed for the yeast translational initiation factor (eIF-5A), encoded by *TIF51A* and *TIF51B* in yeast (Schwelberger *et al*., 1993). The two proteins eIF-5Aa and eIF-5Ab are constitutively expressed under aerobic and anaerobic conditions respectively, with both having an approximate molecular weight of 17 kDa (Schwelberger *et al*., 1993). For this reason these proteins can be used as a marker during Western analysis to show that equal amounts of protein were analysed for each sample.

3.2.4 Northern analysis

Total yeast RNA was purified from ten $OD_{600\ nm}$ units of culture using the hot phenol method of Leeds *et al*., (1991). The cells were harvested in a microfuge at 15500 ×g and re-suspended in 300 µL buffer A [(50 mM NaOAc (pH 5.2); 10 mM EDTA (pH 8.0); 1% SDS (weight/volume)]. Two volumes of acid phenol [(equilibrated to below pH 4.0 with 50 mM sodium acetate (pH 4.0)] was added to the lysate and the

suspension incubated at 65°C for five minutes. The suspension was gently mixed by inversion every 30 seconds during the incubation period. The two phases were separated by microfuging at 15500 ×g for 3 minutes. The phenol phase was removed while ensuring the pellet was not disrupted. The same volume of acid phenol was added as before followed by incubation at 65°C to disperse the pellet. To ensure that the pellet was properly re-suspended the sample was vortexed, followed by microfuging at 15500 ×g for 3 minutes. The aqueous phase was removed and the volume adjusted to 500 µL. An equal volume of phenol:chloroform:isoamyl alcohol (25:24:1) (pH 4.0) and 0.15 M sodium acetate (pH 5.5) was added to the suspension, which was subsequently vortexed and then microfuged at 15500 ×g for 3 minutes. The upper aqueous was removed and placed into a fresh eppendorf. Three volumes of ethanol (at room temperature) was added to the aqueous phase which was briefly homogenised and then microfuged at 15500 ×g for 5 minutes. The supernatant was discarded and the pellet washed with 70% ethanol. The pellet was subsequently air dried for 5 minutes in a vacuum dryer and re-suspend in 20 µL diethyl pyrocarbonate (DEPC)–treated triple distilled water. Approximately 5 µg of total yeast RNA was extracted from each preparation.

RNA was purified from HaSV VLPs according to Schneemann *et al*. (1993). One volume of phenol:chloroform:isoamyl alcohol (25:24:1) (pH 4.0) was added to approximately 1×10^{11} sucrose gradient purified VLPs. The suspension was vortexed for 1 minute and then microfuged for 3 minutes at 4°C. The aqueous phase was removed and 1 volume of DEPC–treated H_2O added to the phenol phase. The suspension was vortexed, microfuged at 15500 ×g for 5 minutes and the aqueous phase removed as indicated above. Next, 0.3 M sodium acetate (pH 5.2), 20 mg of glycogen (Roche), and 3 volumes ice cold 200 proof ethanol (Sigma) was added to each RNA extract. The RNA was allowed to precipitate at -20°C over night and collected at 15500 ×g for 10 minutes. The pellets were subsequently washed with ice-cold 75% ethanol and dried in a vacuum dryer for 5 minutes. Ten microliters of DEPC–treated H_2O was added to the pellets, which were re-suspended and pooled. Approximately 1-2 µg of RNA was used for Northern analysis.

Northern blot analysis, electrophoresis using a denaturing 1% agarose-formaldeyde gel and the transfer to a Hybond N+ nylon membrane (Amersham), were performed according to the manufacturers protocol (Roche). The probe used for the hybridisation was DIG–UTP labelled and complementary to nucleotides 2309-761 of HaSV RNA2 (Appendix 2; Figure A2.1). Plasmid pMT20F was used as a template to generate the negative sense HaSV RNA2 probe (Figure 3.4). The plasmid was generated by inserting a PCR product, which represented the HaSV *P71* coding sequence, into the pGEM-T Easy vector. The PCR product was amplified with primers MT1 and RD2, which bind to nucleotides 1-23 and 1944-1924 of HaSV *P71* respectively (Appendix 4; Table A4.1) The thermal cycling conditions are shown in appendix 5, program 3. To synthesise the negative sense probe plasmid pMT20F was linearised with *Bgl* II and transcribed *in vitro* with SP6 RNA polymerase according to the manufacturers instructions (Roche). Subsequent hybridisation of the probe to the target sequence and autographic detection using a CDP–star substrate were also performed according to the manufacturer's instructions (Roche).

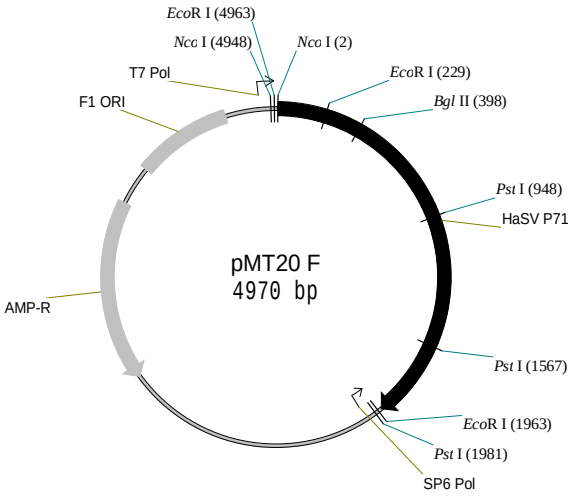

Figure 3.4 Diagrammatic representation of pMT20F, which was used as a template to generate the HaSV RNA2 probe for (+) RNA2 detection. The vector was generated by inserting a PCR fragment, which included the HaSV *P71* sequence, into pGEM-T Easy (Promega). The resultant plasmid contains the HaSV cDNA flanked by bacteriophage RNA polymerase T7 and SP6. The plasmid confers resistance to ampicillin (AMP-R) for selection in *E. coli*. F1 ORI, *E.coli* origin of replication. TCYC1, *CYC1* terminator (T_{CYC1})

3.3 RESULTS

In the previous chapter, it was shown that increased expression of *P71* under control of P_{GADH} led to more efficient VLP assembly and maturation *in vivo*. As discussed previously, this result was in contrast to the data obtained by Venter (2001) using the P_{GAL}-derived expression system, where VLP assembly was very inefficient and no maturation was observed. Thus it was hypothesised that the increase in the levels of viral RNA (represented by *P71* mRNA) produced by the P_{GADH} system and encapsidation of this RNA promoted efficient VLP assembly and maturation in the yeast cells. To test this hypothesis, the approach was to co-express viral RNA (*P71* mRNA or RNA2) with *P71* to determine whether increased levels of viral RNA resulted in more efficient capsid assembly and maturation.

3.3.1 Low versus high-level expression of *P71* and VLP assembly

First the efficiency of VLP assembly supported by low, medium and high level expression of *P71* was investigated. Low-level expression of *P71* was achieved using yeast strain INVScI 3#20.1 (Venter, 2001), which contained a single chromosomal copy of the *P71* gene under control of P_{GAL}, while the multicopy plasmid pAV3 (P_{GAL}), was used for medium levels of expression. Cells containing the multicopy plasmid pMT9, with *P71* expressed under the control of P_{GADH}, was used for high-level expression. For induction of *P71* the yeast strains were grown in minimal medium containing 0.01% galactose and 5% glycerol, which induces transcriptional activation by P_{GAL} and provides the carbon-limiting conditions required for inducing P_{GADH} activity.

Substantially higher levels of p71 were produced from the multicopy expression vectors compared to chromosomal expression (Figure 3.5). This was expected because 2μ-based vectors are present at a copy number of approximately 50 per cell (Rose and Broach, 1990). Lower levels of p71 were detected in cells with P_{GAL1}-derived plasmid expression of *P71* when compared to P_{GADH} expression of *P71*. In both cases where *P71* was expressed using the *GAL1* promoter, the protein could not be detected after 12 hours or 48 hours in cells carrying the chromosomal copy versus pAV3, respectively (Figure 3.5). In contrast p71 could be detected in cells containing

pMT9 (P_{GADH}) after up to 72 hours of incubation and there was no difference in the levels of p71 over the incubation time. In addition, p64 could be detected in these cells after 12 hours, indicating the VLPs matured in these cells. No p64 was detected in cells expressing *P71* from the chromosome or plasmid using P_{GAL}. This result confirmed that higher levels of *P71* expression promoted VLP assembly and maturation. It still remained unclear whether the reason for the improved VLP assembly in P_{GADH}-*P71* expression was as a consequence of increased protein or viral RNA concentrations.

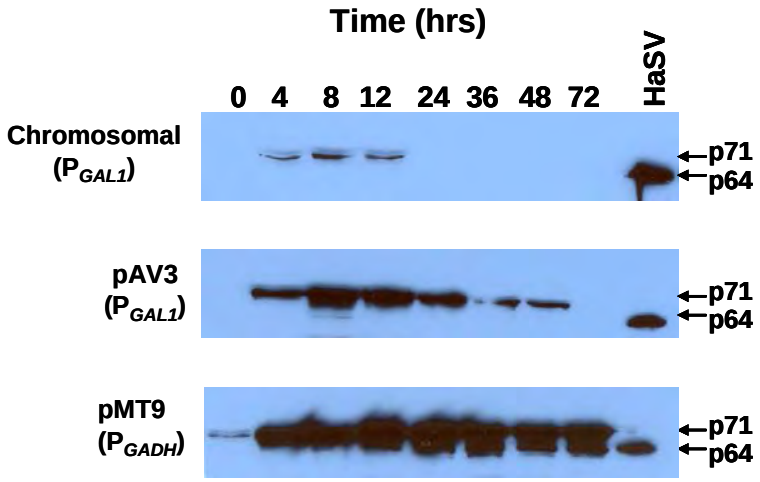

Figure 3.5 Comparison between chromosomal P_{GAL1}-directed *P71* (**A**) and plasmid expression of *P71* by P_{GAL1} (**B**) or P_{GADH} (**C**). Western analysis of total yeast lysates extracted from cells that were induced for the expression of *P71* as indicated in section 3.2.2. Arrows indicate the position of bands migrating at an approximate molecular weight of 64 kDa (p64) and 71 kDa (p71). HaSV refers to wild-type HaSV.

3.3.2 Co-expression of *P71* and *P71* mRNA

If an increase in viral mRNA was the reason for increased VLP assembly then it was expected that an increase in *P71* mRNA would result in an increase in VLP assembly in cells expressing P_{GAL1}-*P71* (pAV3). To test the hypothesis a system enabling the co-expression of *P71* under the control of P_{GAL1} (pAV3) or P_{GADH} (pMT9) together with *P71* mRNA (pMT9-AUG) under control of P_{GADH} was devised. Throughout this chapter two methods of expression will be described. Where P_{GAL1} and P_{GADH}-dependent co-expression was required, cells were initially grown in SMM with 0.1%

glucose and 5% glycerol for 20 hours. The cells were then re-suspended in SMM supplemented with 0.01% galactose and 5% glycerol (galactose-induction medium). Where only P_{GADH}-dependent expression was required, cells were grown in SMM with 0.1% glucose (glucose-starvation medium).

First it was important to confirm that the *P71* mRNA expression vector did not result in the translation of p71. Cells were transformed with the high-level *P71* (pMT9) or *P71* mRNA expression vector (pMT9-AUG) and grown in galactose-induction or glucose-starvation medium. As expected no p71 was translated from the *P71* mRNA expression vector in the two different sets of media (Figure 3.6, lanes 5-8 and 12-14), while p71 was detected in cells containing pMT9 (Figure 3.6, lanes 1- 4 and 9-11). These results showed that p71 was not detectable from the *P71* mRNA expression vector, pMT9-AUG

Figure 3.6 Mutation of the p71 methionine start abolishes translation. Western analysis of total yeast lysates prepared from cells containing either pMT9 (+AUG) or pMT9 minus the p71 translational start (-AUG). Cells were grown in galactose–induction or glucose–starvation conditions at 28°C for the times indicated. The arrows indicate the position of bands migrating at an approximate molecular weight of 64 kDa (p64) and 71 kDa (p71). HaSV refers to wild type virus loaded as a positive control.

To test whether increased mRNA levels in cells expressing *P71* at lower levels would favour VLP assembly. Yeast cells transformed with pAV3 and pMT9-AUG (*P71* mRNA minus the p71 start codon) were examined for the presence of p71 and p64. The levels of the constitutively expressed yeast translation factor, eIF-5A were used to ensure that comparable levels of protein were being analysed for the different samples.

A small increase in the amount of p71 could be detected when mRNA was co-expressed with P_{GAL1}-derived *P71* (pAV3), compared to when no additional mRNA was co-expressed (Figure 3.7, A). After 48 hours p71 could not be detected in the lysates (Figure 3.7, A lane7). After 12 hours a protein, which co-migrated with wild-type HaSV, was detected in the yeast lysate where *P71* mRNA and *P71* were co-expressed (Figure 3.7, A, lane 3). Since this band was not detected in later samples (24 hours-72 hours) this most likely represented a degradation product. Medium levels of p71 with additional mRNA did not therefore improve p71 solubility and the absence of p64 suggested that there was no increase in the assembly of the VLPs.

This result showed that the reason for increased VLP assembly in P_{GADH}-*P71* cells was not due to an increased mRNA level and was therefore likely due to the increased p71 concentrations. However the presence of pMT9-AUG did appear to increase levels of p71 in these cells. Since the AUG codon of p71 is missing in this clone, the increase in p71 must be due to increased mRNA concentrations.

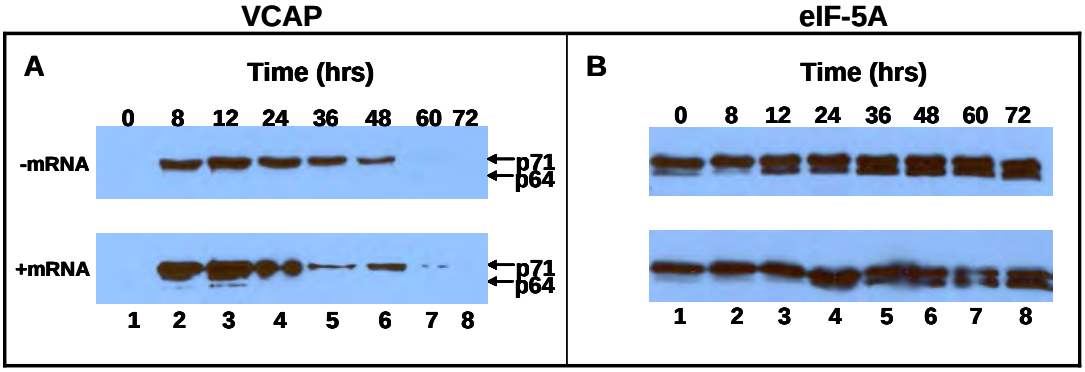

Figure 3.7 Co-expression of P_{GAL1}-derived *P71* with *P71* mRNA. Western analysis of total yeast lysates, expressing medium-level *P71* (pAV3) with (+mRNA) or without (-mRNA) high-level *P71* mRNA. Cells were grown in galactose–induction medium as described in the text. Blots were either probed for p71/p64 (VCAP) or eIF-5A with anti-HaSV (**A**) or anti-eIF-5A (**B**) antibodies respectively. The eIF-5A blots illustrate that equivalent amounts of total yeast protein were loaded into each lane. Arrows indicate the position of bands migrating at an approximately molecular weight of 64 kDa (p64) and 71 kDa (p71).

To test whether an increase in *P71* mRNA would have an effect on p71 expressed from P_{GADH}, cells containing plasmids pMT9-AUG and pMT9 were grown in

galactose-induction medium. Elevated levels of p71 were also detected when *P71* mRNA was co-expressed with P_{GADH}-*P71*, when compared to the control (expression of *P71* only) (Figure 3.8, A). This could not be attributed to loading different amounts of total yeast protein on the Western blot as the levels of eIF-5A protein were equivalent in all the samples (Figure 3.8, B). Furthermore, p64 was detected in cells co-expressing *P71* mRNA with high-level *P71* after 8 hours induction compared to 48 hours for the control (expression of *P71* only) (Figure 3.8, A, compare lane 2 to 6).

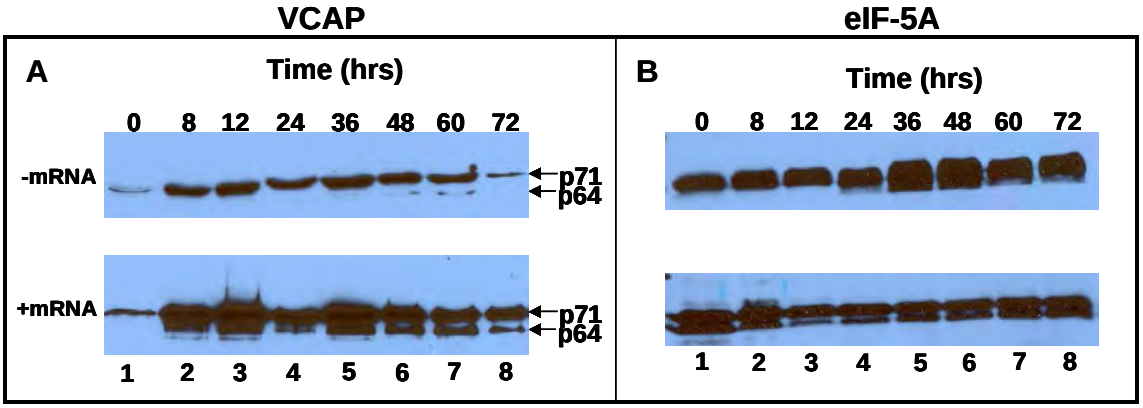

Figure 3.8 Co-expression of P_{GADH}-derived *P71* with *P71* mRNA. Western analysis of total yeast lysates, expressing high-level *P71* (pMT9) with (+mRNA) or without (-mRNA) high-level *P71* mRNA. Cells were grown in galactose–induction medium as described in the text. Blots were either probed for p71/p64 (VCAP) or eIF-5A with anti-HaSV (**A**) or anti-eIF-5A (**B**) antibodies respectively. The eIF-5A blots illustrate that equivalent amounts of total yeast protein were loaded into each lane. Arrows indicate the position of bands migrating at an approximately molecular weight of 64 kDa (p64) and 71 kDa (p71).

3.3.3 Co-expression of *P71* and RNA2

The co-expression of the *P71* mRNA appeared to result in an increase in the detectable levels of p71 and the appearance of p64 indicated that the VLPs had the increased ability to mature. This indicated that assembly may be dependent on high p71 and viral RNA concentrations. Next it was important to determine the effect RNA2 would have on ability of p71 to assemble. First it was important to show that no p71 was translated from the low-level and high-level RNA2 constructs, pMT22L and pMT29. No p71 was detected from either RNA2 construct, but p71 was detected from the positive control (pMT9) (Figure 3.9).

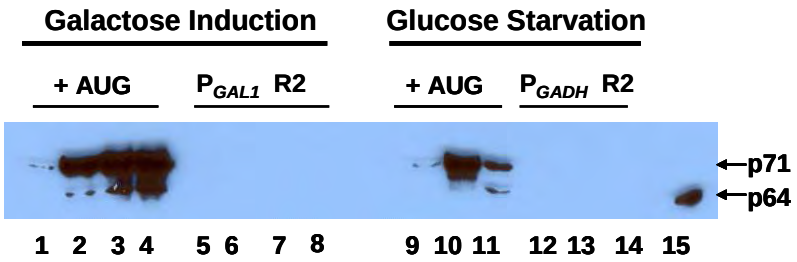

Figure 3.9 Expression of HaSV RNA2 in yeast cells does not result in the translation of p71. Western analysis of total yeast lysates prepared from cells containing pMT9 (+AUG), the P_{GAL1}-dependent (pMT22L; P_{GAL1}R2) or P_{GADH}-dependent (pMT29; P_{GADH}R2) RNA2 expression constructs incubated under galactose–induction or glucose–starvation conditions at 28°C for the times indicated. The arrows indicate the position of bands migrating at an approximate molecular weight of 64 kDa (p64) and 71 kDa (p71) and HaSV refers to wild-type virus loaded as a positive control.

As observed before, when *P71* mRNA was expressed in conjunction with medium concentrations of *P71* (pAV3), elevated levels of p71 were produced when compared to cells expressing *P71* only, and in both cases no p71 was detected after 60 hours of induction (Figure 3.10). A similar trend was observed when RNA2 was co-expressed with *P71*, except that p71 could be detected after 72 hours of induction (Figure 3.10). The levels of p71 decreased dramatically after 24 hours when RNA2 was co-expressed with *P71*, but more importantly no p64 was detected in any of the experiments. This indicated that the presence of RNA2, like *P71* mRNA, do not increase the assembly of HaSV VLPs. The presence of the viral RNA did however increase the levels of p71.

3.3.4 Effect of increased viral RNA concentration on VLP maturation

The difference in the levels of p71 detected when viral RNA was expressed had to be as a consequence of the RNA. The eventual disappearance of p71 indicated that the protein was unable to form stable VLPs. To determine if p71 in the presence of viral RNA increased VLP assembly, *P71* (pAV3) was co-expressed with or without viral RNA for an induction time of 12 hours and maturation induced with acetic acid. The reasoning was that the presence of mature capsid protein (p64) would indicate the assembly and maturation of the VLPs.

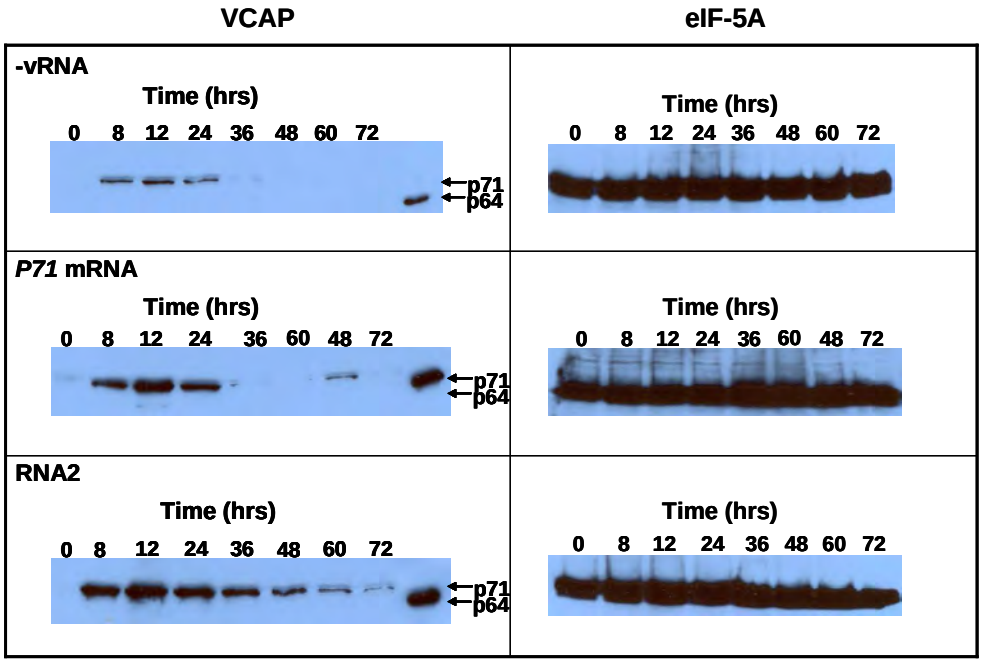

Figure 3.10 Co-expression of *P71* mRNA and RNA2 with *P71*. Western analysis of total yeast lysates from cells co-expressing P_{GAL1}–directed *P71* with no RNA (-RNA), P_{GADH} –directed *P71* mRNA (*P71* mRNA), or P_{GAL1}–directed RNA2 (RNA2). The cells were grown under galactose-induction conditions. Blots were either probed with anti-HaSV (VCAP) or anti-eIF-5A (eiF-5A) antibodies. Arrows indicate the position of bands migrating at an approximately molecular weight of 64 kDa (p64) and 71 kDa (p71).

Western analysis of crude cell extracts showed the presence of p64 in all samples treated with acetic acid, indicating the presence of mature VLPs irrespective of whether or not the viral RNA was present (Figure 3.11). Interestingly p64 was detected in cells co-expressing *P71* and HaSV RNA2 that had not been treated with acetic acid (Figure 3.11, lane 5). This was in contrast to untreated cells co-expressing *P71* and *P71* mRNA or *P71* alone, where only p71 was detected (Figure 3.11, lanes 1 and 3). This suggested that the presence of HaSV RNA2 stimulated the spontaneous maturation of VLPs. This could be as a consequence of the cells inducing apoptosis because of the metabolic load imposed on the cells by expressing high concentrations of RNA2.

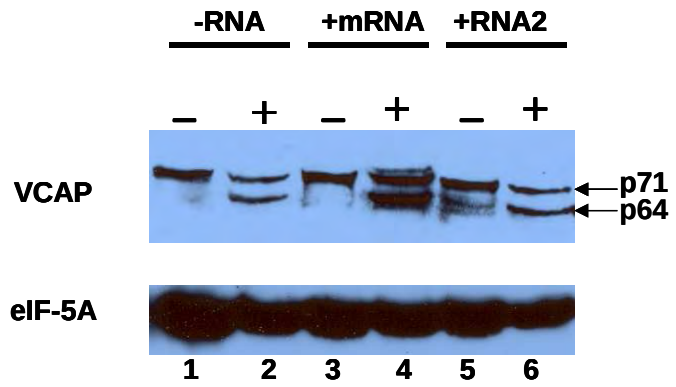

Figure 3.11 Maturation of procapsids purified from cells co-expressing medium-level *P71* and viral RNA. Western analysis of total yeast lysates prepared from cells co-expressing medium-level *P71* (pAV3) with *P17* mRNA (+mRNA), P_{GAL1}-derived RNA2 (pMT22L) or without RNA (-RNA), grown in galactose-induction medium for 12 hours at 28ºC. Cells were then treated with (+) or without (-) 80 mM acetic acid for 200 minutes at 28ºC. Arrows indicate the position of bands migrating at an approximately molecular weight of 64 kDa (p64) and 71 kDa (p71). Blots were either probed with anti-HaSV (VCAP) or anti-eIF-5A (eIF-5A) antibodies respectively.

3.3.5 p71 solubility in the presence of viral RNA

To determine whether an increase in RNA levels would influence p71 solubility, yeast cells expressing P_{GADH}–derived *P71* (pMT9) were co-transformed with plasmids pMT9-AUG or pMT29, which express either *P71* mRNA or RNA2 under control of $P_{GADH.}$ Western analysis showed that the co-expression of RNA2 resulted in substantially higher levels of total p71 and p64, as compared to cells co-expressing *P71* with *P71* mRNA or *P71* alone (Figure 3.12, A, lanes 5 and 6). In cells expressing *P71* only or co-expressing *P71* and mRNA, the majority of both p71 and p64 appeared to remain in the insoluble fraction (Figure 3.12, A, lanes 1 and 3 versus 2 and 4). However, in the case of cells co-expressing *P71* and RNA2, a significant increase in the levels of soluble p71 and p64 were observed with more than 50% of the protein remaining in the soluble fraction (Figure 3.10, A, lanes 5 and 6). The difference in the amounts of protein detected cannot be as a consequence of different protein levels loaded onto the blot (Figure 3.12, C). The presence of HaSV RNA2 significantly increases the solubility of both p71 and p64 in the yeast cells and consequently VLP assembly and maturation.

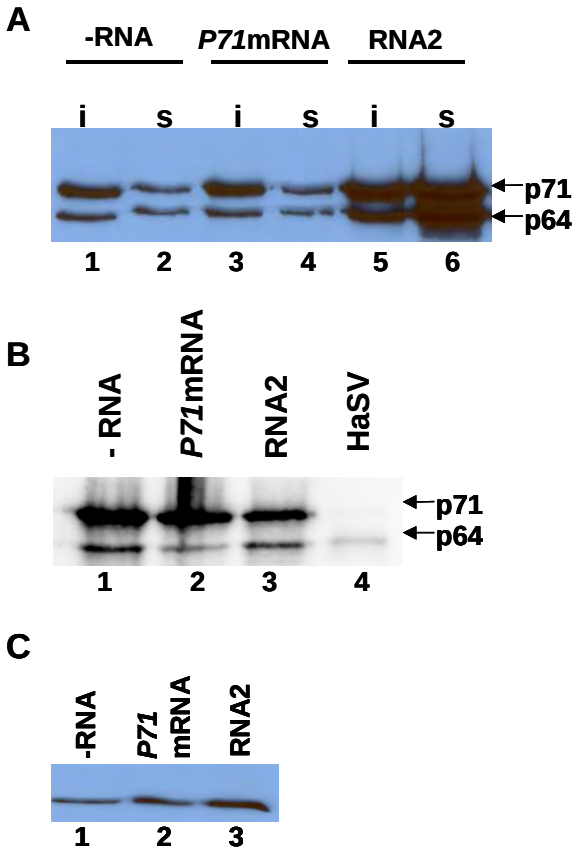

Figure 3.12 Effect of the presence of viral RNA on the solubility of VLPs. Western analysis of total yeast lysates (i), soluble yeast lysates (s) (**A**) or VLPs purified through a 10-40% sucrose gradient (**B**), prepared from cells co-expressing high level *P71* with (*P71* mRNA/RNA2) or without (-RNA) viral RNA under glucose-starvation conditions at 28ºC for 48 hours. Blots were either probed for p71/p64 with anti-HaSV (**A** and **B**) or for eIF-5A with anti-eIF-5A (**C**) antibodies respectively. Arrows indicate the position of bands migrating at an approximately molecular weight of 64 kDa (p64) and 71 kDa (p71).

Yeast cells expressing *P71* with or without viral RNA (*P71* mRNA or RNA2) were subjected to VLP purification to determine whether or not the presence or absence of viral RNA was affecting the efficiency of VLP assembly. Western analysis of samples collected from the sucrose gradients showed the presence of both p71 and p64 in approximately the same concentration in all three samples, indicating the presence of both procapsids and mature capsids (Figure 3.12, B). The relatively high concentration of p71 remaining after VLP purification indicated that these particles may represent a proportion of p71 which were either able to assemble, but did not mature, or were aberrant VLPs. These results indicate that the HaSV RNA improved the solubility of the VLPs, but did not necessarily improve assembly of the VLPs. This is similar to what was observed before (chapter 2).

3.3.6 Encapsidation of viral RNA

VLPs were purified from cells co-expressing *P71* in the absence or presence of viral RNA, which were incubated in glucose-starvation medium for 48 hours and then treated with acetic acid for 200 minutes to induce maturation *in vivo* to stabilize the VLPs. Western analysis of the VLP preparations revealed that only capsid protein was present whether additional RNA was expressed or not implying the presence of mature VLPs (Figure 3.13). This was in contrast to earlier experiments where both p71 and p64 could be detected when cells expressing *P71* were not treated with acetic acid (Figure 3.12, B). The presence or absence of viral RNA had no added effect on the ability of the VLPs to assemble and subsequently mature.

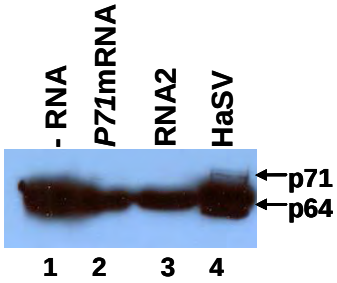

Figure 3.13 Western analysis of HaSV VLPs prepared from cells co-expressing *P71* and viral RNA. The VLPs were purified from cells expression *P71* with (*P17*mRNA or P_{GADH}-dependent RNA2) or without (-RNA) one of the RNA transcripts as indicated. Cells were incubated in SMM with 0.1% glucose for 48 hours at 28°C. Acetic acid was added to a final concentration of 80 mM and the culture was incubated for 200 minutes at 28°C.

TEM analysis of the purified VLPs revealed that the there was a wide distribution of particle in terms of both size and shape in the different experimental systems (Figure 3.14, A-D and E). When no additional viral RNA was expressed, the majority of particles (40%) had a diameter of 32 nm and a mean diameter of 30 nm (Figure 3.14, A 1-4). These particles were semicircular in shape and 8 nm smaller on average than wild-type HaSV (30 nm versus 38 nm). These particles may represent a species, which encapsidate random cellular RNAs. Additionally the surface morphology of these particles was different to wild-type HaSV. No predominant surface features were detected on the particles, which appeared smooth in texture compared to the pitted surface structure of wild-type HaSV particles (Figure 3.14, Compare A4 to

D4). In contrast when *P71* mRNA was expressed with *P71*, the majority of particles (62%) were 38 nm in diameter, varied in shape to wild-type HaSV and thus did not represent the customary icosahedral symmetry (Figure 3.14, B2-4 and E).

When *P71* mRNA was co-expressed, 15% of the particles were less than or equal to 32 nm in diameter, while 23% of the particles were greater than or equal to 44 nm in diameter. A large proportion of particles in this sample were aberrant (Figure 3.14, B1). In contrast when RNA2 was co-expressed, 35% of particles were 32 nm or smaller and 18% were 44 nm and larger (Figure 3.14, C and D). Similarly, the majority of particles were 38 nm in diameter (47%) (Figure 3.14, compare C4 to D4). A proportion of the particles were aberrant. These particles also had a wide assortment of shapes, but few were miss formed or appeared to have collapsed, as was observed when *P71* mRNA was co-expressed. Particles purified from cells co-expressing viral RNA had the largest size distribution.

These results signified that HaSV particle assembly is affected by the increased presence of viral RNA. The wide size distribution seen when viral RNA was expressed with *P71* may represent particles which co-packaged cellular RNA and viral RNA, with the RNA dictating the final shape of the virus. In order to determine the species of RNA encapsidated in the VLPs, RNA was purified from the VLPs. The RNA was then subjected to Northern analysis and the blots were probed for viral RNA to determine if the VLPs specifically encapsidated their own RNA.

Initially it was important to determine if the viral RNA was being expressed off the expression constructs. Total yeast RNA was analysed by Northern analsysis after an incubation time of 24 hours and 48 hours. Both *P17* mRNA and RNA2, at nucleotides 1941 and 2489 respectively, were detected from the total yeast lysates (Figure 3.15, A, lanes 1-4). The levels of RNA decreased from 24 to 48 hours, which was most likely due to mRNA degradation in the yeast cells (Figure 3.15, A, lanes 2 and 4).

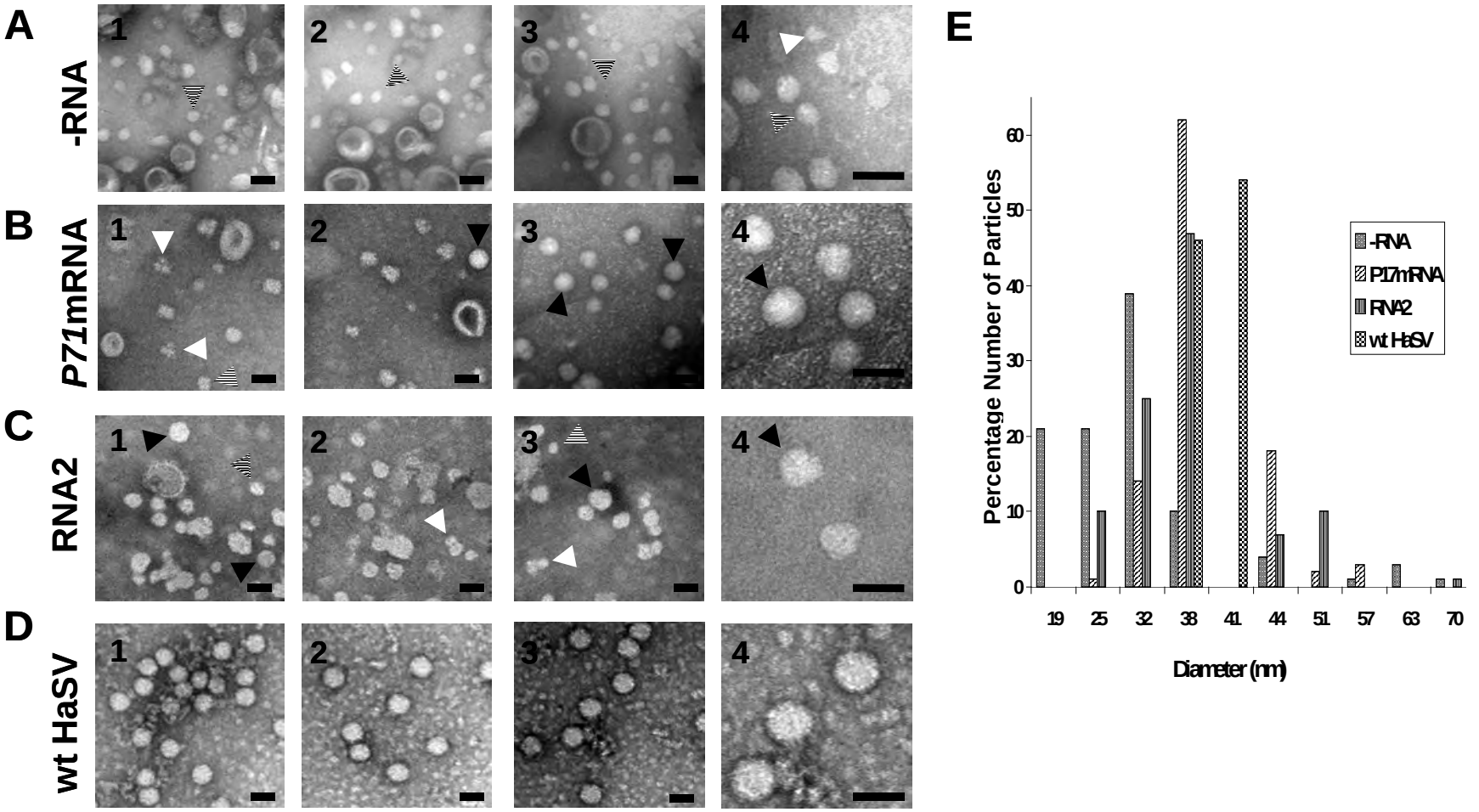

Figure 3.14 Effect of co-expressing viral RNA on HaSV VLP assembly. (**A-D**) Transmission electron micrograph and (**E**) size distribution of virus particles from 100 particles counted. Solid black and white arrows indicate particles that closely resemble wild-type HaSV particles or miss formed particles respectively. Stripped arrows indicate particles that are significantly smaller than wild-type HaSV particles. The VLPs were purified from cells expression *P71* without (-RNA; **A**) or with (*P17*mRNA; **B** or P_{GADH}-RNA2; **C**) one of the RNA transcripts as indicated. Cells were incubated in SMM with 0.1% glucose for 48 hours at 28°C, 80 mM acetic acid was added and the culture incubated for a further 200 minutes at 28°C. The bar represents 50 nm in each micrograph.

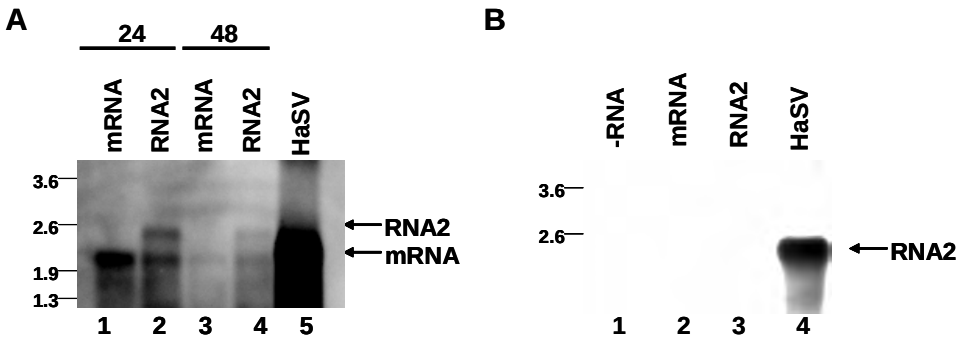

Figure 3.15 HaSV VLPs do not have the ability to encapsidate transcribed *P71* mRNA and RNA2 in yeast. (**A**) Northern analysis of total RNA extracted from cells expressing *P71* with *P17* mRNA or RNA2 in glucose–starvation medium for 48 hours at 28ºC probed for (+) RNA2. (**B**) Northern analysis of RNA extracted from VLPs which were purified through a 10-40% sucrose gradient from cells expressing *P71* with or without viral RNA (*P17* mRNA/RNA2) probed for (+) RNA2 as indicated above.

Next, RNA was extracted from 7 μg of VLPs purified from each experimental system and probed for the presence of the HaSV *P71* coding sequence, using a negative sense RNA2 probe corresponding to nucleotides 2309-766 of the *P71* coding sequence (Appendix 2, Figure A2.2). No HaSV RNA was detected in any of the VLPs purified from the yeast expression systems (Figure 3.15, B, lanes 1-3). Only the positive control was detected, which represented 42 ng of genomic RNA extracted from 2.45×10^{11} particles (Figure 3.15, B, lane 4). Approximately 1.5 μg of RNA was loaded from each VLP preparation, which represented RNA from 1.75×10^{11} particles. So if the amount of viral RNA required for detection by Northern analysis was 42 ng, then less than 2.8% of the total RNA from each viral RNA preparation (expressing RNA2 and *P71*) represented viral RNA. This would indicate that less than 4.38×10^{9} particles encapsidated RNA2 or mRNA. If approximately half of the particles purified from cells expressing *P71* and viral RNA represented wild-type HaSV (approximately 50% of particles had a diameter of 38 nm), and its assumed that these particles encapsidated viral RNA only, then less than 2.2×10^{9} particles contained viral RNA. These results indicated that the majority of the RNA species encapsidated by the VLPs represented cellular RNA. This data indicates that the VLPs produced in yeast do not encapsidate viral RNA specifically.

3.4 DISCUSSION

Viral RNA was thought to play a crucial role in the assembly of omegatetraviruses as genomic RNA has been shown to be an essential component of the inner capsid shell in other RNA viruses (Fisher and Johnson, 1993; Tang *et al*., 2001). NωV and HaSV have been shown to package their own mRNA by a replication-independent mechanism and the authors hypothesised that the message contained encapsidation signals (Agrawal and Johnson, 1995; Gordon *et al*., 2001). Similarly it was believed that viral RNA was the rate-limiting component during assembly. It was expected that the HaSV VLPs would specifically encapsidate viral RNA in the yeast cells. To answer this question *P71* was co-expressed with viral RNA.

3.4.1 Viral RNA and VLP assembly

Data presented in this chapter shows that efficient VLP assembly in yeast cells requires a threshold concentration of p71. The increase in p71 levels detected in crude cell extracts when viral RNA was expressed with medium-level *P71* indicated that the RNA might offer p71 limited stability. In some way the RNA may play a role in protecting p71 from proteolytic degradation *in vitro*, prehaps by increasing the solubility of p71. This was shown to be true when high levels of both RNA2 and *P71* were co-expressed. The eventual disappearance of p71 however suggested that the protein was degraded by proteolysis. A more logical argument was that the increased levels of RNA expressed caused a shock response in the cells. This would cause the expression of a toxic response, which would improve the folding of p71, making it more soluble.

Expression of high-level *P71* and *P71* mRNA appeared to improve the assembly of the VLPs. The spontaneous maturation of p71 in this system indicated that high-levels of viral RNA might induce apoptosis through the increased metabolic load of expressing two genes within the same cell. The continued presence of p71 even after VLP purification indicated that the p71 which remained, had assembled. The inability of the particles to mature indicated that they may require an acidic pH. *In vivo* maturation with acetic acid successfully matured the remaining p71. The levels of p64 detected were similar when increased levels or no additional viral RNA was

expressed. This indicated that the viral RNA ultimately had no effect on the efficiency of assembly of the VLPs. This result substantiates the previous observation that chaperone proteins (elicited by a shock response imposed by expression of additional RNA) enabled improved protein folding which led to the increased stability (Santoro, 1996).

The fact that the VLPs did not encapsidate either mRNA or RNA2 indicate that the packaging mechanism of the VLPs was random. It appeared that the VLPs had the ability to assemble without any detectable viral RNA. This indicates that the particles must have encapsidated cellular RNAs as omegatetraviruses and nodaviruses do not form empty particles devoid of RNA (Fisher and Johnson, 1993; Agrawal and Johnson, 1995). This result contradicts those of Agrawal and Johnson (1995), who reported that baculoviral-derived NωV VLPs encapsidated *P70* mRNA. The concentrations of viral RNA produced in yeast may have been insufficient for encapsidation of their RNA. Considering that baculoviral expression of heterologous proteins may represent a 3-fold increase in expression levels when compared to yeast expression using P_{GADH} (Cousens *et al*., 1987; Miller, 1988). This could be one possible reason why the capsid encoding sequence of NωV was encapsidated in baculoviral-derived VLPs (Agrawal and Johnson, 1995).

In the absence of replicating RNA the HaSV VLPs may encapsidate random RNAs. Replication-dependent encapsidation is required in FHV (Venter *et al*., 2005; Venter and Schneemann, 2007). In the absence of replication the FHV VLPs encapsidate cellular RNA (Venter and Schneemann, 2007). This requirement for replication competent transcripts ensures that the RNA and capsid subints are in association with one another (Venter *et al*., 2005). The omegatetraviruses may co-package their genome, like the nodaviruses (Schneemann *et al*., 1994; Krishna and Schneemann, 1999). In the absence of RNA1, RNA2 may not be packaged.

Another possibility is that the additional 5’ extension on the RNA2 may have interfered with its ability to be encapsidated. The exact transcriptional start of the hybrid promoter used for the expression of high-level HaSV RNA2 is unknown. It is

possible that a number of additional nucleotides exist at the 5' end of the mRNA, which could interfere with viral RNA encapsidation.

3.4.2 VLP morphology

TEM analysis revealed that the there was a wide distribution of VLP sizes in the presence or absence of viral RNA. A significantly higher proportion of VLPs with a diameter of 38 nm in size (which correspond to wild-type virus particles) were detected when additional viral RNA was expressed with *P71* compared to when no additional RNA was expressed with *P71*. In contrast the majority of particles (39%) purified from the control (expression of *P71* alone) were 32 nm in diameter. In some instances the particles appeared to be aberrant, which could have been as a consequence of these particles failing to encapsidate RNA. This RNA is believed to stabilise the interior of the particle (Munshi *et al*., 1996; Helgstrand *et al*., 2004). The distribution of particle sizes may be a result of mismaturation (Taylor, 2003) as a result of the particles encapsidating random RNAs. Therefore, it is possible that the RNA may dictate the overall assembled intermediate and the way in which the particles mature.

The formation of *T*=1 particles has been elucidated by the cryoEM reconstruction of baculovirus-derived HaSV VLPs purified at pH of 6.0 (Taylor, 2003). These particles were missing their γ–peptide and thus only bent contacts could form between the subunits. This would dictate that they only had the ability to form the *T*=1 arrangement. In addition the interior of these particles contained disordered RNA. In contrast, cryoEM image reconstruction of HaSV *T*=4 particles purified at pH 5.0 revealed that RNA forms a highly ordered structure. This is similar to the scenario in PaV particles (Tang *et al*., 2001; Taylor, 2003). The structure of HaSV procapsids at pH 7.6 and the subsequent transition to mature capsids at pH 5.0 was almost identical to the model elucidated for NωV VLPs by Canady *et al.* (2000). Taylor (2003) also purified an intermediate particle (like NωV), which did not represent procapsids or mature capsids. It is possible that both the *T*=1 and larger intermediate particles were purified in this study. The *T*=1 particles had a diameter of 24 nm (Taylor, 2003), which could represent the VLPs purified when no additional viral RNA was co-expressed with *P71*.

A similar result was obtained for the *T*=4 *Aura virus* (AV) and *T*=3 *Brome mosaic virus* (BMV), where formation of the particles was a direct consequence of the type of RNA encapsidated (Krol *et al*., 1999; Zhang *et al*., 2002). In the case of BMV, the *T*=3 quasi-equivalent symmetry of wild-type BMV was achieved when genomic RNA was packaged. BMV particles which encapsidated random mRNAs formed particles with a *T* =2 quasi-equivalent symmetry. The viral RNA was hypothesised to nucleate the capsid subunits which are only associated through weak hydrophobic interactions when viral RNA was not present (Krol *et al*., 1999). Similarly, *Hepatitis B virus* forms *T*=3 and *T*=4 particles under certain conditions and bromoviruses have been shown to form *T*=1 and even larger *T*=4 or *T*=7 particles (Lane, 1981; Zlotnick *et al*., 1996). These larger *T*=7 particles have also been shown to form in bacteriophage P22 particles (Thuman–Commike *et al*., 1998). So in terms of this study, the different sized particles most likely represent particles with different quasi-equivalent symmetries. The large distribution of particles could represent *T*=1, *T*=2, *T*=3 and *T*=7 symmetry, where the structure of the particle was dictated by the RNA they encapsidated.

The high–levels of p71 produced from the hybrid promoter ensure that there was an abundance of subunits in association with one another. An acidic pH has been shown to drive the maturation event in particles. It seems that the symmetry of these particles may be tightly regulated by the RNA they encapsidate and a certain complement or size of encapsidated RNA ensures formation of particles with a *T*=4 conformation. In essence the acidic pH forces the particles to mature even if they are assembled in a different way to wild-type virions.

CHAPTER 4. EXPLOITING THE POTENTIAL OF NODAVIRAL REPLICATION SYSTEMS FOR THE ASSEMBLY OF OMEGATETRAVIRUS VLPs

CHAPTER 4. EXPLOITING THE POTENTIAL OF NODAVIRAL REPLICATION SYSTEMS FOR THE ASSEMBLY OF OMEGATETRAVIRUS VLPs

4.1 INTRODUCTION

The inability of the virus particles to encapsidate viral RNA may be a consequence of the insufficient RNA levels produced by transcription. The virus particles may require a replication-dependent encapsidation mechanism to specifically package viral RNA. Replication would ensure that the RNA and capsid protein are present at high concentrations in the vicinity of one another.

In Chapter 3, it was shown that HaSV VLPs assembled in yeast cells did not specifically encapsidate capsid mRNA or HaSV RNA2. There are several potential explanations including: (1) the effect of small non-viral extensions at the 5' end of the RNA2 transcript; (2) RNA encapsidation requires the presence of a further factor such as, for example, a host factor (3) as in the nodaviruses, tetravirus RNA encapsidation is replication-dependent; (4) or as in the nodaviruses, the omegatetraviruses use a co-packaging mechanism where both RNA1 and RNA2 are required for viral RNA packaging.

The nodaviruses are infectious and replicate their genomes in a wide variety of cells which include insects, plants, mammals and yeast (Scotti *et al*., 1983; Selling *et al*., 1990; Ball *et al.,* 1992; Price *et al*., 1996; 2005). In yeast, the levels of replicating RNA produced approach the levels of ribosomal RNA and the levels of FHV RNA1 and RNA3 replicated in yeast can represent as many as 32 000 and 120 000 copies per cell respectively (Price *et al*., 1996; 2005). The relative ratios of the RNA molecules replicated are similar to what was reported for *Drosophila* cells (Price *et al*., 1996; 2000). The ability of FHV and NoV to produce very high levels of RNA during replication in yeast has been exploited to produce heterologous proteins (Price *et al*., 2002; 2005). Unlike RNA1, the only regions important for FHV RNA2 synthesis appear to be within the first 14 nucleotides, the last 50 to 60 nucleotides and an internal region between nucleotides 538 and 616 (Ball and Li, 1993; Ball *et*

al., 1994). Price *et al*., (2005) showed that nucleotides 53 to 423 were dispensable for NoV RNA2 replication. Thus, as long as these sequences are present, heterologous sequences inserted into the FHV or NoV RNA2 will be replicated by the viral replicase (Price *et al*., 2002; 2005) By fusing the *HIS3* gene to the first 11 amino acids of the capsid-encoding sequence of FHV and NoV in RNA2, the growth of the yeast strain in the absence of histidine was dependent on the RNA molecule being replicated by the viral replicase (Price *et al*., 2002; 2005). A similar result was obtained by constructing a RNA2-based replicon for the replication-dependent synthesis of *URA2* (Price *et al*., 2002).

Dorrington *et al*. (2007) explored the possibility of using these nodavirus replication systems to replicate HaSV and NωV capsid-encoding sequences in yeast cells. The FHV and NoV capsid-encoding sequences were replaced with the capsid-encoding sequence of either HaSV or NωV while retaining the 5' and 3' ends of RNA2 required for nodavirus RNA1-dependent replication (Figure 4.1). The *GAL1* promoter, for which the transcription start is well characterised (Johnson and Davis, 1984), and the *Hepatitis delta virus* (HDV) ribozyme were used to ensure the transcripts carried the correct 5' and 3' ends, respectively.

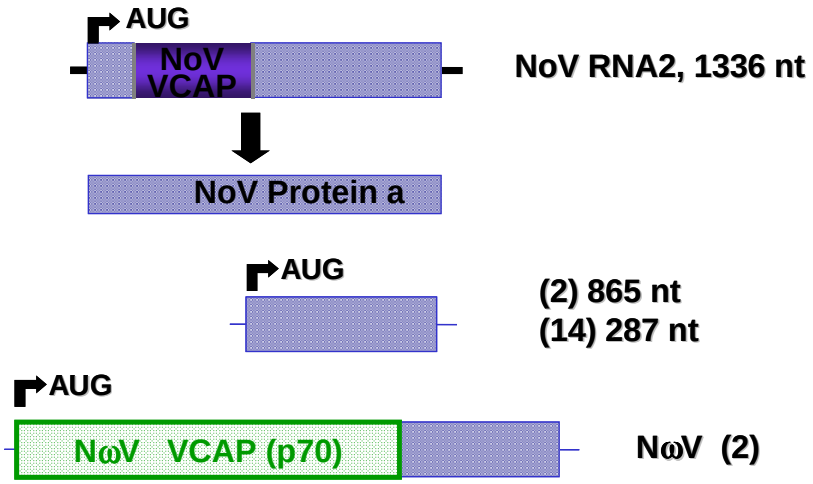

Figure 4.1 Schematic representation of the recombinant system designed for NoV-based replication of NωV *P70* designed by Dorrington *et al*. (2007). The capsid encoding sequences, *P70*, was fused upstream from the first 14 nucleotides and downstream from either the last 287 (14) or 865 (2) nucleotides of NoV RNA2, replacing the NoV VCAP. (2) and (14) are related to the Northern blot (Figure 4.2) indicating constructs with the last 287 or 865 nucleotides of NoV RNA2 upstream from NωV *P70*.

The replication system of FHV has been one of the most excessively studied ss (+) RNA virus. For this reason Dorrington *et al*. (2007) wanted to determine if the FHV RNA1-derived RdRp had the ability to replicate the FHV RNA2-HaSV (*P71*) or NωV (*P71*) chimeras *in vivo*. The levels of positive sense RNA2 detected from both chimeras were low, with higher levels of the NoV RNA2-based *P70* chimera being detected when compared to the *P71* construct (Figure 4.2). The levels of positive sense RNA2 detected for the positive control were significantly higher than the two RNA2 chimeras (Figure 4.2).

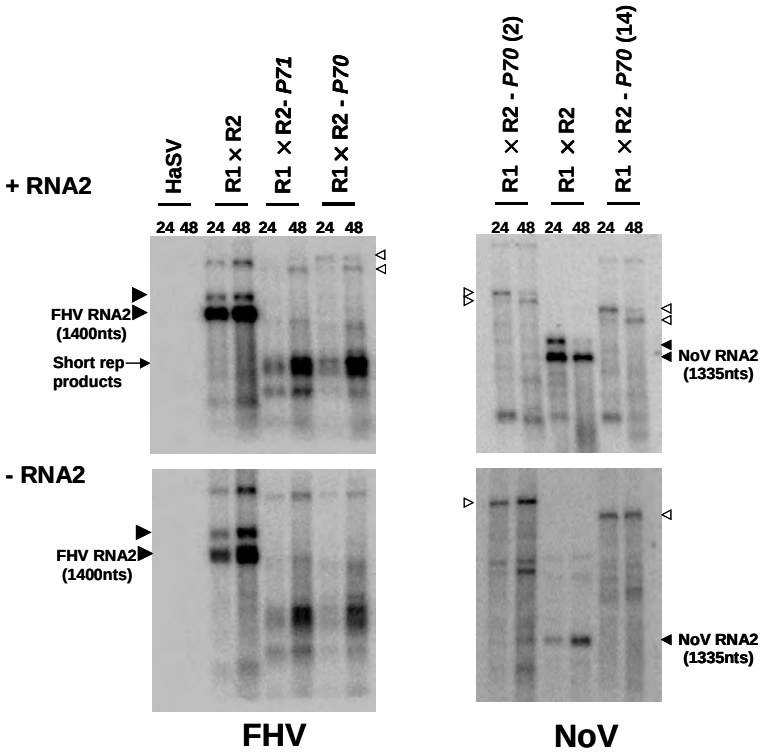

Figure 4.2 Northern blot analysis of transcription-derived FHV and NoV RNA2 replication in yeast cells. The blots were either probed for positive (+RNA2) or negative (-RNA2) sense FHV/NoV RNA2 from plasmid-initiated RNA2 replication as indicated. RNA from yeast cells expressing either wild-type FHV or NoV RNA1 (R1) in conjunction with either wild-type FHV or NoV RNA2 (R2) or a HaSV or NωV capsid precursor RNA2 chimera (R2-*P71* or R2-*P70* respectively) are shown. The solid and open arrows indicate the relative positions of +/- sense wild-type RNA2 or the +/- sense NoV RNA2NωV/HaSV chimera respectively. The primary transcripts that have not been cleaved by the HDV ribozyme are also shown. The shortened FHV RNA2 chimeric replication products generated by the FHV replicase are shown (Dorrington *et al.*, 2007).

It appeared that the chimeras were being replicated inefficiently. A high concentration of truncated products were detected (Figure 4.2), indicating that the

FHV RdRp constantly produced shortened transcripts. This indicated that the *P71* and *P70* genes were not compatible with the FHV RdRp. There was some evidence that negative sense RNA2 could be detected for the two chimeras, indicating that the RNAs had the ability to replicate in the yeast cells.

The production of truncated replication products led Dorrington *et al*. (2007) to determine whether the NoV replication system would efficiently replicate omegatetravirus capsid-encoding sequences. The observation that higher levels of the NωV-based RNA2 chimera were replicated when compared to the HaSV-based RNA2 chimera, led to the investigation of possibility using the NoV replication system for NωV *P70* only (Figure 4.2). Two NωV constructs were investigated for their potential to be replicated by the NoV RNA1-dependent replicase. The constructs contained the first 18 nucleotides of the NoV RNA2 5' sequence, followed by the NωV *P70* sequence downstream from either the last 865 nucleotides (2) or 287 nucleotides (14) of NoV RNA2 (Figure 4.1). Positive and negative sense RNA2 were detected for both chimeras. The presence of the negative strands indicated that both constructs were replicating *in vivo* (Figure 4.2). No truncated RNA products were observed suggesting that the NoV replication system was compatible with the NoV RNA1-dependent replicase. In addition, the NoV replication system had the ability to replicate an RNA2-based chimera containing the *P70* cDNA.

This chapter describes a NoV replication system for the *de novo* synthesis of omegatetravirus VLPs with the aim of determining if replication results in the specific encapsidation of viral RNA.

4.2 MATERIALS AND METHODS

4.2.1 Microbial strains and culture conditions

Yeast strain INVScI was used for P_{GADH}-derived *P70* expression. Yeast strain BY4733 (*Mat*α, *his3*Δ200, *leu*2Δ0, *met*15Δ0, *trp*1Δ63, *ura*3Δ0) (Brachmann *et al*., 1998) was used for the P_{GAL1}-derived expression of NoV RNA1, NoV RNA2 and the NoV RNA2-NωV *P70* chimera. Strain INVScI was maintained on SMM

(Appendix 6) agar (1.5%) with 0.002% histidine, 0.002% tryptophan, 0.01% leucine (Sigma) and 2% glucose (volume/volume) to select for pMT13 (section 4.4), which carries a *URA3* auxotrophic marker (Kaiser *et al*., 1994). Strain BY4733 was maintained on SMM agar (1.5%) with 0.002% histidine, 0.002% uracil, 0.002% methionine (Sigma) and 2% glucose (volume/volume) to select for plasmids with *LEU2* and *TRP1* auxotrophic markers. Transformations, patching of colonies and the method of inoculation into liquid media were performed as described in Section 2.2.5.

4.2.2 Yeast expression constructs

Expression plasmids used in this study are listed in Table 4.1. Plasmid TpGN1 carries the complete NoV RNA1 encoding the replicase gene cloned into the vector Tp with a *TRP1* selectable marker (Figure 4.3). Plasmid LpGN2 encodes the complete NoV RNA2 cloned into the vector Lp with a *LEU2* selectable marker (Figure 4.3).

Table 4.1 Characteristics of expression constructs used in this chapter.

Plasmid Name	Yeast Origin of replication	Selectable Marker	Promoter	cDNA	Reference
TpGN1	2μ	*TRP1*	P_{GAL1}	NoV RNA1	Price *et al*., 2005
LpGN2	2μ	*LEU2*	P_{GAL1}	NoV RNA2	Price *et al*., 2005
LpGNωV	2μ	*LEU2*	P_{GAL1}	NoV RNA2-NωV *P70* chimera	Dorrington *et al*., 2007
pMT13	2μ	*URA3*	P_{GADH}	NωV *P70*	This study

The NωV *P70* coding sequence was expressed from pMT13. The plasmid LpGNωV contains the NωV capsid coding sequence flanked by the first 18 nucleotides of NoV RNA2 at the 5' end and the last 865 nucleotides of NoV RNA2 at the 3' end (Figure 4.3).

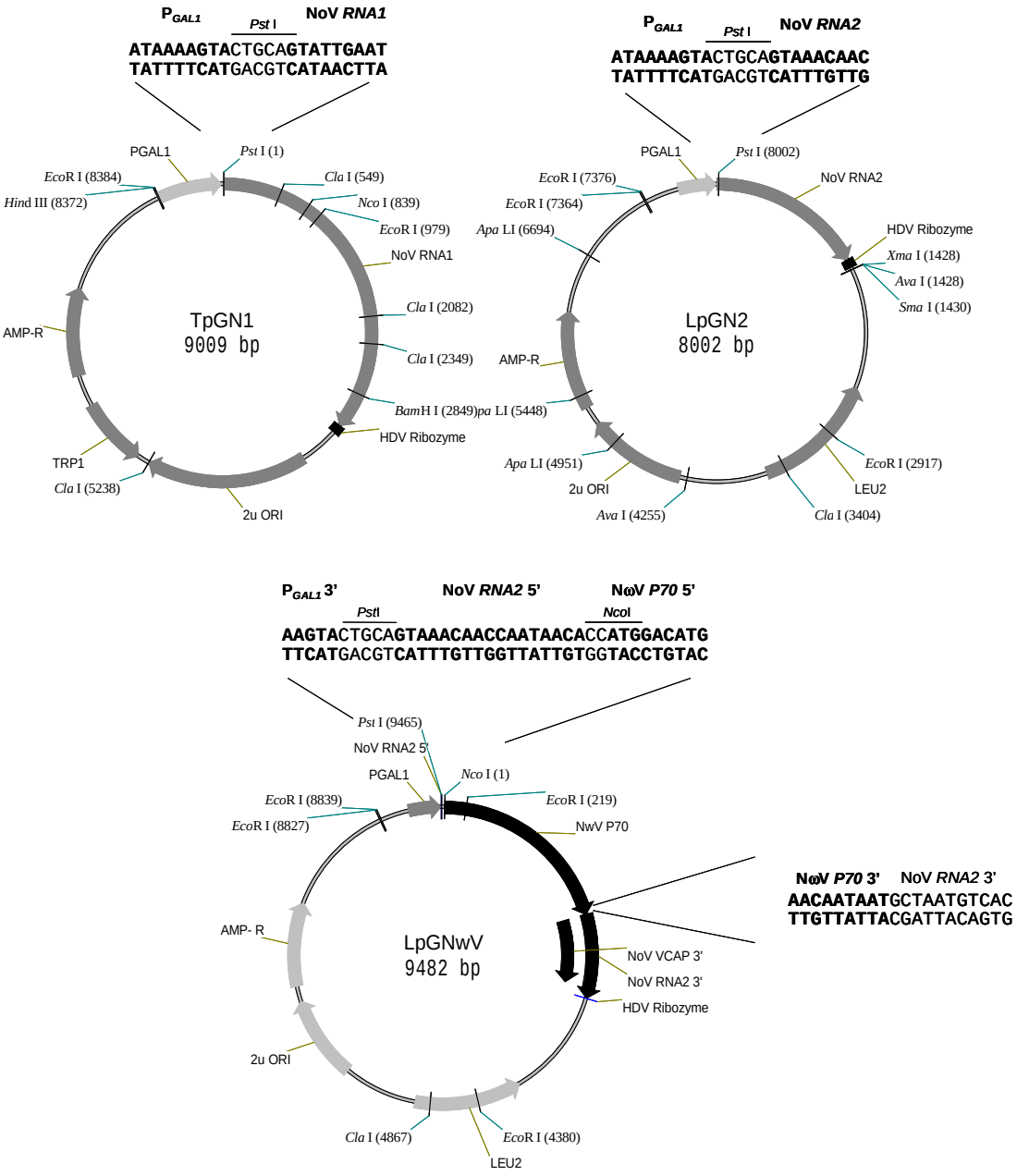

Figure 4.3 Diagrammatic representation of plasmids TpGN1, LpGN2 and LpGNωV used for the expression of NoV RNA1, NoV RNA2 and a NoV RNA2-NωV *P70* chimera respectively. The vectors contain a *LEU2* or *TRP1* auxotrophic marker and all vectors contain a *Hepatitis delta virus* ribozyme (HDV ribozyme) for production of authentic 3' ends and a gene encoding a β-lactamase enzyme for ampicillin resistance (AMP-R).

4.2.3 Construction of NωV *P70* expression vector, pMT13

Plasmid pFBωIIILG, which carries the *P70*-encoding cDNA sequence (du Plessis *et al*., 2005), was used to construct the *P70* expression vector pMT13. A 1448 bp *Bam* HI / *Sma* I fragment was excised from pFBIIILG1, representing the first 1440 nucleotides of the NωV *P70* coding sequence, was inserted into the same restriction sites of pAV16MT, generating pMT10 (Figure 4.4, Step I). The 236 bp sequence between the *GAPDH* translational start and the translational start of p70, was deleted by reverse PCR inserting an optimal Kozak sequence for efficient translational using primers MT5 (Appendix 4; Table A4.1) and MT2 (Appendix 4; Table A4.1) (Figure 4.4, Step II). A 762 bp *Bcl* I / *Eco* RI fragment from the resulting plasmid (pMT11), was inserted into pMT4 (Figure 4.4, Step III). Next, a 1889 bp *Eco* RI / *Xho* I fragment representing the remainder of the *P70* coding sequence was inserted into pMT12, generating pMT13 (Figure 4.4, Step IV). The expression construct pMT13 is a multicopy vector for the P_{GADH}-derived expression of *P70* and carries a *URA3* auxotrophic marker.

4.2.4 *P70* expression

INVScI cells were transformed with pMT4 or pMT13 and plated onto SMM agar (1.5%) with 0.002% histidine, 0.002% tryptophan, 0.01% leucine and 2% glucose. The transformants were incubated at 28°C for 3 days and patched as indicated before. Patched cells were re-suspended into a small volume of $dddH_2O$ and inoculated into SMM with 0.002% histidine, 0.002% tryptophan, 0.01% leucine, 0.1% glucose and 5% glycerol at an OD_{600nm} of 0.1. The culture was initially incubated at 28°C for 12 hours. Ethanol was then added to a final concentration of 3% or no additional carbon source was added (carbon-limiting). The culture was incubated at 28°C and p70 expression monitored by removing two OD_{600nm} units of culture at specific intervals. Total yeast lysates were prepared as indicated before (section 2.2.6) for Western analysis and all blots were probed with anti-NωV antibodies.

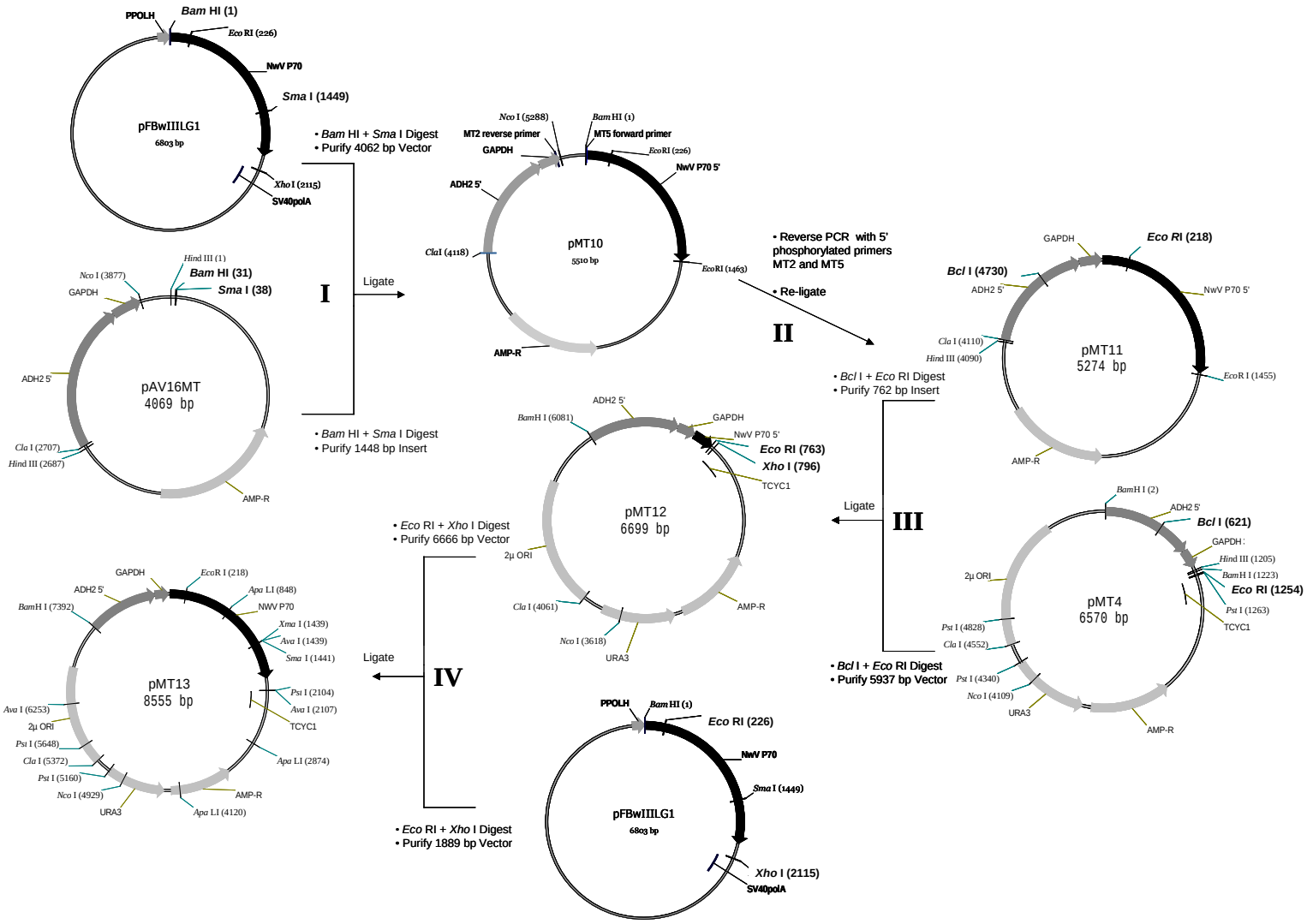

Figure 4.4 Diagrammatic representation of the construction of the NωV *P70* expression vector, pMT13. The restriction enzymes utilized for each cloning step are highlighted in bold font and the steps followed represented by Roman numerals. The 5' end of the *ADH2* promoter and 5'end of the *GAPDH* untranslated region are represented by *ADH2* 5' and *GAPDH* respectively. NωV *P70* refers to the capsid encoding sequence for NωV and AMP-R refers to a gene that encodes a β-lactamase enzyme for ampicillin resistance.

4.2.5 Transcription–dependent NoV replication of a NoV RNA2-NωV *P70* chimera.

BY4733 cells were co-transformed with TpGN1 (NoV RNA1) and either LpGN2 (NoV RNA2), LpGNωV (NoV RNA2-NωV*P70* chimera) or Tp. The transformants were plated onto SMM agar (1.5%) with 0.002% histidine, 0.002% methionine, 0.002% uracil and 2% glucose. The plates were incubated at 28°C for 3 days and patched as described before. Patched cells were re-suspended in a small volume of sterile dddH_2O and inoculated into SMM with 0.002% histidine, 0.002% methionine, 0.002% uracil, 0.1% glucose and 2% galactose at an OD_{600nm} of 0.1. The cells were incubated at 28°C and p71 production monitored by removing two OD_{600nm} units of culture at 24 hours and 48 hours incubation. Total and soluble yeast lysates were prepared as discussed previously (section 2.2.6) for Western analysis. Blots were probed with anti-NωV antibodies obtained from Professor Donald Hendry (Department of Microbiology, Biochemistry and Biotechnology, Rhodes University).

4.2.6 Northern analysis.

Total yeast RNA was purified from ten OD_{600nm} units of cell culture using a hot phenol method described by Leeds *et al*., (1991) (section 3.2.4). RNA was purified from sucrose gradient purified NωV VLPs using the RNAgents™ kit (Promega) according to the manufacturer's instructions.

Strand-specific ^{32}P-ATP-labeled RNA probes were generated by *in vitro* transcription of a PCR product containing bacteriophage RNA polymerase T7/SP6 using the Riboprobe™ kit (Promega) (Price *et al*., 2005). The appropriate sense NoV RNA1 and RNA2 probes corresponded to nucleotides 2732 to 3204 and nucleotides 1100 to 1336 respectively (Price *et al*., 2005). To synthesise the negative sense NωV RNA2 probe plasmid pCW17R (Cheryl Walter, Rhodes University, Figure 4.5) was linearised with *Nco* I and transcribed by *in vitro* transcription with [α-^{32}P]-CTP using SP6 RNA polymerase (Riboprobe kit™, Promega). Excess radioisotopes, dNTPs and salts were

removed using the QIAquick PCR Purification Kit (Qiagen). The purified total yeast RNA or RNA purified from the VLPs was resolved on a 1% agarose gel containing 2% formaldehyde at 120 volts for approximately 2.5 hours in 1 × MOPS buffer. After electrophoresis the RNA was transferred by capillary transfer to a Hybond N+ nylon membrane (Amersham) in 20 × SSC buffer (Appendix 7, A7.3). The membrane was briefly rinsed in 2 × SSC and then baked at 80°C for 2 hours. After incubation the membrane was place in a hybridisation bottle to which pre-heated (65°C) hybridization solution (Appendix 7, A7.3) was added and the membrane allowed to pre-hybridise at 60°C for 4 hours with rotation. The solution was poured off and fresh pre-warmed hybridisation solution added, which contained 2×10^6 cpm of radiolabelled probe. Hybridisation was allowed to proceed overnight with rotation at 60°C. After incubation the membrane was briefly rinsed in wash buffer (0.2% SSC and 0.2% SDS) at room temperature and then washed twice at 65°C for 2 to 4 hours. The membrane was dried with 3MM Watmann, wrapped in cling wrap and exposed to a Phosphor storage screen (Amersham Biosciences). The image on the screen was processed using a Molecular Dynamics PhosphorImager and quantitated using ImageQuant software (Amersham Biosciences).

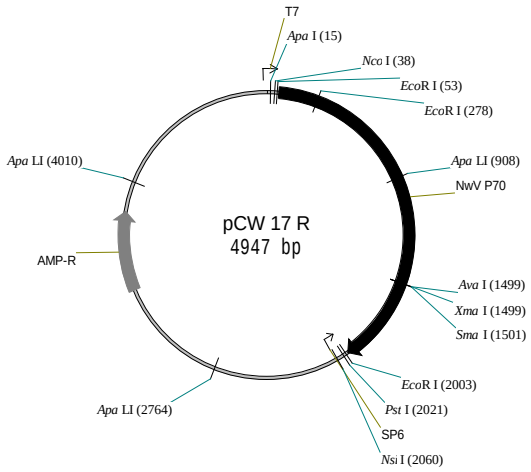

Figure 4.5 Diagrammatic representation of pCW17R which was used to generate the NωV RNA2 negative sense RNA probe. The vector was generated by inserting a PCR fragment, which included the entire NωV RNA2 sequence, into pGEM-T Easy (Promega). The resultant plasmid contains the entire NωV RNA2 cDNA flanked by bacteriophage RNA polymerase T7 and SP6. Plasmid pCW17R confers resistance to ampicillin (AMP-R) for selection in *E. coli*.

4.2.7 Purification of NωV-like particles from infected *N. capensis* larvae

Virus particles were purified from *N. capensis* larvae collected in 2002 from the Western Province of South Africa according to a protocol described by Morris *et al*. (1979). Approximately 250 g of larvae were homogenised in 3.3 volumes (weight/volume) of ice-cold larval homogenisation buffer (LHB) [0.2% β-mercaptoethanol (volume/volume), 0.5 M Tris-Cl (pH 7.5), 0.01 M Na_2EDTA (pH 8.0) and 250 mL butan-1-ol (volume/volume)] at 4°C. The supernatant was clarified by centrifugation at 8000 rpm for 15 minutes at 4°C in a Beckman JA-10 rotor. The pellet was re-extracted as indicated above and the supernatants pooled. The volume of the clarified supernatant was measured, 8% polyethyleneglycol (PEG) 6000 (weight/volume) and 0.1 M NaCl added and the mixture stirred at room temperature for 1 hour. The proteins in the supernatant were allowed to precipitate at 4°C for 3 hours and collected by centrifugation at 8000 rpm for 15 minutes at 4°C in a Beckman JA-10 rotor. The supernatant was discarded and the pellet re-suspended in one-tenth volume (volume/volume), which represented the volume of the original homogenate in 0.1 M Tris-EDTA (pH 7.5). The protein suspension was centrifuged at 8000 rpm for 10 minutes at 4°C in a Beckman JA-20 rotor to remove any insoluble proteins. The supernatant was then layered onto 2 mL of 30% sucrose [prepared in EB (50 mM Tris-Cl (pH 7.5), 250 mM NaCl)] and centrifuged at 40000 rpm in a SW-28 rotor at 11°C for one hour and fifteen minutes. The supernatant was discarded and pellet allowed to re-suspended in 500 µL of EB at 4°C overnight.

4.3 RESULTS

In the previous chapters it was found that HaSV VLPs assembled in yeast encapsidated no viral RNA. One possible explanation for this was RNA encapsidation is replication-dependent. It was hypothesised that viral replication allowed for replicated RNA and capsid assembly to occur in close proximity within the site of replication. This would enable higher levels of viral RNA encapsidation by the VLPs. An *in vivo* replication system is not available for the omegatetraviruses, as they are not infectious in tissue

culture. It was therefore decided to explore the possibility of using a yeast-based replication system based upon the nodavirus NoV to determine whether proximity of the capsid protein and RNA would result in specific viral RNA encapsidation.

4.3.1 Assembly of NωV VLPs in yeast

Agrawal and Johnson (1995) showed that the expression of the capsid-encoding sequence of NωV using a baculoviral expression system allowed p70 to assemble and mature into VLPs. VLPs produced by this highly productive system were used by Canady *et al*. (2000; 2001) and Taylor *et al*. (2002) for detailed analysis of the process of procapsid maturation. The first step was to confirm the assembly of NωV VLPs in yeast cells expressing *P70* (the NωV capsid protein precursor-encoding gene). The expression vector pMT13 was constructed, in which the NωV *P70* coding sequence was fused to the translational start of the *GAPDH* gene. This plasmid was transformed into yeast cells and expression of *P70* was induced by carbon-limitation or induction with ethanol.

Western analysis of cell-free extracts showed the presence of p70 even at the time of induction (Figure 4.6, A, lanes 2 and 3). After 2 hours, a band co-migrating with the wild-type NωV capsid protein, p62, was detected suggesting that as with HaSV, NωV VLPs might be undergoing spontaneous maturation *in vivo* (Figure 4.6, A, lanes 5, 6, 8 and 9 as compared with lane 10). There was no apparent difference in the levels of p70 and p64 in cells grown in carbon-limiting medium versus those induced with ethanol (Figure 4.6, A, lane 8 vs. lane 9). As with HaSV, the proportion of p70 versus p62 appeared to be approximately equal, suggesting that VLP assembly was not as efficient as in virus-infected cells. To confirm that p70 and p62 detected by Western analysis represents assembled procapsids and mature capsids respectively, VLPs were purified from cells expressing P_{GADH}-derived *P70* in carbon-limiting medium for 16 hours. TEM analysis confirmed that the predominant type of particle purified represented wild-type NωV with a mean diameter of 40 nm (Figure 4.6, B).

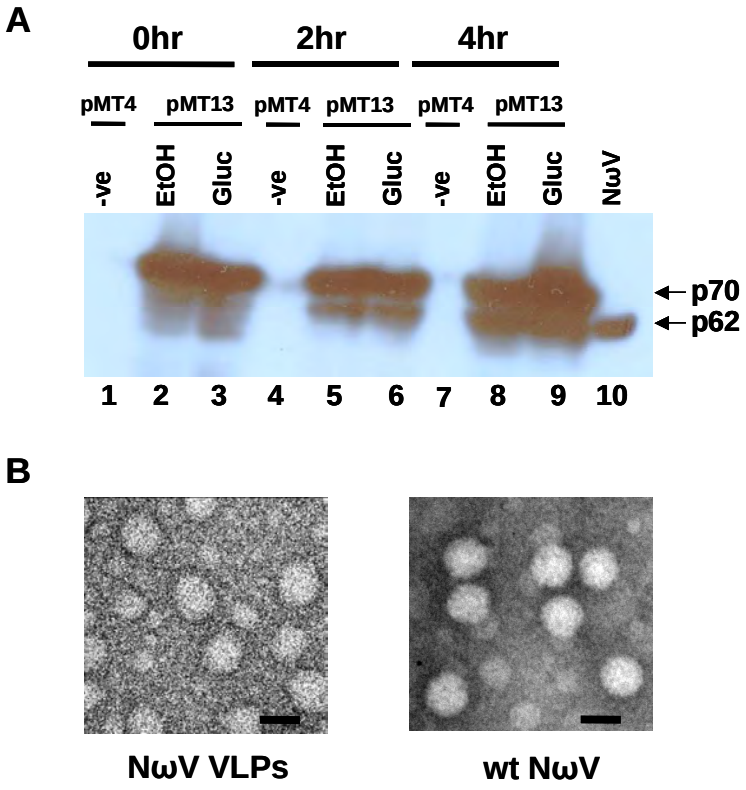

Figure 4.6 Assembly of NωV VLPs in yeast. **(A)** Western analysis of total yeast lysates from cells containing pMT4 or pMT13 initially incubated in SMM with 0.1% glucose and 5% glycerol for 12 hours at 28°C. Ethanol was then added to a final concentration of 3% (EtOH) or no additional carbon source was added (Gluc, -ve; carbon-limiting) to the media. Arrows indicate the relative positions of proteins migrating at 70 kDa and 62 kDa and NωV represents wild-type NωV used as a positive control. **(B)** TEM analysis of VLPs (NωV VLPs) or wild-type NωV (wt NωV) purified by sucrose gradient ultracentrifugation from cells expressing *P70* incubated in carbon-limiting media for 16 hours at 28°C. The bar represents 50nm.

4.3.2 Transcription–dependent NoV replication of the NoV RNA2-NωV *P70* chimera in yeast.

Having established that NωV VLPs were able to assemble and mature in yeast cells, the next step was to confirm the results of Dorrington *et al*. (2007) with respect to replication of an NoV RNA2-NωV *P70* chimera in yeast cells. The plasmid LpGNωV, (Figure 4.3), constructed by Kyle Johnson (University of Alabama at Birmingham) was designed such that the NωV *P70* coding sequence was flanked at the 5' end by the first 18 nucleotides and at the 3' end by the last 865 nucleotides of NoV RNA2. The

minimum sequences required for replication of RNA2 by the NoV replicase were retained. The coding sequence for the NoV RNA2-NωV *P70* chimera was flanked by the *GAL1* promoter and the HDV ribozyme such that the 5' and 3' ends of the transcript would be authentic relative to NoV RNA2. LpGNωV was transformed into yeast cells together with TpGN1 (expressing the NoV RNA1 encoding the viral replicase). Expression of RNA1 and the NoV RNA2-NωV *P70* chimera was induced by growing the cells in medium containing galactose. RNA was extracted from the cells and probed by Northern analysis for the presence of (+) and (-) sense RNA2. The (+) sense NoV RNA2-NωV *P70* chimera (2899 nucleotides) could be detected 24 hours after induction with an approximately two-fold increase detected after 48 hours (Figure 4.7 compare lane 8 to 7). In addition, the mRNA transcript, which acted as a template for replication and migrated at a slower rate than the replicated RNA was also detected (Figure 4.7). The smaller size of the replicated RNA when compared to mRNA is due to the activity of the HDV ribozyme which cleaves downstream of the 3' end of the NoV RNA2 sequence to remove the terminator and poly (A) tail of the transcript.

Only the NoV RNA2-NωV *P70* mRNA sequence was detected in the absence of the NoV replicase and there was no negative transcript due to the absence of replication (Figure 4.7, lanes 3, 11 and 12). The (-) NoV RNA2-NωV *P70* chimera was detected in cells with TpGN1 and LpGNωV (Figure 4.7, lanes 9 and 10). In contrast no (-) NoV RNA2-NωV *P70* chimera could be detected in cells without the NoV replicase (Figure 4.7, lanes 11 and 12). As expected, the NoV RNA2-NωV *P70* chimera mRNA was not detected. This confirmed that the NoV RNA2-NωV *P70* chimera was being replicated by the NoV replicase. This experiment also showed that substantially higher levels of the NωV *P70*-encoding RNA was present in cells as a result of replication when compared to the level of mRNA produced by transcription (Figure 4.7, compare lanes 17 and 18 with 21 and 22).

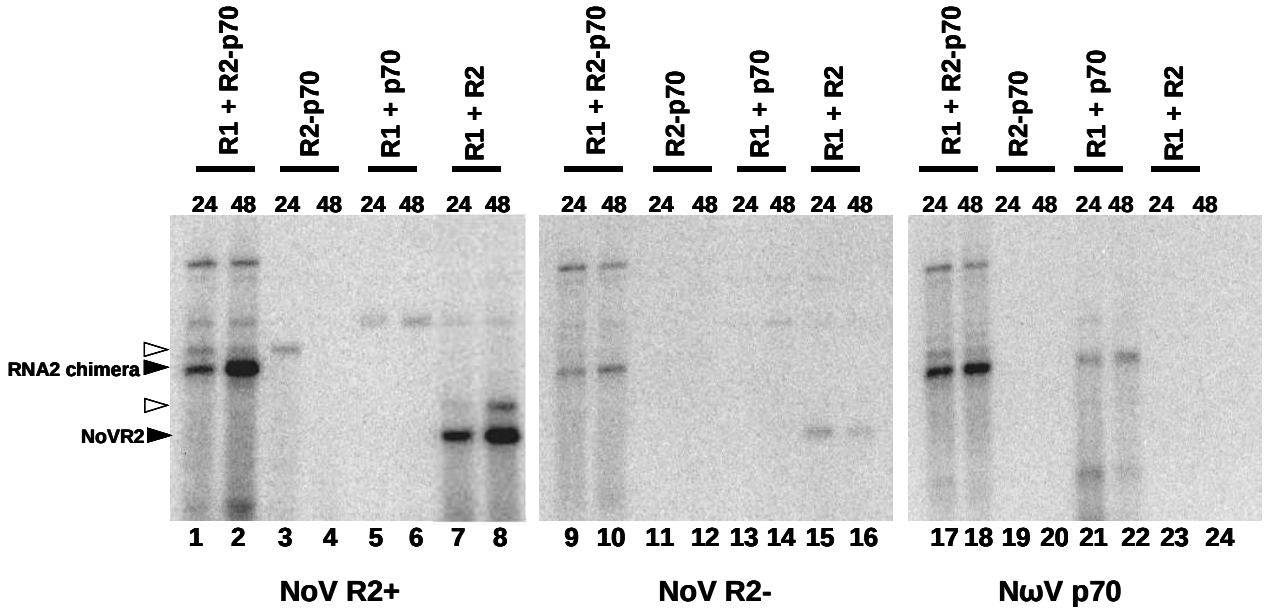

Figure 4.7 Northern blot hybridisation analysis of plasmid–initiated NoV RNA2 replication in yeast cells. NoV R2+, NoV R2- and NωV p70 indicate Northern blot hybridisations to positive (+) and negative (-) sense RNAs as indicated. Total yeast RNA was extracted using a hot phenol method from cells induced for expression of NoV RNA1 (R1; TpGN1), NoV RNA2 (R2; LpGN2), NωV *P70* (p70; pMT13) or an NoV RNA2-NωV *P70* chimera (R2-p70; LpGNωV) as indicated using the *GAL1* promoter for the induction times indicated. Solid arrowheads indicate the relative positions of the NoV RNA2-NωV *P70* chimera and wild-type NoV RNA2, while open arrowheads indicate primary transcripts, which have not been cleaved by the HDV ribozyme.

4.3.3 Expression of NωV *P70* and assembly of NωV VLPs

To determine whether the NωV *P70* sequence encoded by the NoV RNA2-NωV *P70* chimera resulting from replication was translated, cell-free extracts were examined for the presence of p70. Western analysis of total and soluble yeast protein from cells which co-expressed the NoV RNA2-NωV *P70* chimera (LpGNωV) and NoV RNA1 (TpGN1) showed the presence of p70 and p62 after 24 hours of incubation (Figure 4.8, lanes 1 and 2). At 48 hours incubation an increase in the level of p70 and p62 were detected (Figure 4.8, lanes 3 and 4). In cells expressing the NoV RNA2-NωV *P70* chimera only (no replicase) both p70 and p62 were detected after 24 hours (Figure 4.8, lane 5). However, at 48 hours the level of p70 appeared to have substantially decreased (Figure 4.8, compare lanes 7 and 8 with lanes 5 and 6). The decreased levels of protein detected were

a result of the ceasing of transcription from the *GAL1* promoter after a prolonged incubation time (Figure 4.7, compare lane 3 to 4). In contrast, the replication-dependent synthesis would ensure the continued translation of the protein resulting in the elevated levels detected. These results demonstrated that translation of p70 by a replication competent transcript produced more protein than transcription alone. Furthermore, p70 translated from replicated RNA was able to mature *in vivo* implying that the VLPs were assembled.

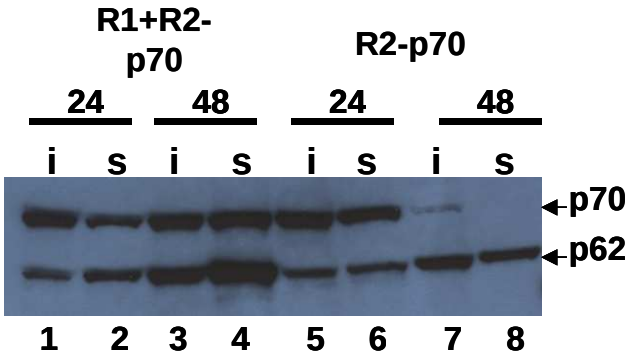

Figure 4.8 Replication-dependent assembly of NωV VLPs *in vitro*. Western analysis of total (i) and soluble (s) yeast lysates prepared from cells containing TpGN1 and LpGNωV (R1 + R2-p70) or LpGωV only (R2-p70), incubated in SMM with 0.1% glucose and 2% galactose for the times indicated at 28ºC. Arrows indicate protein migrating at the approximate molecular weighs of 70, 62 and 57 kDa. (+) refers to a virus which is serologically related to wild-type NωV (NωV-like).

4.3.4 RNA encapsidation in NωV VLPs

To determine whether the VLPs (formed from p70 translated from replicated RNA) encapsidated the NωV *P70*-encoding transcript, VLPs were purified from cells co-expressing NoV RNA1 (TpGN1) and the NoV RNA2-NωV *P70* chimera (LpGNωV) after 48 hours incubation as indicated before. To determine which species of RNAs were being encapsidated, RNA was purified from the VLPs and analysed. The RNA from the VLPs was compared to the RNA extracted from wild-type NoV particles. RNAs corresponding to NoV RNA1 and NoV RNA2 as well as an RNA1-RNA2 dimer (Ball, L.A personal communication) were detected from wild-type NoV particles (Figure 4.9, A, lane 2). In contrast, the NωV VLPs appeared to encapsidate RNA migrating at

approximately the same size as the NoV RNA1-RNA2 dimer. This suggested the presence of cellular RNAs in the VLPs rather than the replication-derived transcripts (Figure 4.9, A, lane 2).

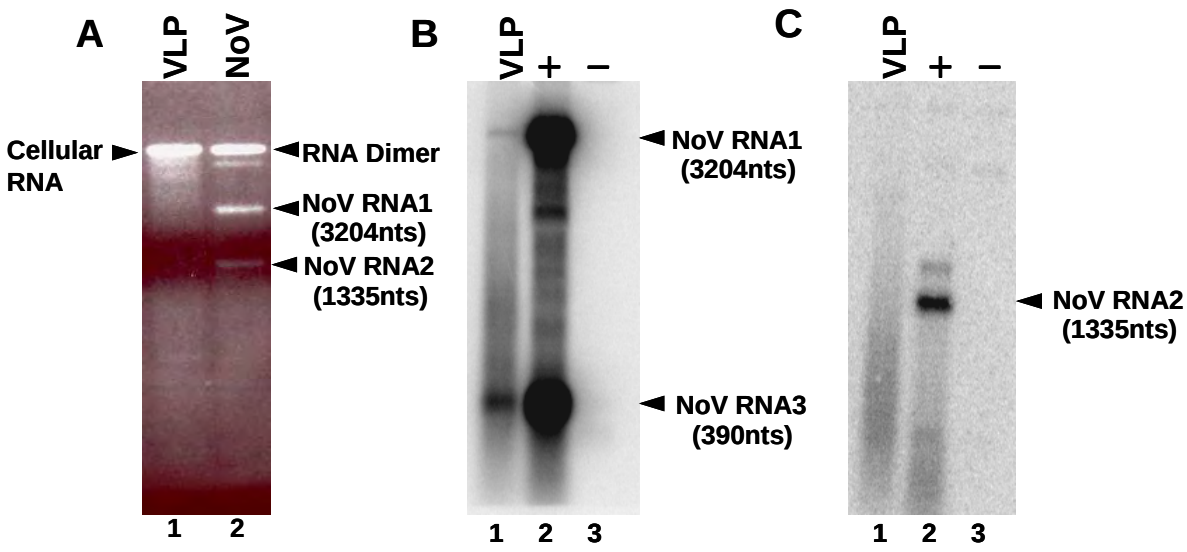

Figure 4.9 RNA encapsidation by NωV VLPs in yeast cells. VLPs were purified from cells co-expressing P_{GAL1}–derived NoV RNA1 (TpGN1) and the NoV RNA2-NωV *P70* chimera (LpGNωV) incubated in SMM with 0.01% glucose and 2% galactose for 48hrs at 28°C. (**A**) Agarose gel electrophoresis of RNA purified from NωV VLPs and wild-type NoV. The relative positions at which the genomic RNAs of NoV resolved on the agarose gel are indicated. Northern analysis of RNA purified from the NωV VLPs probed for positive sense NoV RNA1, NoV RNA3 (**B**) and NoV RNA2 (**C**). Solid arrowheads indicate the relative positions of NoV RNA1, NoV RNA2, NoV RNA3 and a NoV RNA1/RNA2 dimer. (+) represents NoV RNA and (-) in each case refers to mock RNA.

The RNA purified from the VLPs was probed for positive sense NoV RNA1, NoV RNA3 and NoV RNA2. As expected, the Northern blot revealed the presence of all three RNAs in the positive control (Figure 4.9, B and C, lane 2). This however, was not the case for the NωV VLPs, where small amounts of NoV RNA1 and NoV RNA3 were detected, but no RNA corresponding to the NoV RNA2-NωV *P70* chimera was observed (Figure 4.9, B and C, lane 1). The amount of RNA3 detected in the NωV VLPs was higher than RNA1. These results indicated that the VLPs randomly encapsidated RNA that was in abundance during assembly. This resulted in the VLPs encapsidating a mixture of viral and cellular RNAs.

4.4 DISCUSSION

Price *et al* (1996; 2005) demonstrated that nodavirus replication systems could be applied to the synthesis of heterologous proteins. These viruses were also shown to replicate their genomes to high-levels in yeast cells. In addition the nodaviruses encapsidate their genomic RNA in a replication-dependent mechanism (Venter *et al*., 2005). In the absence of replication, the virus particles encapsidate random cellular mRNAs (Venter *et al*., 2005; Venter and Schneemann, 2007). Replication-dependent encapsidation ensure that the viral RNA and capsid protein are in constant contact with one another (Venter *et al*., 2005). To mimic this situation during omegatetravirus assembly, a nodavirus replication system was developed for the *de novo* synthesis of NωV VLPs

P_{GADH}-derived expression of the capsid coding sequence of NωV (*P70*) in yeast resulted in the assembly of VLPs, which had the ability to mature *in vivo*. Similarly, the replication of a NoV RNA2-NωV *P70* chimera resulted in translation of p70 and assembly of NωV VLPs that had the ability to mature. The relative levels of VLPs detected as a result of replication compared to transcription, showed that more VLPs were produced in the replication-dependent system. These results correlated with earlier observations for the assembly of HaSV VLPs where increased translation led to improved assembly.

The ability of the VLPs to encapsidate nodaviral RNA1 and RNA3 but not the NoV RNA2-NωV *P70* chimera suggested that RNA encapsidation by the NωV VLPs may be random and the RNAs most likely to be encapsidated are those that are the most prevalent. Thus the NωV VLPs might package the NoV RNA because they are the most abundant RNAs in close proximity to the assembling particles. The absence of any detectable levels of the NoV RNA2-NωV *P70* chimera in the NωV VLPs indicates that, as with co-expression of HaSV *P71* mRNA, the 5’ and 3’ ends of the wild-type NωV RNA2 might encode encapsidation signals ensuring their specific encapsidation. This would imply that the NωV particle encapsidates the NoV genomic RNAs non-specifically, in the same way as cellular RNAs. The encapsidation of the genomic RNA

in the omegatetraviruses may be co-packaged. In the absence of RNA1 or full length RNA2 the VLPs encapsidate RNA randomly. A system could be developed where full length NωV RNA1 and RNA2 chimeras were constructed that were flanked by the NoV RNA2 sequences required for NoV RNA1-dependent replication. In this way it may be possible to replicate NωV RNA1 and RNA2 by the NoV replicase.

The hybrid NoV replication system is potentially useful as an alternative to the transcriptional production of omegatetravirus capsid protein precursor-encoding mRNA with the resulting assembly of VLPs. The system has however, no effect upon the ability of VLPs to specifically encapsidate tetraviral RNA. This implies that there are other factors involved in RNA encapsidation.

CHAPTER 5. GENERAL DISCUSSION AND CONCLUSIONS

CHAPTER 5. GENERAL DISCUSSION AND CONCLUSIONS

The principal aim of this thesis was to study the assembly of omegatetravirus particles in yeast focussing on the encapsidation of viral RNA. Two different approaches were used to achieve this aim. Capsid precursor protein was translated from mRNA produced by transcription or capsid precursor protein was produced via replication. The first approach was based upon the experimental system developed by Venter (2001). The system was inefficient in terms of VLP assembly. This system was optimised by significantly increasing the expression of the capsid precursor protein. The second system relied upon the replication of a chimeric NoV RNA2-NωV *P70* template encoding the NωV capsid precursor gene, by the replicase of NoV.

5.1 ASSEMBLY OF HaSV AND NωV VLPS IN YEAST

P_{GADH}-derived expression of HaSV *P71* resulted in higher levels of p71 compared to expression of HaSV *P71* from P_{GAL1}. Both expression systems were able to support VLP assembly. However, the P_{GADH} system was much more efficient and resulted in spontaneous maturation of VLPs *in vivo*. Similarly, expression of the NωV capsid encoding sequence (*P70*) with the hybrid promoter resulted in the assembly of VLPs. The assembly of the VLPs was more efficient but the equal proportion of p71 versus p64 and p70 versus p62 detected in the cell free extracts suggested that a substantial proportion of the VLPs did not mature. The improved assembly of the VLPs was believed to be as a consequence of the elevated *P71* mRNA concentrations transcribed from the hybrid promoter. TEM analysis of the particles isolated from yeast cells co-expressing viral RNA revealed that there was a large distribution in VLPs size and morphology. The large distribution of particles observed by acetic acid maturation as opposed to spontaneous maturation *in vivo* may be due to the stabilisation of the particles at a low pH. Only VLPs, which resembled wild-type HaSV, were purified by spontaneous maturation *in vivo*. This may be because the particles were unstable before

maturation and subsequently degraded during VLP purification. When no additional RNA was co-expressed, the majority of particles were smaller than wild-type HaSV capsids. Similarly, baculoviral expression of *P71* and *in vitro* maturation at a pH of 6.0 resulted in the assembly of smaller *T*=1 HaSV VLPs (Taylor, 2003). At a pH of 5.0 Taylor (2003) managed to purify virus particles, which were representative of wild-type virions. This raises an interesting question. Are the VLPs that differ from wild-type virions a result of mismaturation as was observed by Taylor (2003)? It is possible that correct maturation may only occur at a specific pH and in the presence of RNA near the cleavage site? In the absence of either one of these requirements, virus particles mature with different symmetries and during assembly, the virus particles may encapsidate a certain complement of RNAs, which dictates the final mature structure of the VLPs. The ability of the VLPs to assemble by expressing *P71* with P_{GADH}, indicated that the rate-limiting factor during assembly was the protein concentration and not the viral RNA as was previously proposed by Venter (2001).

5.2 RNA ENCAPSIDATION

The success of the omegatetravirus lifecycle relies on their ability to efficiently replicate and package their genomes. The rate at which assembly of these particles occurred in yeast was hypothesized to be governed by the ability of these virus particles to encapsidate viral RNA (Venter, 2001). The improved assembly when high-level *P71* and *P71* mRNA were co-expressed was not as a consequence of viral RNA being encapsidated. This suggested that neither *P71* mRNA nor RNA2 contain any encapsidation signals. This result also contradicted the earlier observation that the capsid-encoding message of both NωV and HaSV were encapsidated in the VLPs (Agrawal and Johnson, 1995; Gordon *et al.*, 2001). Expression of HaSV *P71* and the genomic RNAs in plant protoplasts was proposed to result in the assembly of infectious VLPs (Gordon *et al.*, 2001). In addition to the encapsidation of the *P71* message, Gordon *et al.* (2001) also detected RNA1 in the VLPs. Surprisingly no RNA2 was detected. The production of infectious virus would require the encapsidation of RNA2. This suggests two possible scenarios. Firstly, the diseased larvae from the bioassays may

have an inherent HaSV infection, which was manifested by stressing the animals. Secondly, RNA2 may be present at low levels resulting in few VLPs encapsidating the RNA2 molecule. If the latter scenario is true, then both the message and RNA2 contain an encapsidation signal. However the results presented here show otherwise. The HaSV VLPs in this study must have encapsidated cellular RNA (Agrawal and Johnson, 1995).

In the nodaviruses, encapsidation of cellular RNA was observed in PaV and FHV VLPs that were assembled from capsid protein translated from mRNA (Schneemann *et al*., 1993; Krishna *et al*., 2003; Johnson *et al*., 2004; Venter and Schneemann 2007). Only 6% of the RNA packaged in PaV VLPs represented genomic RNA. Northern analysis of the RNA purified from the HaSV VLPs indicated that less than 2.8% of the total RNA analysed represented viral RNA. In PaV VLPs the RNA formed a helical cage of RNA similar to wild-type PaV (Tang *et al*., 2001; Johnson *et al*., 2004). Like the nodaviruses it is possible that the HaSV VLPs package a mixture of viral RNA and cellular mRNAs in the absence of replication. It was hypothesised that even though the hybrid promoter produced significantly higher levels of the RNA transcripts, the concentrations of RNA expressed were low and not in the vicinity of the capids. This resulted in the particles encapsidating cellular RNAs. Furthermore, the ability of the VLPs to assemble in the absence of additional viral RNA indicated that the particles possibly encapsidated random cellular RNAs, which contributed to the instability of the particles.

There were a number of possible explanations why viral RNA was not encapsidated:
1. Absence of encapsidation signals. The *P71* mRNA and RNA2 do not carry an encapsidation signal as was originally proposed (Gordon *et al*., 2001). This is supported by Gordon *et al*. (2001), where no RNA2 was encapsidated in VLPs assembled in plant protoplasts.

2. Precise copies of viral RNA. Because the exact transcriptional start of P_{GADH} is unknown, there would have been several additional nucleotides at the 5' end. Extensions at the 5' end of the RNA may interfere with the ability of the RNA to be accommodated into the capsid shell or may block encapsidation signals. This theory could be tested by

co-expressing *P71* with P_{GAL1}-derived RNA2, for which the transcriptional start of the promoter is known. The disadvantage of using P_{GAL} is that low levels of RNA2 would be produced. The transcriptional start of P_{GADH} could be determined by primer extension and a precise fusion between RNA2 and -1 of the promoter could be constructed. The advantage of using this promoter would ensure high-level expression of exact RNA2 transcripts.

3. Sequential packaging. RNA1 might be required for the packaging of RNA2 in HaSV VLPs. In the nodaviruses RNA1 and RNA2 are co-packaged in equimolar concentrations (Schneemann *et al*., 1994; Krishna and Schneemann, 1999). Gordon *et al*. (2001) detected RNA1 in plant protoplast-derived HaSV VLPs. Interestingly no RNA2 was encapsidated and Gordon *et al*. (2001) hypothesised that RNA1 can be encapsidated in the absence of RNA2. There is evidence to suggest that FHV requires dimerisation of both RNAs for efficient packaging (Krishna and Schneemann, 1999). However, Venter *et al*. (2005) showed that RNA2 was packaged in the absence of RNA1. Critical to this process is the requirement for RNA2 replication, suggesting that packaging occurs in an ordered manner where RNA2 was packaged before RNA1 (Venter *et al*., 2005). This may indicate that viral RNA encapsidation is replication-dependent in the omegatetraviruses.

It is now widely acknowledged that the tetraviruses most likely evolved from the nodaviruses and it is possible that this method of packaging displayed by the nodaviruses may be an evolutionary advantage, ensuring that both RNAs are efficiently packaged in the virus particle (Johnson *et al*., 1994; Johnson and Reddy, 1998). On the other hand the omegatetraviruses could adopt a different strategy, whereby RNA1 is required to be packaged first in order for RNA2 to be packaged. RNA1 could open the binding site for RNA2 exposing residues important for its binding. This sequential manner of RNA packaging would ensure that the encapsidation event is specific. This model would be largely inefficient, as it would require a high initial concentration of RNA1 to be readily available for the capsid subunits to encapsidate. To test this hypothesis RNA1 and RNA2 could be co-expressed using different promoters. RNA1

could be expressed with the *GADH* promoter and RNA2 with the *GAL1* promoter. In this way high levels of RNA1 could be initially expressed under glucose-starvation conditions with RNA2 expression induced by the addition of galactose.

4. A role for p17. Recent data generated in the laboratory by Vlok (2006) suggests that p17, which is encoded by a conserved ORF that overlaps the capsid protein precursor ORF in all three omegatetraviruses, might play an important role in virus particle assembly. Vlok showed that p17 was present in infected *H. armigera* larval midgut cells. The presence of the protein in wild-type HaSV virus particles at approximately 1/10–1/20 the concentration of the capsid protein was also detected (Vlok, 2006). As structural studies have identified the presence of only the capsid protein and as the assembly of VLPs requires only expression of the capsid protein precursor, it is unlikely that p17 interacts directly with the capsid shell. However, p17 might interact with and possibly order viral RNA during encapsidation in the omegatetraviruses.

Since the expression system used in this study does not include the expression of p17, (no p17 was translated from the RNA2 construct, results not shown), the absence of this protein might account for the lack of viral RNA encapsidation. To test this hypothesis an expression system could be devised in yeast where *P17* is expressed from a single, chromosomal copy and *P71* or viral RNA from multicopy expression vectors. This would mimic the elevated expression levels of *P17* and *P71* that have been detected in infected insect midgut cells.

5. Replication-dependent packaging of viral RNA.

In the omegatetraviruses RNA encapsidation may be coupled to replication. This seems likely if one considers the argument that most if not all ss (+) RNA viruses replicate in association with membranes (for a review see Salonen *et al*., 2004). This ensures that the capsid and RNA are in close contact with one another. The NoV replicase had the ability to replicate a NoV RNA2-NωV *P70* chimeric replicon, which contained the capsid-encoding sequence of NωV. Replication of the NoV RNA2-NωV *P70* chimera resulted in the *de novo* synthesis of NωV VLPs, which had the ability to encapsidate the NoV

RNA1 and RNA3. This was not expected because the nodaviruses co-package RNA1 and RNA2 in equal quantities. The ability of the VLPs to encapsidate RNA3 suggested that RNA packaging was random and dependent on RNA that was present at the highest concentrations in the proximity of the assembling VLPs. These results indicated that the close proximity of the viral RNA and capsid protein might occur for the encapsidation of the NoV RNAs

5.3 THE ROLE OF APOPTOSIS IN THE LIFE CYCLE OF TETRAVIRUSES

The work presented here suggests that there may be a possible link between HaSV VLP maturation and apoptosis *in vivo*. Two possible scenarios exist to explain how apoptosis could be triggered in the yeast cells. Firstly the ability of the VLPs to mature earlier in cells expressing *P71* compared to the negative control suggests that the metabolic load of the mRNA transcripts and subsequent translation of p71 may induce apoptosis (results not shown). Second p71 could specifically induce apoptosis like some picornaviruses (Carthy *et al*., 1998; Barco *et al*., 2000; Calandria *et al*., 2004; Liu *et al*., 2004). In both these cases apoptosis may be important in the lifecycle of the virus because the response of *H. armigera* to HaSV infection culminates in cell sloughing, which has been linked to apoptosis (Brookes *et al*., 2002). Induction of apoptosis by the virus could ensure two biological advantages. First, induction of apoptosis causes acidification of the cytosol, which may be required for maturation of the virus, and secondly, apoptosis may be used as a mechanism for cellular exit.

Another point to consider is that FHV replicates as spherules in the outer mitochondrial membrane (Miller *et al*., 2001). In this case the protein and RNA are always in close association with one another (Venter *et al*., 2005). Tetraviruses may need to replicate *in situ* with cellular organelles. The trigger for maturation might be caused by the acidification of the cytosol by mitochondrial (Ludovico *et al*., 2002) or lysosomal (Nilsson *et al*., 2006) lysis. In the laboratory, the HaSV replicase has been shown to localise to either the lysosomes or endosomes, but further research is required to

conclusively demonstrate this (James Short, unpublished data). It seems feasible that the virus would replicate in association with the organelles to cause the acidification required during maturation. Replication in association with cellular membranes would also ensure that the RNA, capsid proteins and replication factors are localized and concentrated for assembly (Ahlquist *et al*., 2003). Membrane complexes could also offer the virus particles protection and ensure that the host translational factors do not out compete the replicating RNA (Ahlquist *et al*., 2003).

5.4 CONCLUDING REMARKS

While the mechanism of omegatetravirus maturation has been elucidated *in vitro*, little is known about how these viruses enter their host, replicate their genomes, assemble and mature *in vitro*. An expression system was developed to study the assembly of HaSV VLPs in yeast. The work presented in this dissertation indicates that the virus almost certainly required a high concentration of capsid precursor protein during assembly. The ability of the virus to specifically encapsidate its own RNA may not rely on viral RNA and capsid protein association in the vicinity of one another. Instead the omegatetraviruses may require replication for specific assembly. Replication of the virus in association with organelles could also induce apoptosis reducing the pH of the immediate environment where assembly occurs, causing maturation. The challenges, which arose from this work indicate that in the absence of a wild-type replication system, the virus may assemble and encapsidate RNA in a different way. In order to study the assembly and RNA encapsidation mechanisms of the omegatetraviruses, a wild-type replication system needs to be developed.

APPENDICES

APPENDIX 1. BACTERIAL AND YEAST STRAINS

Table A1.1 Bacterial and yeast strains used in this study

Strain	**Genotype**	**Reference**
S. cerevisiae INVScI	Matα, *trp1* - 289, *his3* Δ1, *leu2*, *ura3*-52	Invitrogen
S. cerevisiae INVScI 3#20.1	Matα, *his*3, *P71*:*LEU2*::*p71*, *trp*1, *ura*3)	Venter (2001)
S. cerevisiae INVScI L+	Matα, *his*3, *LEU*2, *trp*1, *ura*3	Venter (2001)
S. cerevisiae BY4733	Matα, *his3*Δ200, *leu*2Δ0, *met*15Δ0, *trp*1Δ63, *ura*3Δ0	Brachmann *et al*., 1998
E. coli DH5α	*F-(80dlacZ M15) (lacZYA-argF)U169hsdR17(r-m+) recA1 endA1 relA1 deoR*	Hanahan, 1983
E. coli JM110	*rpsL* (Strr) *thr leu thi-1 lacY galK galT ara tonA tsx dam dcm supE44* Δ(*lac-proAB*) [F´ *traD36 proAB lacI*qZΔ*M15*]	Yanisch-Perron *et al*., 1985

APPENDIX 2. SEQUENCE OF THE HaSV GENOME

```
  1                                                 Met Tyr Ala Lys
  1  GUUCUGCCUC CCCCGGACGG UAAAUAUAGG GGAACA AUG UAC GCG AAA

  5  Ala Thr Asp Val Ala Arg Val Tyr Ala Ala Ala Asp Val Ala
 49  GCG ACA GAC GUG GCG CGU GUC UAC GCC GCG GCA GAU GUC GCC

 19  Tyr Ala Asn Val Leu Gln Gln Arg Ala Val Lys Leu Asp Phe
 91  UAC GCG AAC GUA CUG CAG CAG AGA GCA GUC AAG UUG GAC UUC

 33  Ala Pro Pro Leu Lys Ala Leu Glu Thr Leu His Arg Leu Tyr
133  GCC CCG CCA CUG AAG GCA CUA GAA ACC CUC CAC AGA CUG UAC

 47  Tyr Pro Leu Arg Phe Lys Gly Gly Thr Leu Pro Pro Thr Gln
175  UAU CCG CUG CGC UUC AAA GGG GGC ACU UUA CCC CCG ACA CAA

 61  His Pro Ile Leu Ala Gly His Gln Arg Val Ala Glu Glu Val
217  CAC CCG AUC CUG GCC GGG CAC CAA CGU GUC GCA GAA GAG GUU

 75  Leu His Asn Phe Ala Arg Gly Arg Ser Thr Val Leu Glu Ile
259  CUG CAC AAU UUC GCC AGG GGA CGU AGC ACA GUG CUC GAG AUA

 89  Gly Pro Ser Leu His Ser Ala Leu Lys Leu His Gly Ala Pro
301  GGG CCG UCU CUG CAC AGC GCA CUU AAG CUA CAU GGG GCA CCG

103  Asn Ala Pro Val Ala Asp Tyr His Gly Cys Thr Lys Tyr Gly
343  AAC GCC CCC GUC GCA GAC UAU CAC GGG UGC ACC AAG UAC GGC

117  Thr Arg Asp Gly Ser Arg His Ile Thr Ala Leu Glu Ser Arg
385  ACC CGC GAC GGC UCG CGA CAC AUU ACG GCC UUA GAG UCU AGA

131  Ser Val Ala Thr Gly Arg Pro Glu Phe Lys Ala Asp Ala Ser
427  UCC GUC GCC ACA GGC CGG CCC GAG UUC AAG GCC GAC GCC UCA

145  Leu Leu Ala Asn Gly Ile Ala Ser Arg Thr Phe Cys Val Asp
469  CUG CUC GCC AAC GGC AUU GCC UCC CGC ACC UUC UGC GUC GAC

159  Gly Val Gly Ser Cys Ala Phe Lys Ser Arg Val Gly Ile Ala
511  GGA GUC GGC UCU UGC GCG UUC AAA UCG CGC GUU GGA AUU GCC

173  Asn His Ser Leu Tyr Asp Val Thr Leu Glu Glu Leu Ala Asn
553  AAU CAC UCC CUC UAU GAC GUG ACC CUA GAG GAG CUG GCC AAU
```

Figure A2.1 RNA sequence of HaSV RNA1 (Genome sequence accession number: U18246). The amino acid sequence of the replicase gene is shown above the sequence.

```
 187  Ala Phe Glu Asn His Gly Leu His Met Val Arg Ala Phe Met
 595  GCG UUU GAG AAC CAC GGA CUU CAC AUG GUC CGC GCG UUC AUG

 201  His Met Pro Glu Glu Leu Leu Tyr Met Asp Asn Val Val Asn
 637  CAC AUG CCA GAA GAG CUG CUC UAC AUG GAC AAC GUG GUU AAU

 215  Ala Glu Leu Gly Tyr Arg Phe His Val Ile Glu Glu Pro Met
 679  GCC GAG CUC GGC UAC CGC UUC CAC GUU AUU GAA GAG CCU AUG

 229  Ala Val Lys Asp Cys Ala Phe Gln Gly Gly Asp Leu Arg Leu
 721  GCU GUG AAG GAC UGC GCA UUC CAG GGG GGG GAC CUC CGU CUC

 243  His Phe Pro Glu Leu Asp Phe Ile Asn Glu Ser Gln Glu Arg
 763  CAC UUC CCU GAG UUG GAC UUC AUC AAC GAG AGC CAA GAG CGG

 257  Arg Ile Glu Arg Leu Ala Ala Arg Gly Ser Tyr Ser Arg Arg
 805  CGC AUC GAG AGG CUG GCC GCC CGC GGC UCC UAC UCC AGA CGC

 271  Ala Val Ile Phe Ser Gly Asp Asp Asp Trp Gly Asp Ala Tyr
 847  GCC GUC AUU UUC UCC GGC GAC GAC GAC UGG GGU GAU GCG UAC

 285  Leu His Asp Phe His Thr Trp Leu Ala Tyr Leu Leu Val Arg
 889  UUA CAC GAC UUC CAC ACA UGG CUC GCC UAC CUA CUG GUG AGG

 299  Asn Tyr Pro Thr Pro Phe Gly Phe Ser Leu His Ile Glu Val
 931  AAC UAC CCC ACU CCG UUU GGU UUC UCA CUC CAU AUA GAA GUC

 313  Gln Arg Arg His Gly Ser Ser Ile Glu Leu Arg Ile Thr Arg
 973  CAG AGG CGC CAC GGC UCC AGC AUU GAG CUG CGC AUC ACU CGC

 327  Ala Pro Pro Gly Asp Arg Met Leu Ala Val Val Pro Arg Thr
1015  GCG CCA CCU GGA GAC CGC AUG CUG GCC GUC GUC CCA AGG ACG

 341  Ser Gln Gly Leu Cys Arg Ile Pro Asn Ile Phe Tyr Tyr Ala
1057  UCC CAA GGC CUC UGC AGA AUC CCA AAC AUC UUU UAU UAC GCC

 355  Asp Ala Ser Gly Thr Glu His Lys Thr Ile Leu Thr Ser Gln
1099  GAC GCG UCG GGC ACU GAG CAU AAG ACC AUC CUU ACG UCA CAG

 369  His Lys Val Asn Met Leu Leu Asn Phe Met Gln Thr Arg Pro
1141  CAC AAA GUC AAC AUG CUG CUC AAU UUU AUG CAA ACG CGU CCU

 383  Glu Lys Glu Leu Val Asp Met Thr Val Leu Met Ser Phe Ala
1183  GAG AAG GAA CUA GUC GAC AUG ACC GUC UUG AUG UCG UUC GCG

 397  Arg Ala Arg Leu Arg Ala Ile Val Val Ala Ser Glu Val Thr
1225  CGC GCU AGG CUG CGC GCG AUC GUG GUC GCC UCA GAA GUC ACC

 411  Glu Ser Ser Trp Asn Ile Ser Pro Ala Asp Leu Val Arg Thr
1267  GAG AGC UCC UGG AAC AUC UCA CCG GCU GAC CUG GUC CGC ACU
```

Figure A2.1 Continued…

```
 425  Val Val Ser Leu Tyr Val Leu His Ile Ile Glu Arg Arg Arg
1309  GUC GUG UCU CUU UAC GUC CUC CAC AUC AUC GAG CGC CGA AGG

 439  Ala Ala Val Ala Val Lys Thr Ala Lys Asp Asp Val Phe Gly
1351  GCU GCG GUC GCU GUC AAG ACC GCC AAG GAC GAC GUC UUU GGA

 453  Glu Thr Ser Phe Trp Glu Ser Leu Lys His Val Leu Gly Ser
1393  GAG ACU UCG UUC UGG GAG AGU CUC AAG CAC GUC UUG GGC UCC

 467  Cys Cys Gly Leu Arg Asn Leu Lys Gly Thr Asp Val Val Phe
1435  UGU UGC GGU CUG CGC AAC CUC AAA GGC ACC GAC GUC GUC UUU

 481  Thr Lys Arg Val Val Asp Lys Tyr Arg Val His Ser Leu Gly
1477  ACU AAG CGC GUC GUC GAU AAG UAC CGA GUC CAC UCG CUC GGA

 495  Asp Ile Ile Cys Asp Val Arg Leu Ser Pro Glu Gln Val Gly
1519  GAC AUA AUC UGC GAC GUC CGC CUG UCC CCU GAA CAG GUC GGC

 509  Phe Leu Pro Ser Arg Val Pro Pro Ala Arg Val Phe His Asp
1561  UUC CUG CCG UCC CGC GUA CCA CCU GCC CGC GUC UUU CAC GAC

 523  Arg Glu Glu Leu Glu Val Leu Arg Glu Ala Gly Cys Tyr Asn
1603  AGG GAA GAG CUU GAG GUC CUU CGC GAA GCU GGC UGC UAC AAC

 537  Glu Arg Pro Val Pro Ser Thr Pro Pro Val Glu Glu Pro Gln
1645  GAA CGU CCG GUA CCU UCC ACU CCU CCU GUG GAG GAG CCC CAA

 551  Gly Phe Asp Ala Asp Leu Trp His Ala Thr Ala Ala Ser Leu
1687  GGU UUC GAC GCC GAC UUG UGG CAC GCG ACC GCG GCC UCA CUC

 565  Pro Glu Tyr Arg Ala Thr Leu Gln Ala Gly Leu Asn Thr Asp
1729  CCC GAG UAC CGC GCC ACC UUG CAG GCA GGU CUC AAC ACC GAC

 579  Val Lys Gln Leu Lys Ile Thr Leu Glu Asn Ala Leu Lys Thr
1771  GUC AAG CAG CUC AAG AUC ACC CUC GAG AAC GCC CUC AAG ACC

 593  Ile Asp Gly Leu Thr Leu Ser Pro Val Arg Gly Leu Glu Met
1813  AUC GAC GGG CUC ACC CUC UCC CCA GUC AGA GGC CUC GAG AUG

 607  Tyr Glu Gly Pro Pro Gly Ser Gly Lys Thr Gly Thr Leu Ile
1855  UAC GAG GGC CCG CCA GGC AGC GGC AAG ACG GGC ACC CUC AUC

 621  Ala Ala Leu Glu Ala Ala Gly Gly Lys Ala Leu Tyr Val Ala
1897  GCC GCC CUU GAG GCC GCG GGC GGU AAA GCA CUU UAC GUG GCA

 635  Pro Thr Arg Glu Leu Arg Glu Ala Met Asp Arg Arg Ile Lys
1939  CCC ACC AGA GAA CUG AGA GAG GCU AUG GAC CGG CGG AUC AAA

 649  Pro Pro Ser Ala Ser Arg Thr Gln His Val Ala Leu Ala Ile
1981  CCG CCG UCC GCC UCG CGU ACG CAA CAU GUC GCC CUU GCG AUU
```

Figure A2.1 Continued…

```
 663  Leu Arg Arg Ala Thr Ala Glu Gly Ala Pro Phe Ala Thr Val
2023  CUC CGU CGU GCC ACC GCC GAG GGC GCC CCU UUC GCU ACC GUG

 677  Val Ile Asp Glu Cys Phe Met Phe Pro Leu Val Tyr Val Ala
2065  GUU AUC GAC GAG UGC UUC AUG UUC CCG CUC GUG UAC GUC GCG

 691  Ile Val His Ala Leu Ser Pro Ser Ser Arg Ile Val Leu Val
2107  AUC GUG CAC GCC UUG UCC CCG AGC UCA CGA AUA GUC CUU GUA

 705  Gly Asp Val His Gln Ile Gly Phe Ile Asp Phe Gln Gly Thr
2149  GGG GAC GUC CAC CAA AUC GGG UUU AUA GAC UUC CAA GGC ACA

 719  Ser Ala Asn Met Pro Leu Val Arg Asp Val Val Lys Gln Cys
2191  AGC GCG AAC AUG CCG CUC GUU CGC GAC GUC GUU AAG CAG UGC

 733  Arg Arg Arg Thr Phe Asn Gln Thr Lys Arg Cys Pro Ala Asp
2233  CGU CGG CGC ACU UUC AAC CAA ACC AAG CGC UGU CCG GCC GAC

 747  Val Val Ala Thr Thr Phe Phe Gln Ser Leu Tyr Pro Gly Cys
2275  GUC GUU GCC ACC ACG UUU UUC CAG AGC UUG UAC CCC GGG UGC

 761  Thr Thr Thr Ser Gly Cys Val Ala Ser Ile Ser His Val Ala
2317  ACA ACC ACC UCA GGG UGC GUC GCA UCC AUC AGC CAC GUC GCC

 775  Pro Asp Tyr Arg Asn Ser Gln Ala Gln Thr Leu Cys Phe Thr
2359  CCA GAC UAC CGC AAC AGC CAG GCG CAA ACG CUC UGC UUC ACG

 789  Gln Glu Glu Lys Ser Arg His Gly Ala Glu Gly Ala Met Thr
2401  CAG GAG GAA AAG UCG CGC CAC GGG GCU GAG GGC GCG AUG ACU

 803  Val His Glu Ala Gln Gly Arg Thr Phe Ala Ser Val Ile Leu
2443  GUG CAC GAA GCG CAG GGA CGC ACU UUU GCG UCU GUC AUU CUG

 817  His Tyr Asn Gly Ser Thr Ala Glu Gln Lys Leu Leu Ala Glu
2485  CAU UAC AAC GGC UCC ACA GCA GAG CAG AAG CUC CUC GCU GAG

 831  Lys Ser His Leu Leu Val Gly Ile Thr Arg His Thr Asn His
2527  AAG UCG CAC CUU CUA GUC GGC AUC ACG CGC CAC ACC AAC CAC

 845  Leu Tyr Ile Arg Asp Pro Thr Gly Asp Ile Glu Arg Gln Leu
2569  CUG UAC AUC CGC GAC CCG ACA GGU GAC AUU GAG AGA CAA CUC

 859  Asn His Ser Ala Lys Ala Glu Val Phe Thr Asp Ile Pro Ala
2611  AAC CAU AGC GCG AAA GCC GAG GUG UUU ACA GAC AUC CCU GCA

 873  Pro Leu Glu Ile Thr Thr Val Lys Pro Ser Glu Glu Val Gln
2653  CCC CUG GAG AUC ACG ACU GUC AAA CCG AGU GAA GAG GUG CAG

 887  Arg Asn Glu Val Met Ala Thr Ile Pro Pro Gln Ser Pro Thr
2695  CGC AAC GAA GUG AUG GCA ACG AUA CCC CCG CAG AGU CCC ACG
```

Figure A2.1 Continued…

```
 901  Pro His Gly Ala Ile His Leu Leu Arg Lys Asn Phe Gly Asp
2737  CCG CAC GGA GCA AUC CAU CUG CUC CGC AAG AAC UUC GGG GAC

 915  Gln Pro Asp Cys Gly Cys Val Ala Leu Ala Lys Thr Gly Tyr
2779  CAA CCC GAC UGU GGC UGU GUC GCU UUG GCG AAG ACC GGC UAC

 929  Glu Val Phe Gly Gly Arg Ala Lys Ile Asn Val Glu Leu Ala
2821  GAG GUG UUU GGC GGU CGU GCC AAA AUC AAC GUA GAG CUU GCC

 943  Glu Pro Asp Ala Thr Pro Lys Pro His Arg Ala Phe Gln Glu
2863  GAA CCC GAC GCG ACC CCG AAG CCG CAU AGG GCG UUC CAG GAA

 957  Gly Val Gln Trp Val Lys Val Thr Asn Ala Ser Asn Lys His
2905  GGG GUA CAG UGG GUC AAG GUC ACC AAC GCG UCU AAC AAA CAC

 971  Gln Ala Leu Gln Thr Leu Leu Ser Arg Tyr Thr Lys Arg Ser
2947  CAG GCG CUC CAG ACG CUG UUG UCC CGC UAC ACC AAG CGA AGC

 985  Ala Asp Leu Pro Leu His Glu Ala Lys Glu Asp Val Lys Arg
2989  GCU GAC CUG CCG CUA CAC GAA GCU AAG GAG GAC GUC AAA CGC

 999  Met Leu Asn Ser Leu Asp Arg His Trp Asp Trp Thr Val Thr
3031  AUG CUA AAC UCG CUU GAC CGA CAU UGG GAC UGG ACU GUC ACU

1013  Glu Asp Ala Arg Asp Arg Ala Val Phe Glu Thr Gln Leu Lys
3073  GAA GAC GCC CGU GAC CGA GCU GUC UUC GAG ACC CAG CUC AAG

1027  Phe Thr Gln Arg Gly Gly Thr Val Glu Asp Leu Leu Glu Pro
3115  UUC ACC CAA CGC GGC GGC ACC GUC GAA GAC CUG CUG GAG CCA

1041  Asp Asp Pro Tyr Ile Arg Asp Ile Asp Phe Leu Met Lys Thr
3157  GAC GAC CCC UAC AUC CGU GAC AUA GAC UUC CUU AUG AAG ACU

1055  Gln Gln Lys Val Ser Pro Lys Pro Ile Asn Thr Gly Lys Val
3199  CAG CAG AAA GUG UCG CCC AAG CCG AUC AAU ACG GGC AAG GUC

1069  Gly Gln Gly Ile Ala Ala His Ser Lys Ser Leu Asn Phe Val
3241  GGG CAG GGG AUC GCC GCU CAC UCA AAG UCU CUC AAC UUC GUC

1083  Leu Ala Ala Trp Ile Arg Ile Leu Glu Glu Ile Leu Arg Thr
3283  CUC GCC GCU UGG AUA CGC AUA CUC GAG GAG AUA CUC CGU ACC

1097  Gly Ser Arg Thr Val Arg Tyr Ser Asn Gly Leu Pro Asp Glu
3325  GGG AGC CGC ACG GUC CGG UAC AGC AAC GGU CUC CCC GAC GAA

1111  Glu Glu Ala Met Leu Leu Glu Ala Lys Ile Asn Gln Val Pro
3367  GAA GAG GCC AUG CUG CUC GAA GCG AAG AUC AAU CAA GUC CCA

1125  His Ala Thr Phe Val Ser Ala Asp Trp Thr Glu Phe Asp Thr
3409  CAC GCC ACG UUC GUC UCG GCG GAC UGG ACC GAG UUU GAC ACC
```

Figure A2.1 Continued…

```
1139  Ala His Asn Asn Thr Ser Glu Leu Leu Phe Ala Ala Leu Leu
3451  GCC CAC AAU AAC ACG AGU GAG CUG CUC UUC GCC GCC CUU UUA

1153  Glu Arg Ile Gly Thr Pro Ala Ala Ala Val Asn Leu Phe Arg
3493  GAG CGC AUC GGC ACG CCU GCA GCU GCC GUU AAU CUA UUC AGA

1167  Glu Arg Cys Gly Lys Arg Thr Leu Arg Ala Lys Gly Leu Gly
3535  GAA CGG UGU GGG AAA CGC ACC UUG CGA GCG AAG GGU CUA GGC

1181  Ser Val Glu Val Asp Gly Leu Leu Asp Ser Gly Ala Ala Trp
3577  UCC GUU GAA GUC GAC GGU CUG CUC GAC UCC GGC GCA GCU UGG

1195  Thr Pro Cys Arg Asn Thr Ile Phe Ser Ala Ala Val Met Leu
3619  ACG CCU UGC CGC AAC ACC AUC UUC UCU GCC GCC GUC AUG CUC

1209  Thr Leu Phe Arg Gly Val Lys Phe Ala Ala Phe Lys Gly Asp
3661  ACG CUC UUC CGC GGC GUC AAG UUC GCA GCU UUC AAA GGC GAC

1223  Asp Ser Leu Leu Cys Gly Ser His Tyr Leu Arg Phe Asp Ala
3703  GAC UCG CUC CUC UGU GGU AGC CAU UAC CUC CGU UUC GAC GCU

1237  Ser Arg Leu His Met Gly Glu Arg Tyr Lys Thr Lys His Leu
3745  AGC CGC CUU CAC AUG GGC GAA CGU UAC AAG ACC AAA CAU UUG

1251  Lys Val Glu Val Gln Lys Ile Val Pro Tyr Ile Gly Leu Leu
3787  AAG GUC GAG GUG CAG AAA AUC GUG CCG UAC AUC GGA CUC CUC

1265  Val Ser Ala Glu Gln Val Val Leu Asp Pro Val Arg Ser Ala
3829  GUC UCC GCU GAG CAG GUC GUC CUC GAC CCU GUC AGG AGC GCU

1279  Leu Lys Ile Phe Gly Arg Cys Tyr Thr Ser Glu Leu Leu Tyr
3871  CUC AAG AUA UUU GGG CGC UGC UAC ACA AGC GAA CUC CUU UAC

1293  Ser Lys Tyr Val Glu Ala Val Arg Asp Ile Thr Lys Gly Trp
3913  UCC AAG UAC GUG GAG GCU GUG AGA GAC AUC ACC AAG GGC UGG

1307  Ser Asp Ala Arg Tyr His Ser Leu Leu Cys His Met Ser Ala
3955  AGU GAC GCC CGC UAC CAC AGC CUC CUG UGC CAC AUG UCA GCA

1321  Cys Tyr Tyr Asn Tyr Ala Pro Glu Ser Ala Ala Tyr Ile Ile
3997  UGC UAC UAC AAU UAC GCG CCG GAG UCU GCG GCG UAC AUC AUC

1335  Asp Ala Val Val Arg Phe Gly Arg Gly Asp Phe Pro Phe Glu
4039  GAC GCU GUU GUU CGC UUU GGG CGC GGC GAC UUC CCG UUU GAA

1349  Gln Leu Arg Val Val Arg Ala His Val Gln Ala Pro Asp Ala
4081  CAA CUG CGC GUG GUG CGU GCC CAU GUG CAG GCA CCC GAC GCU

1363  Tyr Ser Ser Thr Tyr Pro Ala Asn Val Arg Ala Ser Cys Leu
4123  UAC AGC AGC ACG UAU CCG GCU AAC GUG CGC GCA UCG UGC CUU
```

Figure A2.1 Continued…

```
1377  Asp His Val Phe Glu Pro Arg Gln Ala Ala Ala Pro Ala Gly
4165  GAC CAC GUC UUC GAG CCC CGC CAG GCC GCC GCC CCG GCA GGU

1391  Phe Val Ala Thr Cys Ala Lys Pro Glu Thr Pro Ser Ser Leu
4207  UUC GUU GCG ACA UGU GCG AAG CCG GAA ACG CCU UCU UCA CUU

1405  Thr Ala Lys Ala Gly Val Ser Ala Thr Thr Ser His Val Ala
4249  ACC GCG AAA GCU GGU GUU UCU GCG ACU ACA AGC CAC GUU GCG

1419  Thr Gly Thr Ala Pro Pro Glu Ser Pro Trp Asp Ala Pro Ala
4291  ACU GGG ACU GCG CCC CCG GAG UCU CCA UGG GAU GCA CCU GCA

1433  Ala Asn Ser Phe Ser Glu Leu Leu Thr Pro Glu Thr Pro Ser
4333  GCC AAC AGC UUU UCG GAG UUA UUG ACA CCG GAG ACC CCG UCC

1447  Thr Ser Ser Ser Ala Val Ile Val Phe Ile Gly Leu Leu Tyr
4375  ACA UCA UCC UCG GCC GUC AUC GUC UUC AUC GGA CUC CUC UAC

1461  Ile Val Trp Lys Val Ala Gln Trp Trp Arg His Arg Lys Arg
4417  AUC GUG UGG AAG GUC GCU CAG UGG UGG AGA CAC CGC AAG AGG

1475  Thr Glu Asp Leu Asn Ser Arg Lys Pro Pro Ser Gln Asp Arg
4459  ACA GAA GAC UUG AAC AGC AGA AAG CCG CCU UCG CAA GAC AGG

1489  Gln Ser Arg Ser Ser Glu Cys Leu Asp Arg Ser Gly Glu Arg
4501  CAA UCA CGC UCG UCU GAA UGU CUG GAC AGA AGC GGA GAA AGG

1503  Thr Gly Ser Ser Leu Thr Ala Pro Thr Ala Pro Ser Pro Ser
4543  ACA GGC AGU UCG UUA ACU GCC CCC ACU GCU CCG AGC CCC UCA

1517  Phe Ser Phe Ser Glu Arg Ala Arg Leu Ala Thr Gly Pro Thr
4585  UUC UCA UUU UCG GAA AGA GCU CGA CUG GCG ACC GGG CCG ACU

1531  Val Ala Ala Ala Thr Ser Pro Ser Ala Thr Pro Ser Cys Ala
4627  GUC GCC GCU GCG ACA UCA CCU UCG GCA ACC CCA UCC UGC GCC

1545  Thr Asp Gln Val Ala Ala Arg Thr Thr Pro Asp Phe Ala Pro
4669  ACG GAC CAG GUU GCC GCG AGG ACC ACG CCG GAC UUU GCG CCU

1559  Phe Leu Gly Ser Gln Ser Ala Arg Ala Val Ser Lys Pro Tyr
4711  UUC CUG GGU UCC CAG UCU GCC CGU GCU GUC UCG AAG CCG UAC

1573  Arg Pro Pro Thr Thr Ala Arg Trp Lys Glu Val Thr Pro Leu
4753  CGG CCC CCC ACG ACU GCC CGU UGG AAA GAA GUC ACC CCG CUC

1587  His Ala Trp Lys Gly Val Thr Gly Asp Arg Pro Glu Val Arg
4795  CAC GCG UGG AAG GGC GUG ACC GGA GAC CGA CCG GAA GUC AGG

1601  Glu Asp Pro Glu Thr Ala Ala Val Val Gln Ala Leu Ile Ser
4837  GAG GAC CCG GAG ACA GCG GCG GUC GUC CAG GCU CUG AUC AGC
```

Figure A2.1 Continued…

```
1615  Gly Arg Tyr Pro Gln Lys Thr Lys Leu Ser Ser Asp Ala Ser
4879  GGC CGU UAU CCU CAG AAG ACG AAG CUU UCC UCC GAC GCA UCC

1629  Lys Gly Tyr Ser Arg Thr Lys Gly Cys Ser Gln Ser Thr Ser
4921  AAA GGC UAC UCA AGA ACU AAG GGA UGC UCA CAA UCC ACC UCU

1643  Phe Pro Ala Pro Ser Ala Asp Tyr Gln Ala Arg Asp Cys Gln
4963  UUU CCU GCC CCG AGU GCG GAU UAC CAG GCC CGC GAC UGC CAG

1657  Thr Val Arg Val Cys Arg Ala Ala Ala Glu Met Ala Arg Ser
5005  ACA GUC CGA GUC UGC CGC GCC GCU GCA GAG AUG GCG CGC UCA

1671  Cys Ile His Glu Pro Leu Ala Ser Ser Ala Ala Ser Ala Asp
5047  UGU AUU CAC GAG CCG UUG GCU UCA UCU GCC GCC AGU GCC GAC

1685  Leu Lys Arg Ile Arg Ser Thr Ser Asp Ser Val Pro Asp Val
5089  UUG AAG CGC AUA CGC UCU ACC UCG GAC UCU GUU CCC GAU GUA

1699  Lys Ile Ser Lys Ser Ala
5131  AAG AUC AGC AAG AGC GCA UGAAGGAACA AAAUUAGUUU CCUUGUUCGU

5179  AAACAAGGUG GUCCCUCCCA UUGAGGUAAA GACUCUGGUG AGUCCUCAAC

5229  GUUACUCGUU GAGUCUGCUG CGGUUCGAUU CCAUUCCCAA GCAGCAAAGG

5279  GUGCGCAACU AGUACGGCGC CCCCUGGGAU ACCA
```

Figure A2.1 Continued…

```
   1  GUUUUUCUUU CUUUACCAAG UGUGGUAAAA UUUAAACAAA GAAGAAAACC

  51  AGGACCGUAA CCCGGCCCUU ACACACCUCG AGUCCGUGAC CACCGGAUUA

 101  UACGUCGCCC ACCACACGGC GCCUUUUCCG ACCACUCUCG AGAGUCGUUG

 151  GGAGUUUCGU CCGUGACCAC CCGGUUGGCA GUCGACAGAC GCUUCCGGAC

 201  CACUAGAACC UCCUCGAGCG ACGCACACAC AGCACACACA CCGCCUUAGC

 251  UGCACCUACG GCAGCGUUGA UAGCGCGGAU UUAUGAGCGA GCACACCAUC

 301  GCCCACUCCA UCACAUUACC ACCCGGUUAC ACCCUUGCCC UAAUACCCCC

   1                    Met Gly Asp Ala Gly Val Ala Ser Gln
 351  UGAACCUGAA GCAGG AUG GGA GAU GCU GGA GUG GCG UCA CAG

  10  Arg Pro His Asn Arg Arg Gly Thr Arg Asn Val Arg Val Ser
 393  CGA CCU CAC AAC CGU CGC GGA ACC CGU AAC GUU CGG GUC AGC

  24  Ala Asn Thr Val Thr Val Asn Gly Arg Arg Asn Gln Arg Arg
 435  GCC AAC ACC GUC ACC GUC AAU GGU AGA AGA AAC CAA CGG CGU

  38  Arg Thr Gly Arg Gln Val Ser Pro Pro Asp Asn Phe Thr Ala
 477  CGG ACC GGA AGG CAA GUU UCU CCC CCU GAC AAU UUC ACC GCU

  52  Ala Ala Gln Asp Leu Ala Gln Ser Leu Asp Ala Asn Thr Val
 519  GCU GCA CAA GAC CUC GCG CAA AGC CUU GAC GCC AAC ACC GUC

  66  Thr Phe Pro Ala Asn Ile Ser Ser Met Pro Glu Phe Arg Asn
 561  ACU UUC CCC GCU AAC AUC UCU AGC AUG CCC GAA UUC CGG AAU

  80  Trp Ala Lys Gly Lys Ile Asp Leu Asp Ser Asp Ser Ile Gly
 603  UGG GCC AAG GGA AAG AUC GAC CUC GAC UCC GAU UCC AUC GGC

  94  Trp Tyr Phe Lys Tyr Leu Asp Pro Ala Gly Ala Thr Glu Ser
 645  UGG UAC UUC AAG UAC CUU GAC CCA GCG GGU GCU ACA GAG UCU

 108  Ala Arg Ala Val Gly Glu Tyr Ser Lys Ile Pro Asp Gly Leu
 687  GCG CGC GCC GUC GGC GAG UAC UCG AAG AUC CCU GAC GGC CUC

 122  Val Lys Phe Ser Val Asp Ala Glu Ile Arg Glu Ile Tyr Asn
 729  GUC AAG UUC UCC GUC GAC GCA GAG AUA AGA GAG AUC UAU AAC

 136  Glu Glu Cys Pro Val Val Thr Asp Val Ser Val Pro Leu Asp
 771  GAG GAG UGC CCC GUC GUC ACU GAC GUG UCC GUC CCC CUC GAC

 150  Gly Arg Gln Trp Ser Leu Ser Ile Phe Ser Phe Pro Met Phe
 813  GGC CGC CAG UGG AGC CUC UCG AUU UUC UCC UUU CCG AUG UUC
```

Figure A2.2 RNA sequence of HaSV RNA2 (Genome sequence accession number: L37299). The amino acid sequence of the capsid precursor protein gene is shown above the sequence.

```
 164  Arg Thr Ala Tyr Val Ala Val Ala Asn Val Glu Asn Lys Glu
 855  AGA ACC GCC UAC GUC GCC GUA GCG AAC GUC GAG AAC AAG GAG

 178  Met Ser Leu Asp Val Val Asn Asp Leu Ile Glu Trp Leu Asn
 897  AUG UCG CUC GAC GUU GUC AAC GAC CUC AUC GAG UGG CUC AAC

 192  Asn Leu Ala Asp Trp Arg Tyr Val Val Asp Ser Glu Gln Trp
 939  AAU CUC GCC GAC UGG CGU UAU GUC GUU GAC UCU GAA CAG UGG

 206  Ile Asn Phe Thr Asn Asp Thr Thr Tyr Tyr Val Arg Ile Arg
 981  AUU AAC UUC ACC AAU GAC ACC ACG UAC UAC GUC CGC AUC CGC

 220  Val Leu Arg Pro Thr Tyr Asp Val Pro Asp Pro Thr Glu Gly
1023  GUU CUA CGU CCA ACC UAC GAC GUU CCA GAC CCC ACA GAG GGC

 234  Leu Val Arg Thr Val Ser Asp Tyr Arg Leu Thr Tyr Lys Ala
1065  CUU GUU CGC ACA GUC UCA GAC UAC CGC CUC ACU UAU AAG GCG

 248  Ile Thr Cys Glu Ala Asn Met Pro Thr Leu Val Asp Gln Gly
1107  AUA ACA UGU GAA GCC AAC AUG CCA ACA CUC GUC GAC CAA GGC

 262  Phe Trp Ile Gly Gly Gln Tyr Ala Leu Thr Pro Thr Ser Leu
1149  UUU UGG AUC GGC GGC CAG UAC GCU CUC ACC CCG ACU AGC CUA

 276  Pro Gln Tyr Asp Val Ser Glu Ala Tyr Ala Leu His Thr Leu
1191  CCG CAG UAC GAC GUC AGC GAG GCC UAC GCU CUG CAC ACU UUG

 290  Thr Phe Ala Arg Pro Ser Ser Ala Ala Ala Leu Ala Phe Val
1233  ACC UUC GCC AGA CCA UCC AGC GCC GCU GCA CUC GCG UUU GUG

 304  Trp Ala Gly Leu Pro Gln Gly Gly Thr Ala Pro Ala Gly Thr
1275  UGG GCA GGU UUG CCA CAG GGU GGC ACU GCG CCU GCA GGC ACU

 318  Pro Ala Trp Glu Gln Ala Ser Ser Gly Gly Tyr Leu Thr Trp
1317  CCA GCC UGG GAG CAG GCA UCC UCG GGU GGC UAC CUC ACC UGG

 332  Arg His Asn Gly Thr Thr Phe Pro Ala Gly Ser Val Ser Tyr
1359  CGC CAC AAC GGU ACU ACU UUC CCA GCU GGC UCC GUU AGC UAC

 346  Val Leu Pro Glu Gly Phe Ala Leu Glu Arg Tyr Asp Pro Asn
1401  GUU CUC CCU GAG GGU UUC GCC CUU GAG CGC UAC GAC CCG AAC

 360  Asp Gly Ser Trp Thr Asp Phe Ala Ser Ala Gly Asp Thr Val
1443  GAC GGC UCU UGG ACC GAC UUC GCU UCC GCA GGA GAC ACC GUC

 374  Thr Phe Arg Gln Val Ala Val Asp Glu Val Val Val Thr Asn
1485  ACU UUC CGG CAG GUC GCC GUC GAC GAG GUC GUU GUG ACC AAC

 388  Asn Pro Ala Gly Gly Gly Ser Ala Pro Thr Phe Thr Val Arg
1527  AAC CCC GCC GGC GGC GGC AGC GCC CCC ACC UUC ACC GUG AGA
```

Figure A2.2 Continued…

```
 402  Val Pro Pro Ser Asn Ala Tyr Thr Asn Thr Val Phe Arg Asn
1569  GUG CCC CCU UCA AAC GCU UAC ACC AAC ACC GUG UUU AGG AAC

 416  Thr Leu Leu Glu Thr Arg Pro Ser Ser Arg Arg Leu Glu Leu
1611  ACG CUC UUA GAG ACU CGA CCC UCC UCU CGU AGG CUC GAA CUC

 430  Pro Met Pro Pro Ala Asp Phe Gly Gln Thr Val Ala Asn Asn
1653  CCU AUG CCA CCU GCU GAC UUU GGA CAG ACG GUC GCC AAC AAC

 444  Pro Lys Ile Glu Gln Ser Leu Leu Lys Glu Thr Leu Gly Cys
1695  CCG AAG AUC GAG CAG UCG CUU CUU AAA GAA ACA CUU GGC UGC

 458  Tyr Leu Val His Ser Lys Met Arg Asn Pro Val Phe Gln Leu
1737  UAU UUG GUC CAC UCC AAA AUG CGA AAC CCC GUU UUC CAG CUC

 472  Thr Pro Ala Ser Ser Phe Gly Ala Val Ser Phe Asn Asn Pro
1779  ACG CCA GCC AGC UCC UUU GGC GCC GUU UCC UUC AAC AAU CCG

 486  Gly Tyr Glu Arg Thr Arg Asp Leu Pro Asp Tyr Thr Gly Ile
1824  GGU UAU GAG CGC ACA CGC GAC CUC CCG GAC UAC ACU GGC AUC

 500  Arg Asp Ser Phe Asp Gln Asn Met Ser Thr Ala Val Ala His
1863  CGU GAC UCA UUC GAC CAG AAC AUG UCC ACC GCU GUG GCC CAC

 514  Phe Arg Ser Leu Ser His Ser Cys Ser Ile Val Thr Lys Thr
1905  UUC CGC UCA CUC UCC CAC UCC UGC AGU AUC GUC ACU AAG ACC

 528  Tyr Gln Gly Trp Glu Gly Val Thr Asn Val Asn Thr Pro Phe
1947  UAC CAG GGU UGG GAA GGC GUC ACG AAC GUC AAC ACG CCU UUC

 542  Gly Gln Phe Ala His Ala Gly Leu Leu Lys Asn Glu Glu Ile
1989  GGC CAA UUC GCG CAC GCG GGC CUC CUC AAG AAU GAG GAG AUC

 556  Leu Cys Leu Ala Asp Asp Leu Ala Thr Arg Leu Thr Gly Val
2031  CUC UGC CUC GCC GAC GAC CUG GCC ACC CGU CUC ACA GGU GUC

 570  Tyr Pro Ala Thr Asp Asn Phe Ala Ala Ala Val Ser Ala Phe
2073  UAC CCC GCC ACU GAC AAC UUC GCG GCC GCC GUU UCU GCC UUC

 584  Ala Ala Asn Met Leu Ser Ser Val Leu Lys Ser Glu Ala Thr
2115  GCC GCG AAC AUG CUG UCC UCC GUG CUG AAG UCG GAG GCA ACG

 598  Ser Ser Ile Ile Lys Ser Val Gly Glu Thr Ala Val Gly Ala
2157  UCC UCC AUC AUC AAG UCC GUU GGC GAG ACU GCC GUC GGC GCG

 612  Ala Gln Ser Gly Leu Ala Lys Leu Pro Gly Leu Leu Met Ser
2199  GCU CAG UCC GGC CUC GCG AAG CUA CCC GGA CUG CUA AUG AGU

 626  Val Pro Gly Lys Ile Ala Ala Arg Val Arg Ala Arg Arg Ala
2241  GUA CCA GGG AAG AUU GCC GCG CGU GUC CGC GCG CGC CGA GCG
```

Figure A2.2 Continued…

```
 640  Arg Arg Arg Ala Ala Arg Ala Asn
2283  CGC CGC CGC GCC GCU CGU GCC AAU UAGUUUGCUC GCUCCUGUUU

2327  CGCCGUUUCG UAAAACGGCG UGGUCCCGCA CAUUACGCGU ACCCUAAAGA

2377  CUCUGGUGAG UCCCCGUCGU UACACGACGG GUCUGCCGCG GUUCGAUUCC

2427  AUUCCCAAGC GGCAAGAAGG ACGUAGUUAG CUCUGCGUCC CUCGGGAUAC

2477  CA
```

Figure A2.2 Continued…

APPENDIX 3. SEQUENCE OF THE *ADH2-GAPDH* PROMOTER

```
   1  GATCCTTCAA TATGCGCACA TACGCTGTTA TGTTCAAGGT CCCTTCGTTT AAGAACGAAA GCGGTCTTCC TTTTGAGGGA
      CTAGGAAGTT ATACGCGTGT ATGCGACAAT ACAAGTTCCA GGGAAGCAAA TTCTTGCTTT CGCCAGAAGG AAAACTCCCT

  81  TGTTTCAAGT TGTTCAAATC TATCAAATTT GCAAATCCCC AGTCTGTATC TAGAGCGTTG AATCGGTGAT GCGATTTGTT
      ACAAAGTTCA ACAAGTTTAG ATAGTTTAAA CGTTTAGGGG TCAGACATAG ATCTCGCAAC TTAGCCACTA CGCTAAACAA

 161  AATTAAATTG ATGGTGTCAC CATTACCAGG TCTAGATATA CCAATGGCAA ACTGAGCACA ACAATACCAG TCCGGATCAA
      TTAATTTAAC TACCACAGTG GTAATGGTCC AGATCTATAT GGTTACCGTT TGACTCGTGT TGTTATGGTC AGGCCTAGTT

 241  CTGGCACCAT CTCTCCCGTA GTCTCATCTA ATTTTTCTTC CGGATGAGGT TCCAGATATA CCGCAACACC TTTATTATGG
      GACCGTGGTA GAGAGGGCAT CAGAGTAGAT TAAAAAGAAG GCCTACTCCA AGGTCTATAT GGCGTTGTGG AAATAATACC

 321  TTTCCCTGAG GGAATAATAG AATGTCCCAT TCGAAATCAC CAATTCTAAA CCTGGGCGAA TTGTATTTCG GGTTTGTTAA
      AAAGGGACTC CCTTATTATC TTACAGGGTA AGCTTTAGTG GTTAAGATTT GGACCCGCTT AACATAAAGC CCAAACAATT

 401  CTCGTTCCAG TCAGGAATGT TCCACGTGAA GCTATCTTCC AGCAAAGTCT CCACTTCTTC ATCAAATTGT GGAGAATACT
      GAGCAAGGTC AGTCCTTACA AGGTGCACTT CGATAGAAGG TCGTTTCAGA GGTGAAGAAG TAGTTTAACA CCTCTTATGA

 481  CCCAATGCTC TTATCTATGG GACTTCCGGG AAACACAGTA CCGATACTTC CCAATTCGTC TTCAGAGCTC ATTGTTTGTT
      GGGTTACGAG AATAGATACC CTGAAGGCCC TTTGTGTCAT GGCTATGAAG GGTTAAGCAG AAGTCTCGAG TAACAAACAA

 561  TGAAGAGACT AATCAAAGAA TCGTTTTCTC AAAAAAATTA ATATCTTAAC TGATAGTTTG ATCAAAGGGG CAAAACGTAG
      ACTTCTCTGA TTAGTTTCTT AGCAAAAGAG TTTTTTTAAT TATAGAATTG ACTATCAAAC TAGTTTCCCC GTTTTGCATC

 641  GGGCAAACAA ACGGAAAAAT CGTTTCTCAA ATTTTCTGAT GCCAAGAACT CTAACCAGTC TTATCTAAAA ATTGCCTTAT
      CCCGTTTGTT TGCCTTTTTA GCAAAGAGTT TAAAAGACTA CGGTTCTTGA GATTGGTCAG AATAGATTTT TAACGGAATA

 721  GATCCGTCTC TCCGGTTACA GCCTGTGTAA CTGATTAATC CTGCCTTTCT AATCACCATT CTAATGTTTT AATTAAGGGA
      CTAGGCAGAG AGGCCAATGT CGGACACATT GACTAATTAG GACGGAAAGA TTAGTGGTAA GATTACAAAA TTAATTCCCT

 801  TTTTGTCTTC ATTAACGGCT TTCGCTCATA AAAATGTTAT GACGTTTTGC CCGCAGGCGG GAAACCATCC ACTTCACGAG
      AAAACAGAAG TAATTGCCGA AAGCGAGTAT TTTTACAATA CTGCAAAACG GGCGTCCGCC CTTTGGTAGG TGAAGTGCTC

 881  ACTGATCTCC TCTGCCGGAA CACCGGGCAT CTCCAACTTA TAAGTTGGAG AAATAAGAGA ATTTCAGATT GAGAGAATGA
      TGACTAGAGG AGACGGCCTT GTGGCCCGTA GAGGTTGAAT ATTCAACCTC TTTATTCTCT TAAAGTCTAA CTCTCTTACT

 961  AAAAAAAAAA CCCTGAAAAA AAAGGTTGAA ACCAGTTCCC TGAAATTATT CCCCTACTTG ACTAATAAGT ATATAAAGAC
      TTTTTTTTTT GGGACTTTTT TTTCCAACTT TGGTCAAGGG ACTTTAATAA GGGGATGAAC TGATTATTCA TATATTTCTG

1041  GGTAGGTATT GATTGTAATT CTGTAAATCT ATTTCTTAAA CTTCTTAAAT TCTACTTTTA TAGTTAGTCT TTTTTTTAGT
      CCATCCATAA CTAACATTAA GACATTTAGA TAAAGAATTT GAAGAATTTA AGATGAAAAT ATCAATCAGA AAAAAAATCA

1121  TTTAAAAACAC CAAGAACTTA GTTTCGAATA AACACACATA AACAAA AUG
      AAATTTTGTG GTTCTTGAAT CAAAGCTTAT TTGTGTGTAT TTGTTT TAC
```

Figure A3.1. Sequence of the *ADH2-GAPDH* promoter. The 5' end of the *ADH2* promoter and *GAPDH* 5' untranslated region are highlighted in yellow and green respectively respectively. The *ADH2 UAS* is underlined and in bold font. The TATAA element of the *GAPDH* gene is depicted in bold font. The translational start of *GAPDH* is shown.

APPENDIX 4. PRIMERS

Table A4.1 Primers used during the course of this study

Primer	Gene	Location	Direct/ Compliment	Sequence
MT1	HaSV *P71*	nts 366-389 of RNA2	D	ATGGGAGATGCTGGAGTGGCGTCA
MT2	GAPDH	35 nts of the *GAPDH* 5' untranslated region, 2 bases downstream from the *GAPDH* translational start	C	TGTTTATGTGTGTTTATTCGAAACTAAGTT
MT5	NωV *P70*	1 to 22	D	ATGGACAGTAACTCAGCCTCCG
KM2R	NωV P70	313 to 334	C	GTACTCACCGACGGCACGAGC
MT6F	GAPDH – HaSV *P71*	The last 18 nts of the *GAPDH* 5' untranslated region and nts 1–26 of HaSV *P71*	D	CGAATAAACACACATAAACGACGTCAGATGCTGGAGTGGCGTCAC
MT7R	GAPDH – HaSV *P71*	The last 18 nts of the *GAPDH* 5' untranslated and nts 1-26 of HaSV *P71*	C	TGTGACGCCACTCCAGCATCTGACGTCGTTTATGTGTGTTTATTCG

APPENDIX 5. THERMAL CYCLING PARAMETERS

Program 1 (Section 2.2.4)

1 ×	94°C for 90sec
10 ×	94°C for 45sec 53 °C for 90sec 68°C for 4min
1 ×	68°C for 4min

Program 2 (Section 3.2.1)

1 ×	95°C for 30sec
18 ×	95°C for 30sec 63 °C for 1min 68°C for 10min

Program 3 (Section 3.2.4)

1 ×	94°C for 90sec
10 ×	94°C for 45sec 63 °C for 45sec 72°C for 4min
1 ×	72°C for 4min

APPENDIX 6. GROWTH MEDIA

Luria-Bertani agar/broth (Sambrook *et al*., 1989)

Per litre: 10 g peptone
5 g yeast extract
5 g NaCl
∗ 15 g Agar

∗ omit for liquid medium.

Synthetic Minimal Medium (SMM) (Kaiser *et al*., 1994)

Per liter: 1.7 g yeast nitrogen base (YNB) without amino acids and ammonium sulphate (Difco).
5 g Ammonium sulphate
20 g glucose
∗ 15 g Agar

∗ omit for liquid medium.

Supplements (Sigma) were added subsequent to autoclaving at the following final concentrations (mg/L):

Uracil	20
L - Tryptohan	20
L - Histidine	20
L - Leucine	100

Yeast Extract, Peptone, Dextrose Medium (YEPD)

Per liter: 2% yeast extract (weight/volume)
1% peptone (weight/volume)
2% glucose (volume/volume)

APPENDIX 7. GENERAL METHODS

A7.1 TUNEL Test (from Frank Madeo University of Tübingen – personal communication)

Buffers and solutions:

- Buffer B (10x): 350 mM KPP, 5 mM $MgCl_2$
- 37% formaldehyde (Sigma)
- Glucuronidase / arylsulfatase (Roche)
- Lyticase (Sigma, 1000 U/ml)
- PBS: 25 mM KPP; 0,9% (w/v) NaCl (pH 7.0)
- 0,3% H_2O_2 in methanol (100µl H_2O_2 in 10 ml methanol)
- Permeabilisation solution: 0.1% Triton X-100 (Merck), 0.1% (w/v) sodium citrate
- TUNEL-mix: enzyme solution in TUNEL-buffer 1:10 (Roche)
- Converter-POD (Roche)
- DAB-substrate: substrate solution in peroxide buffer 1:10 (Roche)

Method:

Approximately 1 mL of culture was microfuged at 2500 ×g for 5 minutes. The supernatant was discarded and the pellet was washed in 500 µL of buffer B. The washed pellet was re-suspended in 1 mL of buffer B to which 120 µL of 37% formaldehyde was added. The suspension was incubated at room temperature for 1 hour. The fixed cells were washed 3 times in buffer B containing 1.2 M sorbitol. The washed pellet was re-suspended in 330 µL of buffer B containing 1.2 M sorbitol. In order to digest the cell wall of the yeast cells, 75 µL glucuronidase / arylsulfatase (Roche) and 120 U lyticase (Sigma) were added to the suspension. The suspension was vortexed and incubated at 28°C for 2 hours. The cells were washed in 500 µL buffer B containing 1.2 M sorbitol and the pellet was re-suspended in 30µL buffer B containing 1.2 M

sorbitol. Approximately 30 µL of cells was applied to each window of polylysine (10mg/mL) coated slide. The cells were allowed to settle for 30 minutes and the excess buffer was removed with Watman 3MM paper. The slide was allowed to dry at room temperature. At this point the slide can be stored for up to 4 weeks at 4°C. These cells can now be tested by TUNEL or the nuclei can be stained with DAPI.

The slide was washed twice with PBS and incubated with 0.3% methanol for 30 minutes. The methanol was removed with 3MM Watman paper and the slide was washed with PBS. Allow the slide to dry and add 20 µl TUNEL-mix to each window for 1 hour in a humid chamber at 37°C. Remove the mixture and wash the slide three times with PBS. Allow the slide to dry and add 20 µl converter-POD to each window. Incubate the slide for 30 minutes in a humid chamber at 37°C and remove the liquid. Wash the slide three times with PBS and add 30 µl DAB-substrate to each window. Incubate the slide for 10 minutes at room temperature, remove the liquid, wash the slide three times with PBS and allow to dry. Add a small amount of Kaisers mounting gelatine (Merck) to each window, cover with a cover slip and view with a light microscope.

A7.2 DAPI staining (from Frank Madeo University of Tübingen – personal communication)

Buffers and solutions:

PBS as in section A7.1

1 µg/ml DAPI (4,6-diamidino-2-phenylindole) (Roche) in PBS

Method:

Wash each window containing fixed yeast cells twice with PBS and add 30 µL of 1 µg/mL of DAPI. Incubate the slide in a dark room for 15 minutes at room temperature. Wash the slide 6 times with PBS, allow the slide to dry, apply a small amount Kaisers mounting gelatine (Merck) to each window, cover with a cover slip and view with a epifluorescence microscope.

A7.3 Reagents for Northern analysis

50 × Denhardt's solution

1% (w/v) Ficoll 400 (Sigma)

1% (w/v) Polyvinylpyrrolidone (PVP; Sigma PVP-360)

1% (w/v) BSA (Sigma, faction V)

Salmon sperm DNA (10mg/mL)

Dissolve 1g sodium salt type III DNA from salmon testes (Sigma D – 1626) in 100mL ddH_2O. Sheer with a syringe fitted with an 18g needle, passing it through 2 or 3 times. Boil the solution to denature the DNA and aliquot. Store at -20°C.

Hybridization solution

50% de–ionized formamide

50 mM $NaPO_4$

800 mM NaCl

1 mM EDTA (pH 8)

1 × Denhardt's solution

250 μg/mL salmon sperm DNA

0.5% SDS

20 × MOPS

0.4 M MOPS

0.01 M NaOAc

20 mM EDTA

20 × SSC (pH 7.0)

3 M NaCl

0.3 M sodium citrate

REFERENCES

Adams, E.M. and Pringle, J. R. 1984. Relationship of actin and tubulin distribution to bud growth in wild-type and morphogenic-mutant *Saccharomyces cerevisiae*. Journal of Cellular Biology. **98:** 934-945.

Agrawal, D.K. and Johnson, J.E. 1992. Sequence and analysis of the capsid protein of *Nudaurellia* capensis *omega virus*, an insect virus with *T*=4 icosahedral symmetry. Journal of Virology. **190:** 806-814.

Agrawal, D.K. and Johnson, J.E. 1995. Assembly of the *T*=4 *Nudaurelia capensis* ω *virus* capsid protein, post – translational cleavage, and specific encapsidation of its mRNA in a baculoviral expression system. Virology. **207:** 89–97.

Ahlquist, P., Noueiry, A.O., Lee, W-A., Kushner, D.B. and Dye, T. 2003. Host factors in positive–strand RNA virus genome replication. Journal of Virology. **77 (15):** 8181-8186.

Albariño, C.G., Eckerle, L.D. and Ball, L.A. 2003. The *cis*-acting replication signal at the 3' end of *Flock House virus* RNA2 is RNA3-dependent. Virology. **311:** 181-191.

Baker, T.S., Olson, N.H. and Fuller, S.D. 1999. Adding the third dimension to virus life cycles: three-dimensional reconstruction of icosahedral viruses from cryo-electron micrographs. Micorbiology and Molecular Biology Reviews. **63 (4):** 862-922.

Ball, L.A., Amann, J.M. and Garrett, B. K. 1992. Replication of *Nodamura virus* after transfection of viral RNA into mammalian cells in culture. Journal of Virology. **66:** 2326–2334.

Ball, L.A. and Li, Y. 1993. *Cis*-acting requirements for the replication of *Flock House virus* RNA2. Journal of Virology. **67 (6):** 3544-3551.

Ball, L.A., Wohlrab, B. and Li, Y. 1994. Nodavirus RNA replication: mechanism and harnessing to vaccinia virus recombinants . Archives of Virology, Supplement. **9:** 407-416.

Ball, L.A. 1995. Requirements for the self directed replication of *Flock House virus* RNA1. Journal of Virology. **69:** 720-727.

Ball, L.A. and Johnson K.L. 1998. Nodaviruses of insects, pp225-267. In Miller, L.K and Ball, L.A (ed). The Insect viruses. Plenum Press, New York, N.Y.

Barco, A., Feduchi, E. and Carrasco. L. 2000. Poliovirus protease $3C^{pro}$ kills cells by apoptosis. Virology. **266:** 352-360.

Bawden, A.L., Gordon, K.H.J. and Hanzlik, T.N. 1999. The specificity of *Helicoverpa armigera stunt virus* infectivity. Journal of Invertebrate Pathology. **74:** 156-163.

Bothner, B., Schneemann, A., Marshall, D., Reddy, V., Johnson, J. E. and Siuzdak, G. 1999. Chrytallographically identical virus capsids display different properties in solution. Natural Structural Biology. **6:** 114–116.

Bothner, B., Taylor, D., Jun, B., Lee, K.K., Siuzdak, G., Schlutz, C.P. and Johnson, J.E. 2005. Maturation of a tetravirus capsid alters the dynamic properties and creates a metastable complex. Virology. **334:** 17–27.

Brachmann, C.B., Davies, A., Cost, G.J., Caputo, E., Li, J., Hieter, P. and Boeke, J.D. 1998. Designer deletion strains derived from *Saccharomyces cerevisiae* S288C: a useful set of strains and plasmids for PCR-mediated gene disruption and other applications. Yeast. **14:**115–132.

Bradford, M.M. 1976. A rapid and sensitive method for the quantitation of microgram quantities of protein utilizing the principle of protein-dye binding. Analyical Biochemistry. **72:** 248-54.

Brooks, E.M., Gordon, K.H.J., Dorrian, S.J., Hines, E.R. and Hanzlik, T.N. 2002. Infection of its lepidopteran host by the *Helicoverpa armigera* stunt virus (*Tetraviridae*). Journal of Invertabrate Pathology. **80:** 97-111.

Calandria, C., Irurzun, A., Barco, Á. and Carrasco, L. 2004. Individual expression of *Poliovirus* $2A^{pro}$ and $3C^{pro}$ induces activation of caspase-3 and PARP cleavage in HeLa cells. Virus Research. **104:** 39-49.

Canady, M.A., Tihova, M., Hanzlik, T.N., Johnson, J.E. and Yeager, M. 2000. Large conformational changes in the maturation of simple RNA virus, *Nudaurellia capensis* ω *Virus* (NωV). Journal of Molecular Biology. **299:** 573-584.

Canady, M.A., Tsuruta, H. and Johnson, J. E. 2001. Analysis of rapid, large-scale protein quaternary structural changes: time resolved X-ray solution scattering of *Nudaurelia capensis omega virus* (NωV) maturation. Journal of Molecular Biology. **311:** 803-814.

Carthy, C.M., Granville, D.J., Watson, K.A., Anderson, D.R., Wilson, J.E., Yang, D., Hunt, D.W.C. and McManus, B.M. 1998. Caspase activation and specific cleavage of substrates after *Coxsackievirus* B3-induced cytopathic effect in HeLa cells. Journal of Virology. **72** (**9):** 7669-7675.

Caspar, D.L.D. and Klug, A. 1962. Physical principles in the construction of regular viruses. *Cold Spring Harbor Symp.* Quantitative Biology. **27:** 1-24.

Chao, Y.-C., Scott, H.A. and Young S.Y. 1983. An icosahedral RNA virus of the soybean looper (*Pseudoplusia includens*). Journal of General Virology. **64:** 1835-1838.

Chao, J.A., Lee, J.H., Chapados, B.R., Debler, E.W., Schneemann, A. and Williamson, J.R. 2005. Dual modes of RNA-silencing suppression by *Flock House virus* protein B2. Nature Molecular Biology. **12 (11):** 952-7.

Cheng, R. H., Reddy, V. S., Olson, N. H., Fisher, A. J., Baker, T. S. and Johnson, J.E. 1994. Functional implications of a quasi-equivalence in a *T*=3 icosahedral animal virus established by cryo-electron microscopy and X ray crystallography. Structure. **2:** 271–282.

Cigan, A.M. and Donahue, T.F. 1987. Sequence and structural features associated with translational initiator regions in yeast-a review. Gene. **59:** 1-18.

Cousens, L.S., Shuster, J.R., Gallegos, C., Ku, L., Stempien, M.M., Urdea, M.S., Sanchez-Pescardo R., Taylor, A. and Tekamp-Olson, P. 1987. High level expression of proinsulin in the yeast, *Saccharomyces cerevisiae*. Gene. **61:** 265-275.

Dasgupta, R., Ghosh, A., Dasmapatara, B., Guarino, L.A. and Kaesberg, P. 1984. Primary and secondary structure of *Black beetle virus* RNA2, the genomic messanger for BBV coat protein precursor. Nucleic Acids Research. **12:** 7215-7223.

Dasgupta, R. and Sgro, J.Y. 1989. Nucleotide sequences of three nodaviral RNA2's: The messengers for their coat protein precursors. Nucleic Acids Research. **27:** 7525-7526.

Dasgupta, R., Selling, B. and Reuckert, R. 1994. *Flock house virus*: a simple model for studying persistent infection in cultured *Drosophila* cells. Archives of Virology Supplements. **9:**121-132.

Dasgupta, R., Garcia, B.H. and Goodman, R.M. 2001. Systemic spread of an RNA insect virus in plants expressing plant viral movement protein genes. Proceedings of the National Academy of Science. United States of America. **98:** 4910-4915.

Dasgupta, R., L. L. Cheng, L. C. Bartholomay, and B. M. Christensen. 2003. *Flock house virus* replicates and expresses green fluorescent protein in mosquitoes. Journal of General virology. **84:** 1789-1797.

Dasgupta, R., Free, H.M., Zietlow, S.L., Paskewitz, S.M., Aksoy, S., Shi, L., Fuchs, J., Hu, C. and Christensen, B.M. 2007. Replication of *Flock house virus* in three genera of medically important insects. Journal of Medical Entomology. **44(1):**102-110.

Dasmahapatara, B., Dasgupta, R., Ghosh, A. and Kaesberg, P. 1985. Structure of the *Black beetle virus* genome and its functional implications. Journal of Molecular Biology. **182:** 183-189.

Dearing, S.C., Scotti, P.D., Wigley, P.J. and Dhana, S.D. 1980. A small RNA virus isolated from the grass grub, *Costelytra zealandica* (Coleoptera: *Scarabaeidae*), New Zealand Journal of Zoology. **7:** 267-269.

Denis, C.L., Ferguson, J. and Young, E.T. 1982. mRNA levels for the fermentative alcohol dehydrogenase of *Saccharomyces cerevisiae* decrease upon growth on a non-fermentable carbon source. The Journal of Biological Chemistry. **258:** 1165-1171.

Dong, X.F., Natarajan, P., Tihova, M., Johnson, J.E. and Schneemann, A. 1998. Particle polymorphism caused by deletion of a peptide molecular switch in a quasi-equivalent icosahedral virus. Journal of Virology. **72:** 6024–6033.

Donnelley, M.L.L., Luke, G., Mehrotra, A., Li, X., Hughes, E., Gani, D. and Ryan, M.D. 2001. Analysis of the *Aphthovirus* 2A/2B polyprotein 'cleavage' mechanism indicates not a proteolytic reaction but a novel effect: a putative ribosomal 'skip'. Journal of Virology. **82:** 1013-1025.

Donoviel, M.S., Kacherovsky, N. and Young, E.T. 1995. Synergetic activation of *ADH2* expression is sensitive to upstream activation sequence 2 (*UAS2*) orientation, copy number and *UAS1-UAS2* helical phasing. Molecular and Cellular Biology. **15 (6):** 3442-3449.

Dorrington, R.A., Johnson, K.L., Price, D.B. and Ball, L.A. 2007 unpublished data.

Du Plessis, L., Hendry, D.A., Dorrington, R.A., Hanzlik, T.N., Johnson, J.E. and Appel, M. 2005. Revised RNA2 sequence of the tetravirus *Nudaurelia capensis* ω *virus* (NωV). Archives of Virology. **150 (11):** 2397-2402.

Eckerle, L.D., Albariño, C.G. and Ball, L.A. 2003. *Flock House virus* subgenomic RNA3 is replicated and its replication correlates with transactivation of RNA2. Virology. **317 (1):** 95-108.

Fauquet, C.M., Mayo, M.A., Maniloff, J., Desselberger, U. and Ball, L.A. 2005. Virus Taxonomy: 8th Report of the International Committee on Taxonomy of Viruses. Academic Press, London.

Fisher, A.J., and Johnson, J.E. 1993. Ordered duplex RNA controls the capsid architecture of an icosahedral animal virus. Nature. **361**, 176-179.

Finch, J.T. and Crowther, R.A. 1974. The structure of *Nudaurelia capensis* β *Virus*: the first example of a capsid with icosahedral surface symmetry *T*=4. Journal of General Virology. **24:** 191-200.

Francki, R.I.B., Fauquet, C.M., Knudson, D.L. and Brown, F. 1991. Classification and nomenclature of viruses: Fifth report of the International Committee of Taxonomy of Viruses. Springer-Verlag, Vienna.

Friesen, P.D. and Rueckert, R.R. 1981. Synthesis of *Black beetle virus* proteins in cultured *Drosophila* cells: differential expression of RNAs 1 and 2. Journal of Virology. **37(3):** 876-886.

Fu, J., VanDusen, W.J., Kolodin, D.G., O'Keefe, D.O., Herber, W.K. and George, H.A. 1996. Continuous culture study of expression of hepatitis B surface antigen and its self-assembly into virus–like particles in *Saccharomyces cerevisiae*. Biotechnology and Bioengineering. **49:** 578- 586.

Gallagher, T.M., Friesen, P.D. and Rueckert, R.R. 1983. Autonomous replication and expression of RNA1 from *Black beetle virus*. Journal of Virology. **46:** 481-489.

Gallagher, T.M. and Rueckert, R.R. 1988. Assembly-dependent maturation cleavage in provirions of a small icosahedral insect ribovirus. Journal of Virology. **62:** 3399-3406.

Garzon, S., Strykowski, H. and Charpentier, G. 1990. Implication of mitochondria in the replication of *Nodamura virus* in larvae of the Lepidoptera. *Galleria mellanolla* (L.) and in suckling mice. Archives of Virology. **113:** 165–176.

Gordon, K.H.J., Johnson, K.N. and Hanzlik, T.N. 1995. The larger genomic RNA of *Helicoverpa armigera stunt* tetravirus encodes the viral RNA polymerase and has novel 3'-terminal tRNA-like structure. Journal of Virology. **208:** 84-98.

Gordon, K.H.J. and Hanzlik, T.N. 1998. Tetraviruses. pp269-299. In Miller, L.K and Ball, L.A (ed). The Insect viruses. Plenum Press, New York, N.Y.

Gordon, K.H.J., Williams, M.R., Hendry, D.A. and Hanzlik, T.N. 1999. Sequence of the genomic RNA of *Nudaurelia* β virus (*Tetraviridae*) defines a novel virus genome organisation. Virology. **258:** 42-53.

Gordon, K.H., Williams, M.R., Baker, J.S., Gibson, J.M., Bawden, A.L., Millgate, A. G., Larkin, P.J. and Hanzlik, T.N. 2001. Replication-independent assembly of an insect virus (*Tetraviridae*) in plant cells. Virology. **288:** 36-50.

Görgens, J.F., van Zyl, W.H., Knoetze, J.H. and Hahn-Hägerdal. 2000. The metabolic burdon of the *PGK1* and *ADH2* promoter systems for heterologous xylanase production by *Saccharomyces cerevisiae* in defined medium. Biotechnology and Bioengineering. **73 (3):** 238-245.

Grace, T.D.C. and Mercer, E.H. 1965. A new virus of the Saturniid *Antheraea eucalypti* (Scott). Journal of Invertebrate Pathology. **7:** 241-244.

Greenwood, L.K. and Moore, N.F. 1984. Determination of the localisation of an infection in *Trichoplusia ni* larvae by a small RNA-containing virus using enzyme-linked immunosorbent assay and electron microscopy. Microbiologca. **7:** 97-102.

Hanahan, D. 1983. Studies on transformation of *Escherichia coli* with plasmids. Journal of Molecular Biology. **166**: 557-580.

Hanzlik, T.N., Gordon, K.H.J., Dorrain, J. and Christian, P.D. 1993. A novel small RNA virus isolated from the cotton bollworm, *Helicoverpa armigera*. **74:** 1805-1810.

Hanzlik, T.N., Dorrain, J., Gordon, K.H.J. and Christian, P.D. 1995. Sequence of RNA2 of the *Helicoverpa armigera stunt virus* (*Tetraviridae*) and bacterial expression of its genes. Journal of Virology. **76:** 799-811.

Hanzlik, T.N. and Gordon, K.H.J. 1997. The *Tetraviridae*. Advances in Virus Research. **48:** 101-168.

Hendry, D.A., Hodgson, V., Clark, R. and Newman, J. 1985. Small RNA viruses co-infecting the pine emperor moth (*Nudaurellia cytherea capensis*). Journal of General Virology. **66:** 627-632.

Hendry, D.A. and Agrawal, D.K. 1994. Tetraviruses. *In Encyclopaedia of Virology*. (A. Granoff and R.G. Webster, eds), pp. 1416-1422. Academic Press, San Diego, CA.

Helgstrand, C., Munshi, S., Johnson, J. E. and Liljes. L. 2004. The refined structure of *Nudaurelia capensis omega virus* reveals control elements for a *T*=4 capsid maturation. Virology. **318:**192-203.

Herker, E., Jungwirth, H., Lehmann, K. A., Maldener, C., Fröhlich, K-U., Wissing, S., Büttner, S., Fehr, M., Sigrist S. and Madeo. F. 2004. Chronological aging leads to apoptosis in yeast. Journal of Cellular Biology. **164:** 501-507.

Hoffmann, K.J., Cook, J.C., Joyce, J.G., Brown, D.R., Schultz, L.D., George, H.A., Rosolowsky, M., Fife, K.H. and Jansen, K.U. 1995. Sequence determination of *Human papillomavirus* type 6a and assembly of virus–like particles in *Saccharomyces cerevisiae*. Journal of Virology. **209:** 506 – 518.

Hoffmann, K.J., Neeper, M.P., Markus, H.Z., Brown, D.R., Müller, M. and Jansen, K.U. 1996. Sequence conservation within the major capsid protein of *Human papillomavirus* (HPV) type 18 and formation of HPV–18 virus–like particles in *Saccharomyces cerevisae*. Journal of General Virology. **77:** 465-468.

Hosur, M. V., Schmidt, T., Tucker, R. C., Johnson, J. E., Gallagher, T. M., Selling, B. H. and Ruekert, R. R. 1987. Structure of an insect virus at 3.0 Å resolution. Proteins: Structural and Functional Genetics. **2:** 167-176.

Johnston, M. and Davis, R.W. 1984. Sequences that regulate the divergent *GAL1-GAL10* promoter in *Saccharomyces cerevisiae*. Molecular and Cellular Biology. **4:** 1440-1448.

Johnston, M. 1987. A model *GAL* gene regulatory mechanism: the *GAL* genes of *Saccharomyces cerevisiae*. Microbiological Reviews. **51 (4):** 458-476.

Johnson, J.E., Munshi, S., Liljas, L., Agrawal, D., Olson, N.H., Reddy, V., Fisher, A., McKinney, B., Schmidt, T. and Baker, T.S. 1994. Comparative studies of *T*=3 and *T*=4 icosahedral RNA insect viruses. Archives of Virology. **9:** 497-512.

Johnson, J.E. 1996. Functional implications of protein-protein interactions in icosahedral viruses. Proceedings of the National Academy of Science. United States of America. **93:** 27-33.

Johnson, J.E. and Reddy, V. 1998. Structural studies of nodaviruses and tetraviruses. In *The insect viruses*. (L.K. Miller and L.A. Ball, eds.), pp. 171-224. Plenum Press, London.

Johnson, K.N., Tang, L., Johnson, J.E. and Ball, L.A. 2004. Heterologous RNA encapsidated in *Pariacoto virus*–like particles forms a dodecahedral cage similar to genomic RNA in wild–type virions. Journal of Virology. **78 (20):** 11371 – 11378.

Juckes, I.R.M. 1970. Viruses of the pine emperor moth. Bulletin of the South African Society for Plant Pathological Microbiology. **4:** 18.

Juckes, I.R.M. 1979. Comparison of some biophysical properties of the *Nudaurelia* β and ε viruses. Journal of General Virology. **42:** 89-94.

Kaesberg, P., Dasgupta, R., Sgro, J.Y., Wery, J.P., Selling, B.H., Hosur, M.V. and Johnson, J.E. 1990. Structural homology among four nodaviruses as deduced by sequencing and x-ray crystallography. Journal of Biological Chemistry. **214:** 423-435.

Kaiser, C., Michaelis, S. and Mitchell, A. 1994. Methods in Yeast Genetics. Cold Spring Harbour Laboratory Press, New York.

Koonin, E. V., Gorbalenya, A. E., Purdy, M. A., Rozanov, M. N., Reyes, G. R. and Bradley, D. W. 1992. Computer-assisted assignment of functional domains in the nonstructural polyprotein of *Hepatitis E virus*: delineation of an additional group of positive strand RNA plant and animal viruses. Proceedings of the National Academy of Science. United States of America. **89:** 8259–8263.

Krishna, N.K. and Schneemann, A. 1999. Formation of an RNA heterodimer upon heating of nodavirus particles. Journal of Virology. **73 (2):** 1699 – 1703.

Krishna, N.K., Marshall, D. and Schneemann, A. 2003. Analysis of RNA packaging in wild type and mosaic protein capsids of *Flock house virus* using a recombinant baculovirus vectors. Virology. **305:** 10-24.

Krol, M.A., Olson, N.H., Tate, J., Johnson, J.E., Baker, T.S. and Ahlquist, P. 1999 RNA-controlled polymorphism in the *in vivo* assembly of 180–subunit and 120–subunit virions from a single capsid protein. Proceedings of the National Academy of Science. United States of America. **96 (24):** 13650 – 13655.

Laemmli, U.K. 1970. Cleavage of structural proteins during the assembly of the head of a bacteriophage T4. Nature. **227:** 680-685.

La Grange, D.C., Pretorius, I.S. and van Zyl, W.H. 1996. Expression of a *Trichoderma reesei* beta-xylanase gene (XYN2) in *Saccharomyces cerevisiae*. Applied Environmental Microbiology. **62 (3):**1036-44.

Lane, L. (1981) in Handbook of Plant Virus Infections and Comparative Diagnosis, ed. Kurstak, E. (ElsevieryNorth–Holland, Amsterdam), pp. 334–376.

Larson, S. B. and McPherson, A. 2001 *Satellite tobacco mosaic virus* RNA: structure and implications for assembly. Current Opinions in Structural Biology. **11:** 59–65.

Leeds, P., Peltz, S.W., Jacobson, A. and Culbertson, M.R. 1991. The product of the yeast *UPF1* gene is required for rapid turnover of mRNAs containing a premature translational termination codon. Genes and Development. **5:** 2303-2314.

Li, H., Li, W.X. and Ding, S.W. 2002. Induction and suppression of RNA silencing by an animal virus. Science. **296:** 1319-1321.

Lindenbach, B.D., Sgro, J.Y. and Ahlquist, P. 2002. Long-distance base pairing in *Flock house virus* RNA1 regulates subgenomic RNA3 synthesis and RNA2 replication. Journal of Virology. **76(8):** 3905-3919.

Liu, J., Wei, T. and Kwang, J. (2004). *Avian encephalomyelitis virus* non-structural protein 2C induces apoptosis by activating cytochrome c caspase-9 pathway. Virology **318:** 169–182.

Ludovico, P., Sousa, M.J., Silva, M.T., Leao, C. and Corte-Real M. 2001. *Saccharomyces cerevisiae* commits to programmed cell death process in response to acetic acid. Microbiology. **147:** 2409-2415.

Ludovico, P., Rodrigues, F., Almeida, A., Silva, M.T., Barrientos, A. and Corte-Real, M. 2002. Cytochrome c release and mitochondria involvement in programmed cell death induced by acetic acid in *Saccharomyces cerevisiae*. Molecular Biology of the Cell. **13:** 2598-2606.

Lundblad, V. 1997. Yeast cloning vectors and genes. In *Current Protocols in Molecular Biology*. (F.M. Ausubel, R. Brent, R.E. Kingston, D.D. Moore, J.G. Seidman, J.A. Smith and K. Struhl., eds), vol. **2**., unit 13.4. John Wiley and Sons, New York.

Madeo, F., Shlauer, J., Zischka, H., Mecke, D. and Fröhlich, K-U. 1998. Tyrosine phosphorylation regulates cell cycle-dependent nuclear localization of Cdc48p. Molecular Biology and Cell. **9:** 131-141.

Madeo, F., Fröhlich, E., Ligr, M., Grey, M., Sigrist, S., Wolf, D.H. and Fröhlich, K-U. 1999. Oxygen stress: A regulator of apoptosis in yeast. Journal of Cellular Biology. **145:** 757-767.

Madeo, F., Herker, E., Maldener, C., Wissing, S., Lachelt, S., Herlan, M., Fehr, M., Lauber, K., Sigrist, S.J., Wesselborg, S. and Fröhlich, K-U. 2002. A caspase-related protease regulates apoptosis in yeast. Molecular Cell. **9:** 911-917.

Madeo. F., Herker, E., Wissing, S., Jungwirth, H., Eisenberg, T. and Fröhlich, K-U 2004. Apoptosis in yeast. Current Opinions in Microbiology. **7:** 655-60.

Marshall, D. and Schneemann, A. 2001. Specific packaging of nodaviral RNA2 requires the N-terminus of the capsid protein. Journal of Virology. **285:** 165-175.

Matsuyama, S. and Reed J.C. 2000. Mitochondria-dependent apoptosis and cellular pH regulation. Cell Death Differentiation. **7 (12):** 1155-1165.

Matthews, R.E.F. 1982. Classification and nomenclature of viruses. Fourth report of the international committee on taxonomy of viruses. Intervirology. **17:** 1-160.

Miller, L. K. 1988. Baculoviruses as gene expression vectors. Annual Reviews of Microbiology. **42:** 177-199.

Miller, D.J., Schwartz, M.D. and Ahlquist, P. 2001. *Flock house virus* RNA replicates on outer mitochondrial membranes in *Drosophila* cells. Journal of Virology. **75:**11664-11676.

Miller, D.J. and Ahlquist, P. 2002. Flock house virus RNA polymerase is a transmembrane protein with amino-terminal sequences sufficient for mitochondrial localisation and membrane insertion. Journal of Virology. **76 (19):** 9856-9867.

Morris, T.J., Hess, R.T. and Pinnock, D.E. 1979. Physicochemical characterisation of a small RNA virus associated with baculovirus infection in *Trichoplusia ni*. Intervirology. **11:** 238-247.

Mosisili, K. 2003. Non-host production of the *Helicoverpa armigera stunt virus* using a baculovirus expression system in *Spodoptera frugiperda* 21 cell line. Rhodes University MSc Thesis.

Munshi, S., Liljas, L., Cavarelli, J., Bomu, W., McKinney, B., Reddy, V. and Johnson, J.E. 1996. The 2.8 Å structure of a *T*=4 animal virus and its implications for membrane translocation of RNA. Journal of Molecular Biology. **261:** 1-10.

Nilsson, C., Johansson, U., Johansson, A-C., Kågedal, K. and Öllinger, K. 2006. Cytosolic acidification and lysosomal alkalinization during TNF-alpha induced apoptosis in U937 cells. Apoptosis. **11 (7):** 1149-1159.

Neeper, M.P., Hofmann, K.J., Jansen, K.U. 1996. Expression of the major capsid protein of *Human papillomavirus* type 2 in *Saccharomyces cerevisiae*. Gene. **180:** 1-6.

Olson, N.H., Baker, T.S., Johnson, J.E. and Hendry, D.A. 1990. The three-dimensional structure of frozen-hydrated *Nudaurelia capensis β virus*, a *T*=4 insect virus. Journal of Structural Biology. **105:** 11-122.

Price, V.L., Taylor, W.E., Clevenger, W., Worthington, M. and Young, E.T. 1990. Expression of heterologous proteins in *Saccharomyces cerevisiae* using the *ADH* 2 promoter. Methods In Enzymology. **185:** 308-318.

Price, D.B., Reuckert, R. and Ahlquist, P. 1996. Complete replication of an animal virus and maintenance of expression vectors derived from it in *Saccharomyces cerevisiae*. Proceedings of the National Academy of Science. United States of America. **93:** 9465-9470.

Price., D.B., Roeder, M. and Ahlquist, P. 2000. DNA-directed expression of functional *Flock house virus RNA*1 derivatives in *Saccharomyces cerevisiae*, heterologous gene expression, and selective effects on subgenomic mRNA synthesis. Journal of Virology. **74 (24):** 11724 – 11733.

Price, D.B., Ahlquist, P. and Ball, L.A. 2002. DNA-dependent colony formation of an animal virus RNA for the replication–dependent colony formation in *Saccharomyces cerevisiae*. Journal of Virology. **76 (4):** 1610-1616.

Price, D.B., Eckerle, L.D., Ball, L.A. and Johnson, K.L. 2005. *Nodamura virus* RNA replication in *Saccharomyces cerevisiae*: heterologous gene expression allows replication-dependent colony formation. Journal of Virology. **79 (1):** 495-502.

Pringle, F.M., Gordon, K.H.J., Hanzlik, T.N., Kalmakoff, J., Scotti, P.D. and Ward, V. 1999. A novel capsid expression strategy for *Thosea asigna* virus (*Tetraviridae*). Journal of General Virology. **80:** 1855-1863.

Pringle, F.M., Kalmakoff, J. and Vernon, K.W. 2001. Analysis of the capsid processing strategy of *Thosea asigna virus* using baculovirus expression of virus-like particles. Journal of General Virology. **82:** 259-266.

Pringle, F.M., Johnson, K.N., Goodman, C.L., McIntosh, A.H. and Ball, A. 2003. *Providence virus*: a new member of the *Tetraviridae* that infects cultured insect cells. Virology. **306:** 359-370.

Ramjee, M.K., Petithory, J.R., McElver, J., Weber, S.C. and Kirsch, J.F. 1996. A novel yeast expression/secretion system for the recombinant plant thiol endoprotease propapain. Protein Engineering. **9 (11):**1055-61.

Reinganum, C., Robertson, J.S. and Tinsley, T.W. 1978. A new group of RNA viruses from insects. Journal of General Virology. **40:** 195-202.

Romanos, M.A., Scorer, C.A. and Clare, J.J. 1992. Foreign gene expression in yeast: a review. Yeast. **8:** 423-488.

Rombaut, B. and Jore, J.P.M. 1997. Immunogenic, non–infectious polio subviral particles synthesized in *Saccharomyces cerevisiae*. Journal of General Virology. **78:** 1829–1832.

Rose, A.B. and Broach, J.R. 1990. Propagation and expression of cloned genes in yeast: 2μm circle-based vectors. Methods in Enzymology. **185:** 234-279.

Rossmann, M.G. and Johnson, J.E. 1989. Icosahedral RNA virus structure. Annual Reviews of Biochemistry. **58:** 533–573.

Sambrook, J., Fritsch., E.F. and Maniatis, T. 1989. Molecular cloning, a laboratory manual. 2nd ed. Cold Spring Harbour Press, New York.

Santoro, M.G. 1996. Viral infection. EXS. **(77):** 337-57.

Schneemann, A., Zhong, W., Gallagher, T.M. and Rueckert, R.R. 1992. Maturation cleavage required for infectivity of a nodavirus. Journal of Virology. **66 (11):** 6728-6734.

Schneemann, A., Dasgupta, R., Johnson, J.E. and Rueckert, R.R. 1993. Use of recombinant baculoviruses in synthesis of morphologically distinct virus–like particles of *Flock house virus*, a nodavirus. Journal of Virology. **67:** 2756–2763.

Schneemann, A., Gallagher, T.M. and Rueckert, R. R. 1994. Reconstitution of Flock house provirion: a model system for studying structure and assembly. Journal of virology. **68 (7):** 4547– 4556.

Schneemann, A. and Marshall, D. 1998. Specific encapsidation of nodavirus RNAs is mediated through the C-terminus of capsid precursor protein alpha. Journal of Virology. **72 (11):** 8738–8746.

Schneemann, A. 2006. The structural and functional role of RNA in icosahedral virus assembly. Annuals Reviews of Microbiology. **60:** 51-67.

Schwelberger, H.G., Kang. H.A. and Hershey, J.W. 1993. Translation initiation factor eIF-5A expressed from either of two yeast genes or from human cDNA. Functional identity under aerobic and anaerobic conditions. **268 (19):**14018-25.

Scotti, P.D., Dearing, S. and Mosssop, D.W. 1983. *Flock house virus*: a nodavirus isolated from *Costelytra zealandica* (White) (Coleoptera: *Scarabaeidae*). Archives of Virology. **75:** 181-189.

Selling, B.H., Allison, R.F. and Kaesberg, P. 1990. Genomic RNA of an insect virus directs synthesis of infectious virions in plants. Proclamation of the National Academy of Science. United States of America. **87:** 434–438.

Shuster, J.R. 1989. Regulated transcription systems for the production of proteins in yeast: regulation by carbon source. Pp 83–10108. In: Yeast Genetic Engineering. Barr, P.J., Brake, A.J. and Valenzuela, P. (Eds.) Butterworth Publishers, Stoneham, MA.

Salonen, A., Ahola, T. and Kaarianen, L. 2004. Viral RNA replication in association with cellular membranes. Current Topics in Microbiology and Immunology. **285:** 139-73.

Struthers, J.K. and Hendry, D.A. 1974. Studies of the protein and nucleic acid components of *Nudaurelia capensis β virus*. Journal of General Virology. **22:** 355–362.

Sullivan, C. S. and Ganem, D. 2005. A virus-encoded inhibitor that blocks RNA interference in mammalian cells. Journal of Virology. **79 (12):** 7371-9.

Tang, L., Johnson, K.N., Ball, L.A., Lin, T., Yeager, M. and Johnson, J.E. 2001. The structure of *Pariacoto virus* reveals a dodecahedral cage of duplex RNA. Nature Structural Biology. **8 (1):** 77-83.

Taylor, D.J., Krishna, N.K., Canady, M.A., Schneemann, A. and Johnson, J.E. 2002. Large-scale, pH-dependent, quaternary structure changes in an RNA virus capsid are reversible in the absence of subunit autoproteolysis. Journal of Virology. **76 (19):** 9972-9980.

Taylor, D.J. 2003. Molecular and biophysical analysis of a conformational change in a non-enveloped RNA Virus. Ph.D. thesis. University of California-San Diego, California.

Taylor D.J. and Johnson, J.E. 2005. Folding and particle assembly are disrupted by single point mutations near the autocatalytic cleavage site of *Nudaurelia capensis* ω *virus* capsid protein. Protein Science. **14:** 401-408.

Taylor, T.J., Speir, J.A., Reddy, V., Cingolani, C., Pringle, F.M., Ball, L.A. and Johnson, J.E. 2005. Preliminary x-ray characterization of authentic *Providence virus* and attempts to express its coat protein gene in recombinant baculovirus. Archives of Virology. **151 (1):** 155-65.

Thuman-Commike, P.A., Greene, B., Malinski, J.A., King, J. and Chiu, W. 1998. Role of the scaffolding protein in P22 procapsid size determination suggested by *T*=4 and *T*=7 procapsid structures. Journal of Biophysics. **74:** 559–568.

Tihova, M., Dryden, K.A., Le, T.V., Harvey, S.C., Johnson, J.E., Yeager, M. and Schneemann, A. 2004. Nodavirus coat protein imposes dodecahedral RNA structure independent of nucleotide sequence and length. Journal of Virology. **78 (6):** 2897-2905.

Valenzuela, P., Medina, A., Rutter, W.J., Ammerer, G. and Hall, B.D. 1982. Synthesis and assembly of *Hepatitis B virus* surface antigen particles in yeast. Nature. **298:** 347 – 350.

Van Gurp, M., Festjens, N., van Loo, G., Saelens, X. and Vandenabeele. P. 2003. Mitochondrial intermembrane proteins in cell death. Biochemistry and Biophysical Research Communications. **304:** 487–497.

Van Regenmortel, M.H.V., Fauquet, C.M., Bishop, D.H.L., Carstens, E.B., Estes, E.K., Lemon, S.M., Maniloff, J., Mayo, M.A., McGeoch, D.J., Pringle, C.R. and Wickner, R.B. 2000. Virus Taxonomy: Seventh Report of the International Committee on Taxonomy of Viruses. Academic Press, London.

Verdone, L., Camillioni, G., Mauro, E.D. and Caserta, M. 1996. Chromatin remodeling during *Saccharomyces cervisiae ADH2* gene activation. Molecular and Cellular Biology. **16 (5):** 1987-1988.

Verdone, L., Cesari, F., Denis, C.L., Mauro, E.D. and Caserta, M. 1997. Factors affecting *Saccharomyces cerevisiae ADH2* chromatin remodelling and transcription. The Journal of Biological Chemistry. **272 (49):** 30828-30834.

Venter, P.A. 2001. Non-host production of the *Helicoverpa armigera stunt virus* in *Saccharomyces cervisiae*. Rhodes University PhD Thesis.

Venter, P.A., Krishna, N.K. and Schneemann, A. 2005. Capsid protein synthesis from replicating RNA directs specific packaging of the genome of a multipartite, positive-strand RNA virus. Journal of Virology. **79** (**10):** 6239-6248.

Venter, P. A. and Schneemann, A. 2007. Assembly of two independent populations of *Flock house virus* particles with distinct RNA packaging characteristics in the same cell. Journal of Virology. **81:** 613-619.

Vlok, M. 2006. The purification and localisation of the *Helicoverpa armigera stunt virus* p17 protein. Rhodes University Honours thesis.

Ward, A.C., Azad, A.A. and Macreadie, I.G. 1994. Expression and characterization of the *Influenza A virus* non–structural protein NS_1 in yeast. Archives of Virology. **138:** 299–314.

Wery, J.P., Reddy, V.S., Hosur, V.S. and Johnson, J.E. 1994. The refined three–dimensional structure of an insect virus at 2.8Å resolution. Journal of Molecular Biology. **235:** 565–586.

Wodicka, L., Dong, H., Mittmann, M., Ho, M.H. and Lockhart. D.J. 1997. Genome-wide expression monitoring in *Saccharomyces cerevisiae*. Nature Biotechnology. **15:**1359–1367.

Wu, H.L, Chen, P.J, Mu, J.J, Chi, W.K., Kao, T.L., Hwang, L.H. and Chen, D.S. 1997. Assembly of **Hepatitis delta virus**-like empty particles in yeast. Journal of Virology. **236:** 374-381.

Yanisch-Perron, C., Viera, J. and Messing, J. 1985. Improved M13 phage cloning vectors and host strains: nucleotide sequences of the M13mp18 and pUC19 vectors. Gene **33:** 103-119.

Yi, F., Zhang, J., Yu, H., Liu, C., Wang, J. and Hu, Y. 2005. Isolation and identification of a new tetravirus from *Dendrolimus punctatus* larvae collected from Yunnan Province, China. Journals of General Virology. **86:** 789-796.

Zhang, W., Fisher, B.R., Olson, N.H., Strauss, J.H., Kuhn, R.J. and Baker, T.S. 2002. *Aura virus* structure suggests that the *T*=4 organization is a fundamental property of viral structural proteins. Journal of Virology. **76 (14):** 7239–7246.

Zhong, W. and Rueckert, R. 1993. *Flock house virus*: down-regulation of subgenomic RNA3 synthesis does not involve coat protein and is targeted to synthesis of its positive strand. Journal of Virology. **67:** 2716-2722.

Zlotnick, A., Reddy, V.S., Dasgupta, R., Schneemann, A., Ray, W.J., Rueckert, R.R. and Johnson, J.E. 1994. Capsid assembly in a family of animal viruses primes an autoproteolytic maturation that depends on a single aspartic acid residue. The Journal of Biological Chemistry. **269 (18):** 13680–13684.

Zlotnick, A., Cheng, N., Conway, J.F., Booy, F.P., Steven, A.C., Stahl, S.J. and Wingfield, P.T. 1996. Dimorphism of *Hepatitis B virus* capsids is strongly influenced by the C-terminus of the capsid protein. Biochemistry. **35:** 7412–7421.

Zhou, L., Zhang, J., Wang, X., Jiang, H., Yi, F. and Hu, Y. 2006. Expression and characterization of RNA-dependent RNA polymerase of *Dendrolimus punctatus tetravirus*. Journal of Biochemistry and Molecular Biology. **39 (5):** 571-577.

Zeddam, J.-L.A., Gordon, K.H. and Hanzlik, T.N. Genome organization of *Euprosterna elaeasa virus* defines it as a member of a new group of insect RNA viruses. Genebank accession number AF461742. Unpublished